Utjecaj analoga peptida 1 sličnog glukagonu na mehanizme nastanka lijekovima izazvanog jetrenog oštećenja u staničnim kulturama

Omanović Kolarić, Tea

Doctoral thesis / Disertacija

2022

Degree Grantor / Ustanova koja je dodijelila akademski / stručni stupanj: **Josip Juraj Strossmayer University of Osijek, Faculty of Medicine Osijek / Sveučilište Josipa Jurja Strossmayera u Osijeku, Medicinski fakultet Osijek**

Permanent link / Trajna poveznica: https://urn.nsk.hr/urn:nbn:hr:152:881540

Rights / Prava: In copyright / Zaštićeno autorskim pravom.

Download date / Datum preuzimanja: **2024-03-28**

Repository / Repozitorij:

Repository of the Faculty of Medicine Osijek

JOSIP JURAJ STROSSMAYER UNIVERSITY OF OSIJEK

FACULTY OF MEDICINE

Tea Omanović Kolarić

Effect of GLP-1 analogs on the pathophysiological mechanisms of drug-induced liver injury in cell cultures

Doctoral Dissertation

Osijek, 2022.

JOSIP JURAJ STROSSMAYER UNIVERSITY OF OSIJEK

FACULTY OF MEDICINE

Tea Omanović Kolarić

Effect of GLP-1 analogs on the pathophysiological mechanisms of drug-induced liver injury in cell cultures

Doctoral Dissertation

Osijek, 2022.

Mentor: Prof. Martina Smolić, M.D., Ph.D.

Co-Mentor: Prof. George Y. Wu, M.D., Ph.D.

The dissertation contains 84 pages.

PREFACE

The study was funded by grants from Croatian Ministry of Science, Education and Sports dedicated to multi-year institutional funding of scientific activity at the Josip Juraj Strossmayer University of Osijek, Osijek, Croatia - grant numbers: IP10-Mefos-2019 (to Martina Smolic), IP15-Mefos-2021 (to Martina Smolic), and IP8-FDMZ-2021 (to Robert Smolic).

ZAHVALE

Na kraju ove jedne velike etape u mojoj karijeri, ali i u životu, želim zahvaliti osobama koje su me kroz nju vodile, bile mi podrška i zbog kojih sam tu gdje jesam.

Najprije bih zahvalila mentorici, prof.dr.sc. Martini Smolić, na podršci koju mi je pružila u različitim oblicima i razboritosti koju je zadržala i u najizazovnijim trenucima te me sigurno povela do ovog uspjeha.

Hvala i komentoru, prof.dr.sc. George Y Wu, koji je svojim savjetima te ogromnim iskustvom i znanjem koje posjeduje, dao poseban doprinos pri izradi ove disertacije.

Hvala i prof.dr.sc. Ines Bilić-Ćurčić na razumijevanju i podršci bez koje bi bilo puno teže ostvariti ovaj cilj.

Hvala svim mojim kolegama i prijateljima, a među njima moram izdvojiti Vjeru, Kizu i Mileta, koji su sa mnom prošli kroz one najljepše i najteže trenutke od samo početka ovog puta, te mi ga uljepšali svojom podrškom.

"U životu nije bitno jesi li vjernik, agnostik ili ateist, bitno je da si humanist."

prof.dr.sc. M. Omanović, prof. emeritus

Upravo je ova izreka moje misaono nasljeđe i pogotovo u ovim vremenima posebno izazovno za ostvariti- ostati čovjekom. Oni koju si mi u tome nemjerljivo najviše pomogli, te me kroz najteže trenutke bodrili, tješili, volili, a u najljepšima se veselili sa mnom su moja obitelj. Bez njih ni ovaj moj uspjeh ne bi imao pravi smisao, te me čine boljom osobom i da nikad ne zaboravim prave vrijednosti. Hvala im beskonačno na tome, posebno mom mužu Ivanu, koji je svaki trenutak strpljivo proživio sa mnom, te najmlađoj, ali i najsjajnijoj zvijezdi vodilji, a ujedno i mom najvećem životnom postignuću, mojoj Lauri. Volim vas.

Table of contents

1. INTRODUCTION 1
1.1. Drug-induced liver injury (DILI) 1
1.2. Drug-induced fatty liver disease (DIFLD) 2
1.2.1. Epidemiology of DIFLD 3
1.2.2. Histology of DIFLD 3
1.2.3. Risk factors for occurrence of DIFLD 4
1.2.4. Drugs that cause DIFLD 5
1.2.5. Mechanisms of DIFLD development 6
1.2.6. Current and future directions in the treatment of DIFLD 10
1.3. Non-alcoholic fatty liver disease (NAFLD) 11
1.4. NAFLD and DIFLD overlap 12
1.5. *In vitro* models of NAFLD and DIFLD 13
1.6. GLP-1 analogs in NAFLD 13
1.6.1. GLP-1 analogs classes and mechanism of action 13
1.6.2. Hepatoprotective effects of GLP-1 analogs in NAFLD in clinical trials 14
1.6.3. Hepatoprotective effects of GLP-1 analogs in NAFLD in animal and *in vitro* models 15
2. HYPOTHESIS 17
3. RESEARCH OBJECTIVES 18
4. MATERIAL AND METHODS 19
4.1. Study design 19
4.2. Material 19
4.2.1. Chemicals 19
4.2.2. Cell culture 19
4.2.3. Drugs and oleic acid preparation 20

4.3. Methods 21
4.3.1. NAFLD and DIFLD cell culture models 21
4.3.2. Measurement of the Hepatoprotective Effect of LIRA in NAFLD and DIFLD Cell Culture Models 22
4.3.3. Visualization of fat accumulation 22
4.3.4. Measurement of triglyceride levels 23
4.3.5. Measurement of Cellular Glutathione (GSH) Concentration 23
4.3.6. Total RNA isolation and Reverse Transcription Polymerase Chain Reaction (RT-PCR) analysis 25
4.3.7. Statistical analysis 28
5. RESULTS 29
5.1. Establishment of the Cell Culture Model of DIFLD and NAFLD, and Assessment of the Effect of Oleic Acid, Amiodarone, and Tamoxifen on the Cell Viability 29
5.2. Measurement of the Effect of Liraglutide in NAFLD and DIFLD Cell Culture Models on the Cell Viability 33
5.3. Visualization and Quantification of lipid accumulation in NAFLD and DIFLD cell culture models, cotreated with different LIRA concentrations 36
5.4. Measurement of triglyceride content in NAFLD and DIFLD cell culture models, and/or cotreated with different LIRA concentrations 42
5.5. Assessment of the Effect of LIRA on GSH concentration in hepatocyte steatosis NAFLD and DIFLD cell culture models 44
5.6. Evaluation of the effect of LIRA on various gene expression in hepatocyte steatosis NAFLD and DIFLD cell culture models 45
6. DISCUSSION 52
7. CONCLUSIONS 57
8. SUMMARY 58
9. SAŽETAK 59
10. REFERENCES 61
11. CURRICULUM VITAE 75

List of figures:

Figure 1. 1. Three main types (categories) of DILI and numerous different phenotypes, with emphasis on fatty liver, are shown in this scheme. DILI- drug-induced liver injury 1
Figure 1. 2. Most common etiologies of NAFLD, and progression to more severe stages of liver disease are shown in this scheme. NAFLD- non-alcoholic fatty liver disease 12

Figure 5. 1. Determination of cell viability by MTT assay after exposure to varying amiodarone (AMD) and oleic acid (OA) concentrations and varying time periods in the Huh7 cell line.....30
Figure 5. 2. Determination of cell viability by MTT assay after exposure to varying tamoxifen (TAM) concentrations and varying time periods in the Huh7 cell line.....31
Figure 5. 3. Cell survival after exposure of cells to varying amiodarone (AMD) and oleic acid (OA) concentrations and varying time periods in the Huh7 cell line. 32
Figure 5. 4. Cell survival after exposure of cells to varying tamoxifen (TAM) concentrations in the Huh7 cell line.....33
Figure 5. 5. Determination of cell viability by MTT assay after exposure of Huh7 cells to OA, AMD and various LIRA concentrations for 24 h. 34
Figure 5. 6. Determination of cell viability by MTT assay after exposure of Huh7 cells to TAM and various LIRA concentrations for 24h.....35
Figure 5. 7. Cell survival after exposure of Huh7 cells to OA, AMD and various LIRA concentrations for 24 h. 35
Figure 5. 8. Cell survival after exposure of Huh7 cells to TAM and various LIRA concentrations for 24 h. 36
Figure 5. 9. Visualization of lipid accumulation with Oil-Red-O dye.....37
Figure 5. 10. Levels of lipids stained with Oil-Red-O dye in the Huh7 cells treated with OA, AMD, and LIRA. 38
Figure 5. 11. Number of lipids droplets per cell after analyzing the images of Oil-Red-O stained Huh7 cells treated with OA, AMD, and LIRA.....39
Figure 5. 12. Average size of lipid droplets after analyzing images of the Oil-Red-O stained Huh7 cells treated with OA, AMD, and LIRA. 39
Figure 5. 13. Visualization of lipid accumulation with Oil-Red-O dye.....40

Figure 5. 14. Levels of lipids stained with Oil-Red-O dye in the Huh7 cells treated with TAM and LIRA. 40
Figure 5. 15. Number of lipids droplets per cell after analyzing images of Oil-Red-O stained Huh7 cells treated with TAM and LIRA. 41
Figure 5. 16. Average size of lipid droplets after analyzing images of Oil-Red-O stained Huh7 cells treated with TAM and LIRA. 42
Figure 5. 17. Triglyceride content in DIFLD and NAFLD cell culture models incubated with varying concentrations of LIRA. 43
Figure 5. 18. Triglyceride content in TAM NAFLD cell culture model, incubated with varying concentrations of LIRA. 43
Figure 5. 19. GSH levels in the hepatocyte steatosis NAFLD and AMD DIFLD Huh7 cell culture models. 44
Figure 5. 20. GSH levels in the hepatocyte steatosis TAM DIFLD Huh7 cell culture model.45
Figure 5. 21. Expression of *ACSL1*, *CEBPA*, *PPARG*, and *SREBF1* in hepatocyte steatosis cell culture models of NAFLD and AMD DIFLD. 48
Figure 5. 22. Expression of ACSL1, CEBPA, PPARG, and SREBF1 in hepatocyte steatosis cell culture models of TAM DIFLD. 50

List of tables:

Table 1. 1. Classification of Drugs According to Their Ability to Cause Hepatotoxicity: Acute Liver Injury or Progression of Pre-Existing Fatty Liver Disease. 6
Table 1. 2. The roles of various gene pathways in steatosis development.....7
Table 1. 3. Drugs That Cause DIFLD and Summary of Mechanisms Responsible for Their Toxicity. 9
Table 1. 4. Classification of GLP-1 analogs 14
Table 1. 5. List of the main actions of GLP-1 in various organs. 14

Table 4. 1. Reaction mixtures for Reverse Transcription and PCR (total volume 20 µl).....26
Table 4. 2. PCR conditions for amplification of various genes. 26
Table 4. 3. Primer sequences used for RT (Reverse transcription)-PCR. 27

List of abbreviations used in text:

DILI, drug-induced liver injury

ADR, adverse drug reactions

DIFLD, drug-induced fatty liver disease

NAFLD, non-alcoholic fatty liver disease

DISH, drug-induced steatohepatitis

TAM, tamoxifen

AMD, amiodarone

DIS, drug-induced steatosis

NASH, non-alcoholic steatohepatitis

DILIN, drug-induced liver injury network

VLDL, very-low-density lipoprotein

SREBF1, sterol regulatory element binding transcription factor 1c

PPAR, peroxisome proliferator-activated receptor

mtFAO, mitochondrial fatty acid oxidation

ROS, reactive oxygen species

NAS, non-alcoholic steatosis

ACLY, ATP-citrate synthase

THRSP, thyroid hormone responsive

SCD1, stearoyl-CoA Desaturase 1

FASN, fatty acid synthase

CPT1 enzyme, carnitine palmitoyltransferase-1

PLIN4, perilipin-4

MTP, microsomal triglyceride transfer protein

GSH, glutathione

ACSL1, acyl-coa synthetase long chain family member 1,

FA, fatty acid

CEBPA, CCAAT/enhancer-binding protein α

FABP, fatty acid binding protein

HSC, hepatic stellate cells

TGF-β1, transforming growth factor- β1

ACC, acetyl-coa carboxylase

MRC, mitochondrial respiratory chain

FFAs, free fatty acids

ALT, alanine transaminase

AST, aspartate transaminase

ULN, upper limit of normal

INR, international normalized ratio

UDCA, ursodeoxycholic acid

T2DM, type 2 diabetes mellitus

HDL, high-density lipoprotein

GLP-1, glucagon-like peptide-1

LEAN, liraglutide efficacy and action in NASH

LIRA, liraglutide

GGT, gamma-glutamyl transferase

HFD, high fat diet

FTO, fat mass and obesity associated

mRNA, messenger RNA

DMEM, Dulbecco’s Modified Eagle’s Medium

FBS, fetal bovine serum

DMSO, dimethyl sulfoxide

OA, oleic acid

BSA, bovine serum albumin

MTT, 3-(4, 5-dimethylthiazolyl-2)-2, 5-diphenyltetrazolium bromide

IC, inhibitory concentration

PFA, paraformaldehyde

PBS, phosphate buffered saline

ORO, Oil-Red-O stock

WS, working solution

d H_2O, distilled H_2O

RT, room temperature

DAPI, 4’,6’-diamidino-2-phenylindole

GSSG, glutathione disulfide

5% SSA, 5% 5-Sulfosalicylic acid

AB, assay buffer

WM, working mixture

TNB, 5-thio-2-nitrobenzoic acid

RT-PCR, reverse transcription polymerase chain reaction

DEPC, DNA-RNAse free water

cDNA, complementary DNA

1. INTRODUCTION

1.1. Drug-induced liver injury (DILI)

DILI represents one of the most frequent adverse drug reactions (ADR) in clinical practice (1). It is also one of the most common causes of acute liver failure, and reasons for drug restriction or withdrawal from the market (2, 3). Nowadays, the extensive use of numerous drugs, multiple co-existing morbidities, polypharmacy, polypragmasy, and the development of various new drugs, all affect the effectiveness and safety of drug prescription and consumption (4). Accordingly, DILI is becoming an increasingly significant health problem in Western countries (5). DILI classification, along with its main phenotypes are summarized in Figure 1.1.

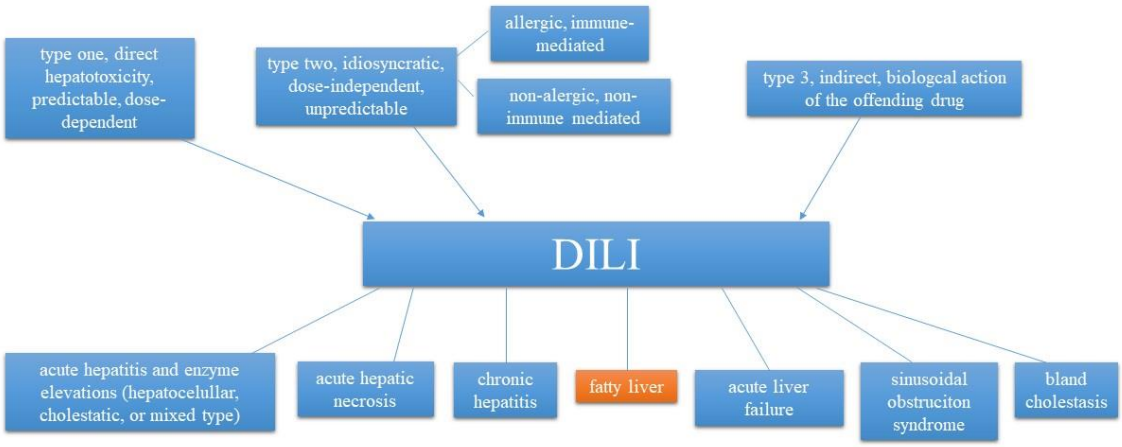


Figure 1. 1. Three main types (categories) of DILI and numerous different phenotypes, with emphasis on fatty liver, are shown in this scheme. DILI- drug-induced liver injury

Data sources: Benic et al., 2021 (6), Hoofnagle and Björnsson, 2019 (7), European Association for the Study of the Liver, 2019 (8), Kuna et al., 2018 (9)

Various interrelated factors are considered risk factors for DILI including gender, genetic factors, advanced age, drug dose, concomitant drugs, nutrition, excessive alcohol consumption, diabetes mellitus, pre-existing liver disease, kidney failure, and HIV infection (10). Due to a lack of adequate diagnostic tools, the true incidence varies significantly among studies and

populations. A temporal link between drug administration and higher levels of liver enzymes and/or alkaline phosphatase, the exclusion of other causes of liver injury, and a seldom repeated drug challenge are all used to diagnose DILI (11, 12). No standardized clinical test has been established for this condition (11, 13). In general, DILI stands for a wide range of clinical symptoms, including abnormally high liver enzymes, hepatitis, hepatocellular carcinoma cirrhosis of the liver, necrosis, cholestasis, fatty liver, and liver necrosis (14-16). The clinical symptoms of DILI, on the other hand, are not specific enough and are insufficient to differentiate DILI from other hepatic illnesses, and unfortunately, no one is immune at any age, but the risk is higher in adults (3). Cirrhosis, caused by drugs that stimulate fibrogenesis and the synthesis of extracellular matrix molecules (ECM) is known as drug-induced cirrhosis (17). Fatty liver induced by drugs (DIFLD, drug-induced fatty liver disease), as one of the phenotypes of DILI, will be discussed in further chapters in detail, especially with emphasis on non-alcoholic fatty liver disease (NAFLD).

1.2. Drug-induced fatty liver disease (DIFLD)

DIFLD is a specific type of fatty liver disease. The most prevalent histological feature of this type of DILI are steatotic changes with internal lipid accumulation in the hepatocytes (18, 19). Despite being necessary for diagnosis, this histologic finding is not specific (20). Drug-induced steatohepatitis (DISH) is the result of DIFLD which is often accompanied by oxidative stress and inflammation (21). Tamoxifen (TAM), an anti-estrogenic medication used to treat and prevent breast cancer, was found to frequently be associated with hepatic steatosis, but not cirrhosis or steatohepatitis, according to Satapathy et al. (22). They also emphasized that chronic exposure to amiodarone (AMD), 4,4'-diethylamino ethoxy hexestrol, or perhexiline maleate rarely results in cirrhosis (22-24). It is well known that phospholipidosis, which occurs after prolonged use of some medications, develops in a dose-dependent manner. But it does not result in steatohepatitis. More investigation is required to clarify the mechanisms by which drug-induced steatosis (DIS) results in steatohepatitis and, ultimately, fibrosis. (25).

Loss of hepatocytes due to chronic liver injury can be followed by activation of hepatic stellate cells (HSCs) and then fibrosis of liver tissue. Various drugs may also accelerate the development of steatohepatitis (26). In the early stages of cirrhosis, necrosis and bridging fibrosis are caused by AMD-induced acute and chronic liver injury without steatosis. (24). AMD-induced hepatotoxicity is well known to cause histological steatosis, phospholipidosis, and fibrosis. The histology in this case report showed no steatosis or phospholipidosis despite years of amiodarone use (24). This means that the diagnosis of DILI should not be ruled out

due to the lack of previously recognized histopathologic features like steatosis and phospholipidosis. It is necessary to conduct more research and confirm this conclusion. Amiodarone has been linked to the development of the potentially fatal liver condition cirrhosis in several studies (27-29). However, it was found that these side effects were relatively infrequent, occurring at a rate of 1-3 percent. Numerous researchers have argued in favor of monitoring of ongoing liver damage in high-risk patients receiving amiodarone (27, 28, 30). A cationic amphiphilic structure is present in the majority of drugs that cause steatosis and steatohepatitis (31). In the sections that follow, the effects of these drugs on liver tissue will be covered in more detail. The drugs are divided into three main categories: those that can sporadically cause steatosis/steatohepatitis, like carbamazepine, those that can independently cause steatosis and steatohepatitis, like perhexiline and amiodarone, and those that can accelerate latent non-alcoholic steatohepatitis (NASH) (18).

1.2.1. Epidemiology of DIFLD

In population-based studies, reported annual incidences of DILI have recently ranged widely from 2,7 to 19,1 cases per 100 000 (32). As a result, it is unknown how common DIFLD actually is in the general population (32). DIS and DISH are uncommon, but well-researched forms of DILI, respectively.

Around 27% of cases of DILI have some form of steatosis with histological damage, according to DILIN (Drug-Induced Liver Injury Network) (33). Only one case in the study by Kleiner et al. had the predominant pattern of microvesicular steatosis while other cases displayed both macrovesicular steatosis and inflammation (33). In the prospective study by Kleiner et al., diagnostic classification in DILIN was based on previously published descriptions of pathologic changes in DILI (33, 34). Standard hepatopathological diagnostic criteria were applied to identify injury patterns (35). Although there was a significant amount of DIFLD in these DILI cases, the pre-existing fatty liver may have distorted the DILIN prevalence. After removing diagnostic challenges and flaws in systematic reporting, the true data on DIFLD epidemiology may become more apparent.

1.2.2. Histology of DIFLD

DIFLD can manifest as DISH or as pure macro- or microvesicular DIS. Histologically, macrovesicular DIS is characterized by the buildup of large lipid vesicles (mostly triglycerides) in hepatocytes. This results in the relocation of the nucleus to the cell's periphery (33, 36). Aminotransferases are typically mildly elevated in steatohepatitis, as they are in other causes of the disease (37). Triglycerides are linked to insulin resistance development, decreased very-

low density lipoprotein (VLDL) secretion, stimulation of *de novo* lipogenesis, direct activation of transcription factors like *SREBF1* and *PPAR*, and deterioration of mitochondrial fatty acid oxidation (mtFAO) (22, 38-41). Hepatocytes that have undergone microvesicular steatosis have a lot of small lipid vesicles in their cytoplasm, but their nucleus is still present in the middle of the cell (42). Microvesicular steatosis is brought on by severe impairment of the mtFAO results in increased free fatty acids esterification into triglycerides, associated with the development of steatosis (22, 43). Hyaline Mallory bodies, lobular inflammation, balloon degeneration, and occasionally perisinusoidal fibrosis are all histopathological characteristics of steatohepatitis (18, 36, 44). Additionally, oxidative stress and increased production of reactive oxygen species (ROS) which primarily arise due to modification of the mitochondrial respiratory chain, play a significant role in DIFLD (38, 45). Drug-induced mitochondrial damage frequently leads to microvesicular steatosis (46, 47). Small fat droplets in the cytoplasm can mark this type of steatosis which can progress to macrovesicular steatosis. Macrovesicular steatosis frequently manifests as a mixture of large and small droplets. (48, 49). DIS/DISH can manifest as micro- or macrovesicular steatosis/steatohepatitis depending on the specific pathogenic mechanism of each lipotoxic drug. However, the majority begin acutely with microvesicular injury (19, 50). DIFLD may have a variable latency before clinical manifestations (19). Hepatic cell injury and liver inflammation are typically confirmed by liver biopsy for DIS/DISH diagnosis (50).

1.2.3. Risk factors for occurrence of DIFLD

Some drugs can increase the risk for developing cirrhosis or progressing from NAFLD to NASH, especially in combination with environmental and genetics factors (38). Obesity and NAFLD may increase the risk of certain drug hepatotoxicity (51). The induction of oxidative stress, decreased mtFAO, increased de novo lipogenesis, and hampered egress of very low-density lipoprotein (VLDL) from liver cells are some of the potential mechanisms by which some medications are able to speed up the progression of NAFLD (52).

Most frequently, DIFLD is a result of the direct effects of drugs on the liver, and commonly prolonged drug consumption. DISH, for instance, can result from the prolonged use of medications like amiodarone, perhexiline, and diethylaminoethyl hexestrol. Additionally, when irinotecan, tamoxifen, and methotrexate are added to therapy, additional risk factors like obesity and cardiometabolic risks are more likely to appear resulting in an exacerbation of steatosis or steatohepatitis. Steatohepatitis, NASH, or DIFLD can also result from antiepileptic drugs, steroids, and insulin resistance and hypertriglyceridemia (22). Adipose tissue dysfunction, insulin resistance, lipid aggregation, endoplasmic reticulum stress, and oxidative stress are all

associated with the progression of fatty liver injury. Additionally, fatty liver may be related to increased plasma endotoxin levels and increased gut permeability (53-55). Genetics, in addition to environmental risk factors, is a major factor in the development of simple steatosis (56). Numerous genetic, epidemiological, and twin studies have demonstrated that the risk of NAFLD is strongly inherited (56). To be effective, clinical algorithms related to the fatty liver must take into account extrinsic (environmental chemicals, alcohol, diet, and drug-drug interactions) as well as intrinsic (gender, age, ethnicity, liver, and renal condition) risk factors (57). Even though environmental risk factors are primarily responsible for the development of simple steatosis, there is mounting evidence that genes play a role in the development of NASH. There is a significant variation in phenotypic penetrance among individuals with similar risk factors, and a strong heritability of sensitivity to NAFLD has been observed in a number of studies (twin, epidemiological, and familial) (56). More research is required to better understand how genetic variations and other risk factors contribute to the development of DIFLD and NAFLD. Studies on the role of genetics in DIFLD are still in their early stages.

1.2.4. Drugs that cause DIFLD

Amiodarone, tamoxifen, glucocorticoids, methotrexate, nonsteroidal anti-inflammatory drugs, estrogens, paracetamol, metoprolol, and 5-fluorouracil, are drugs that have been shown to cause macrovesicular liver steatosis (36, 58-60). Aspirin, glucocorticoids, ibuprofen, valproic acid zidovudine, and tetracycline are among the medications linked to microvesicular steatosis (19, 42). Tamoxifen amiodarone, valproic acid, perhexiline, and propranolol are drugs linked to DISH (42, 61). It is critical to understand which specific drug can increase the risk of developing severe chronic liver disease or can cause acute liver damage on a background of fatty liver. The accumulation of fat in the liver is not always stable, and DIS/DISH are reversible (62). It is frequently unclear whether fatty liver disease is a direct result of an impact on hepatic cells or a side effect of weight gain brought on by drugs like antidepressants or antipsychotics. Drugs can be also classified according to their ability to induce acute liver injury, or progression of pre-existing non-alcoholic steatosis (NAS) to more severe stages of disease, as shown in Table 1.1.

Table 1. 1. Classification of Drugs According to Their Ability to Cause Hepatotoxicity: Acute Liver Injury or Progression of Pre-Existing Fatty Liver Disease.

Drugs capable of inducing acute liver injury	**Drugs capable of causing exacerbation of pre-existing fatty liver or NASH**	**Drugs capable of promoting transition of pre-existing fatty liver disease into NASH, fibrosis, or cirrhosis**
amiodarone, acetaminophen, aspirin, isoflurane, ibuprofen, halothane, fosipronil, valproic acid, vitamin a, tetracycline, losartan, omeprazole, troglitazone, sorafenib, telithromycin, piperacillin/tazobactam nucleoside reverse transcriptase inhibitors	tamoxifen, androgenic steroids, benzbromarone, corticosteroids, nucleoside reverse transcriptase inhibitors, rosiglitazone, tetracycline, methotrexate, phenobarbital, irinotecan	tamoxifen, corticosteroids, androgenic steroids, benzbromarone, irinotecan, methotrexate

Data sources Kolaric et al. (25) and Allard et al. (38)

1.2.5. Mechanisms of DIFLD development

Induction of oxidative stress in hepatocytes and the production of free radicals are thought to be the primary mechanisms in the development of DIFLD (42, 63). According to research by Kim et al., amiodarone increased the levels of acetylcarnitine in the short-, medium-, and long-chain acylcarnitines in the rat livers (64). The effect of amiodarone on mtFAO through blocking the activity of CPT1 enzyme (carnitine palmitoyltransferase-1) directly inhibiting the mitochondrial -oxidation of acyl-CoA to acetyl-CoA and by inhibiting complexes I and II of the MRC is the most likely cause of these disturbances in liver tissue (65, 66). Another demonstrated mechanism of amiodarone-induced DIFLD is the induction of *de novo* lipogenesis by increasing the expression of genes *SREBF1* (sterol regulatory element binding transcription factor 1c), *ACLY* (ATP-citrate synthase), *THRSP*, *SCD1* (acyl-CoA desaturase), and *FASN*, which are all involved in the process of lipogenesis (67). Additionally, Anthérieu et al. showed in vitro that amiodarone administration caused the overexpression of the *ADFP* (adipose differentiation-related protein) and *PLIN4* (Perilipin-4) genes which are involved in

the formation of lipid droplets (67). Similar to amiodarone, tamoxifen is a cationic amphiphilic substance that accumulates in liver tissue and damages the liver (31). It also affects the mtFAO and causes de novo lipogenesis (68). The upregulation of *SREBF1* and its downstream lipogenesis target genes is one potential mechanism for the induction of hepatic steatosis (19). Role of various gene pathways in steatosis development is summarized in Table 1.2. Triglyceride accumulation promotes the expression of the microsomal triglyceride transfer protein (MTP), which is connected to VLDL assembly and secretion (69). The involvement of oxidative stress in tamoxifen hepatotoxicity was supported by numerous in vivo studies. Similar to amiodarone, it lowers liver glutathione GSH levels and increases oxidized glutathione and lipid peroxidation (63, 70).

Table 1. 2. The roles of various gene pathways in steatosis development

Gene pathway	Role in liver
ACSL1	- Activates FAs destined for triacylglycerol synthesis - Channel FAs from fatty acid oxidation to lipid synthesis - Reduces FAs β-oxidation through *PPARG* pathway - Increases triglyceride levels
CEBPA	- Represses liver *FABP1* which is responsible for prevention of lipotoxicity of FAs, and regulation of FAs partition and trafficking - Increases the triglyceride levels through repression of *FABP1* - Induces apoptosis in HSC, followed by possible reduction of fibrosis
PPARG	- Enhances emergence of lipid droplets - Upregulates proteins linked to TAG storage, lipid uptake, and formation of lipid droplets, such as CD36, FABP4, perilipin 2, fat-specific protein 27 (FSP27)/Cidec, monacylglycerol O-acyltransferase 1 - Can directly affect the TGF-β1/Smad signaling pathway and decrease HSC proliferation, resulting in reduction of fibrosis
SREBF1	- Transcription factor in lipogenesis - Promotes expression of lipogenic genes such as FAS, SCD1, ACC, and lipin 1 - Induces activation of *ACSL1* expression

ACSL1- Acyl-CoA Synthetase Long Chain Family Member 1, FA- fatty acid, *CEBPA*- CCAAT/enhancer-binding protein α, FABP- fatty acid binding protein, HSC- hepatic stellate cells, *PPAR* γ- peroxisome proliferator-activated receptor gamma, TGF-β1- Transforming growth factor- β1, *SREBF1*- sterol regulatory element binding transcription factor 1c, FAS- fatty acid synthase, SCD1- Stearoyl-CoA Desaturase 1, ACC- Acetyl-CoA carboxylase

Data sources: Tingting et al. (71), Li et al. (72), Kawano et al. (73), Guzman et al. (74), Tao et al. (75), Wandrer et al. (76), Singh et al. (77), Wang et al. (78), Ni et al. (79)

Hepatocytes store methotrexate and, in particular, its polyglutamated metabolite which has hepatotoxic effects (80). Methotrexate hepatotoxic effects are thought to be caused by a number of mechanisms including prevention of folate from entering mitochondria which causes mitochondrial dysfunction, and the production of ROS, as well as induction of caspase-dependent apoptosis (53, 81, 82). Methotrexate disruption of the intestinal epithelial barrier, which results in leaky gut syndrome and the development of fatty liver injury is another potential mechanism of hepatotoxicity (31, 53). The hepatosteatotic effects of 5-fluorouracil, irinotecan, and l-asparaginase are all mediated through impairment of mtFAO and enhancement of ROS accumulation in hepatocytes (83, 84). The mtFAO is disrupted by the branched-chain fatty acid valproate which causes triglycerides to accumulate and steatosis to progress (42). In competition with other free fatty acids (FFAs), valproate in its free acid form can act as a substrate for mtFAO pathways. It conjugates with CoA once it enters the hepatic mitochondria, leading to a deficiency in CoA (42). By causing systemic insulin resistance and weight gain, long-term valproate use accelerates the progression of fatty liver disease (85, 86). It is well known that tetracycline can cause DIFLD. The inhibition of several genes involved in mtFAO, including CPT-I, peroxisome proliferator-activated receptor alpha (PPAR-alpha), and fatty acid-binding protein 1 (FABP-1), as well as the inhibition of MTP enzyme which results in the accumulation of VLDL, are thought to be the mechanisms of this toxic effect. Additionally, ROS generation is increased by the activation of transcription factor 4 AF4 which up-regulates CYP2E1 (specifically by doxycycline and minocycline) (31, 39, 87, 88). Human DNA polymerase can be inhibited by nucleoside reverse transcriptase inhibitors (NRTI) including zidovudine, didanosine, stavudine, tenofovir, and abacavir. This results in a reduction in mitochondrial DNA replication (89, 90). Oxidative stress and fat accumulation follow as a result (89, 90). Table 1.3 provides a summary of all the aforementioned mechanisms involved in DIFLD development.

Table 1. 3. Drugs That Cause DIFLD and Summary of Mechanisms Responsible for Their Toxicity.

Drugs that cause DIFLD	Proposed mechanisms
Amiodarone	-Induces de novo lipogenesis by upregulating *SCD1, PLIN4, SREBP1, THRSP, ADFP ACLY* genes' expression - Blocks mtFAO and activity of CPT1 enzyme, inhibits MRC I and II complexes, increases acetylcarnitine levels, -Decreases levels of GSH
Tamoxifen	-Induces *de novo* lipogenesis by upregulating *SREBP1c* and its downstream genes -Impairs mtFAO, -Stimulates VLDL accumulation and secretion and MTP expression -Decreases GSH levels
Methotrexate	- generally effects activity of mitochondria: generates of ROS, disrupts the intestinal epithelial barrier, hampers folate entry into mitochondria
5-Fluorouracil, irinotecan, l-asparaginase	-Impairs of mtFAO and enhances ROS accumulation in hepatocytes
Valproate	-Competes with other FFAs for mtFAO, decrease in CoA levels -Induces weight gain and systemic insulin resistance
Tetracycline	-Inhibits MTP enzyme, -Downregulates *CPTI, FABP1 and PAARα* genes' expression (all genes involved in mtFAO) -Enhances ROS generation by activating ATF4
NRTIs	-Decreases mitochondrial DNA replication -Induces oxidative stress -Inhibits human DNA polymerase γ

SCD1, acyl-CoA desaturase; *PLIN4*, perilipin-4; *SREBF1*, sterol regulatory element-binding protein 1; *THRSP*, thyroid hormone-inducible hepatic protein; *ADFP*, adipose differentiation-related protein; *ACLY*, ATP-citrate synthase; mtFAO, mitochondrial fatty acid oxidation; CPTI,

carnitine palmitoyltransferase I; MRC, mitochondrial respiratory chain; GSH, glutathione; VLDL, very low-density lipoprotein; MTP, microsomal triglyceride transfer protein; ATF4, transcription factor 4; CoA, coenzyme A; *FABP-1*, fatty acid-binding protein 1; FFA, free fatty acid; ROS, reactive oxygen species; *PAARα*, peroxisome proliferator-activated receptor α

Data from Kolaric et al. (25).

1.2.6. Current and future directions in the treatment of DIFLD

The removal of the potential offending agent is a fairly common suggestion for the management of DILI and potentially DIFLD. Up to 95% of the patients experience improvement with prompt withdrawal of the harmful drugs, but a few will still develop chronic liver disease (91). The FDA published criteria for drug withdrawal that are summed up in the following recommendations in 2009 (91, 92). ALT or AST levels higher than 3, but followed by nausea, fever, fatigue, vomiting, rash, tenderness or pain (right upper abdominal quadrant), and possibly eosinophilia; ALT or AST levels higher than 8 upper limit of normal (ULN); > 5 ULN (for a period of two weeks); > 3 ULN combined with INR > 1.5 and total bilirubin > 2 ULN (91). The dose should be changed to manage the primary disease if there is no suitable substitute for the hepatotoxic drug, especially in intrinsic DILI (91). When treating DILI and DIFLD, glucocorticoids are occasionally prescribed, but only after thorough risk-benefit analysis. Patients who exhibit significant autoimmune or hypersensitive symptoms even after drug withdrawal can benefit from them (91). In 15 DILI patients, UDCA (ursodeoxycholic acid) has been shown to have a hepatoprotective effect (including for cholangiocytes), and prevent cellular apoptosis, and stimulate hepatobiliary secretion (93). The improvement of the liver function abnormalities, the alleviation of symptoms like fatigue, pruritus, and jaundice, and the improvement of liver tests all contribute to the effectiveness of UDCA in DILI cases and may even postpone the need for liver transplantation (94-99). The protective effects of UDCA have been demonstrated in cohort studies and case reports after administration of the hepatotoxic drugs such as: chlorpromazine, cyclosporine, amoxicillin-clavulanate, ticlopidine, flucloxacillin, paraquat, and methotrexate (96, 100-104). The therapeutic effects of UDCA have been supported by individual, rare case reports. One of those is a pediatric report of toxicity of amoxicillin/clavulanic acid four years after the liver transplantation, in which UDCA showed positive effect. N-acetylcysteine (NAC), vitamins C and E, and other antioxidants ameliorated the hepatotoxic effects of amiodarone (63). Further clinical trials on humans are needed to confirm these observations.

1.3. Non-alcoholic fatty liver disease (NAFLD)

The main cause of chronic liver disease in Europe and the United States is NAFLD, a well-known disease with a high prevalence affecting a quarter of the adult population of the world. (105). Type 2 diabetes mellitus (T2DM), obesity, and genetic polymorphisms that increase susceptibility are all closely related to the prevalence of NAFLD (106). NAFLD progresses to develop into NASH in about one-third of cases. Consequently, it is estimated that between 3 and 5% of people worldwide have NASH (107). About 20% of NASH patients eventually develop cirrhosis. NASH is likely to become the leading cause of liver transplantation in the United States given the strong correlation between NAFLD and obesity and T2DM (108). When other causes of hepatic steatosis such as excessive alcohol consumption, drugs, infections, and other liver pathologies, have been ruled out, NAFLD is diagnosed if the number of liver cells that contain visible fat exceeds 5 % (109, 110). Patients are identified as having NAFLD when they exhibit the hepatic manifestation of metabolic syndrome, which is identified when three or more of the following conditions are present: high glucose, hypertension, obesity, high triglyceride levels, and low HDL (high-density lipoprotein) cholesterol (111). Non-alcoholic fatty liver, non-alcoholic steatohepatitis (NASH), cirrhosis, and cryptogenic cirrhosis are among the subtypes of NAFLD (109). Steatosis in NAFLD is caused by triglyceride accumulation in the hepatocytes. Hepatocellular damage, lobular inflammation, and hepatocyte death result from this. At this point, the illness is referred to using the term NASH. The metabolic syndrome is thought to manifest in the liver as NAFLD. When NAFLD is left untreated, it can eventually progress to NASH. The abnormalities in fat accumulation in the liver are linked to all of the etiologies of NAFLD of which the most are shown in Figure 1.2. Hepatic steatosis can be caused by a number of different factors, including increased dietary fat delivery to the liver, which may result from increased consumption of fatty foods or abnormalities in gut physiology, increased availability of FAs in adipose tissue, insulin resistance induced hyperinsulinemia which triggers *de novo* synthesis of lipids, or drugs consumption as aforementioned (112).

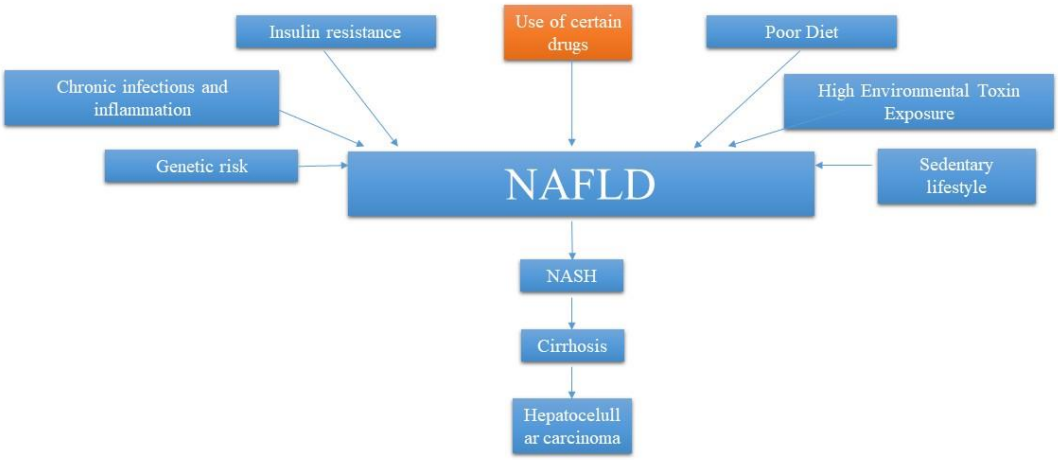


Figure 1. 2. Most common etiologies of NAFLD, and progression to more severe stages of liver disease are shown in this scheme. NAFLD- non-alcoholic fatty liver disease

Data source: Ghazanfar et al. (106)

1.4. NAFLD and DIFLD overlap

Dual etiology fatty liver disease is the term used to describe fatty liver injury that progresses as a result of preexisting NAFLD combined with drug administration (20). A growing number of clinical reports have suggested that certain medications may be more hepatotoxic in obese NAFLD patients than in lean patients (38). DILI in NAFLD manifests in two specific clinical circumstances (38, 51). First, more serious and frequent acute liver injury can be caused by antibiotics like piperacillin-tazobactam, telithromycin, and some analgesics and antipyretics like acetaminophen. It seems that some drugs such as amiodarone and statins do not frequently cause hepatotoxicity in NAFLD patients (38). Antiretroviral medications, corticosteroids, and methotrexate are examples of drugs that seem to alter or exacerbate necroinflammation, pre-existing steatosis, and fibrosis as well as simple fatty liver to NASH. (65, 83). A list of the drugs and their ability to cause or worsen fatty liver is shown in Table 1.1. Because NAFLD is associated with altered activities of metabolizing enzymes like cytochromes P450, some drugs can result in more severe acute liver injury. According to the aforementioned, NAFLD is frequently associated with higher glucuronide formation, decreased CYP3A4 activity, and increased CYP2E1 activity. These enzymes are in charge of the metabolism of drugs like acetaminophen and lorazepam. Since the mechanisms by which drugs and xenobiotics are more

hepatotoxic in NAFLD are not well understood, more *in vitro* and *in vivo* research is necessary to successfully address this issue, especially in light of the global obesity epidemic (113, 114).

1.5. *In vitro* models of NAFLD and DIFLD

Due to aforementioned significant increase in NAFLD and DILI prevalence, various *in vitro* models were established in order to better understand these diseases. Primary cell cultures, such as hepatocytes, HSCs, Kupffer cells seem to represent relevant models and mimic *in vivo* settings for the assessment of these disease (115). However, the downside of these are the ethical issues, limited number of sample of human liver, isolation problem, varying reproducibility in experiments and limited culture time (115, 116). HepG2, Huh7, H4IIE, L-02, SK-Hep-1, and HepaRG are immortalized cell lines derived from hepatocellular carcinoma that have the advantage of having a stable phenotype, an extended replicative capacity, and the ability to be grown and standardized more easily (9, 115). Other approach to study these disease involves not just hepatocytes, but also other cells involved in disease development and progression, per example co-culture models of human hepatocytes and Kupffer cells (AML-12) or macrophages (RAW 264.7) (115). This is important, especially because in order to establish reliable *in vitro* model of more severe stages of NAFLD and DIFLD (steatohepatitis, fibrosis etc.) that could be comparable to *in vivo* models, cells other than hepatocytes are needed. Therefore, hepatocyte cell cultures are most suitable for study of steatosis. As demonstrated by Gupta et al., Huh7 and Hep-G2 cells possess GLP-1 receptor, which makes the study of GLP-1 (glucagon-like peptide-1) analogs direct effects on hepatocytes possible (117). More recently, 3D culturing, per example with H35 rat hepatoma cell line, has been shown as a promising tool in study cell-to-cell cross talk in the disease progression. Its advantages are better mimicking of the *in vivo* liver architecture, and liver specific function and differentiation, but 3D cultures are difficult to cultivate, and more research is necessary to standardize it (115). Numerous drugs, as aforementioned, are capable of causing DILI and DIFLD, and their administration to cell cultures allows *in vitro* study of their effects. For establishing *in vitro* NAFLD model, palmitic and oleic acid (OA) are most often used (116).

1.6. GLP-1 analogs in NAFLD

1.6.1. GLP-1 analogs classes and mechanism of action

GLP-1 (glucagon-like peptide-1) receptor agonists, also known as incretin mimetics or GLP-1 analogs, are a class of drugs used to treat T2DM in adults. Exenatide, lixisenatide, liraglutide, albiglutide, dulaglutide, and semaglutide are a few examples of drugs in this class listed in Table 1.4.

Table 1. 4. Classification of GLP-1 analogs

Backbone	Drug	Dosing frequency
Human GLP-1	Dulaglutide	weekly
	Albiglutide	weekly
	Liraglutide	daily
	Semaglutide	weekly
Exendin-4	Exenatide extended release	weekly
	Exenatide	twice daily
	Lixisenatide	daily

Data source Costello et al. (118).

GLP-1 analogs mimic GLP-1 which is released from the foregut after meal and has a strong blood glucose-lowering effect (119). Numerous effects of GLP-1 in different organs are listed in Table 1.5. All of these actions result in decreased levels of glycated hemoglobin, weight loss, a decrease in systolic blood pressure, and improved β-cell function (119).

Table 1. 5. List of the main actions of GLP-1 in various organs.

GLP-1 analogs increase	GLP-1 analogs decrease
Neuroprotection	Appetite
Memory	Glucose production in liver
Myocardial contractility	Insulin sensitivity in liver
Heart rate	Gastric emptying
Myocardial injury secondary to ischemia	Gastric acid secretion
Glucose uptake by muscles	Pancreatic glucagon secretion
Glucose storage in muscles	β- cell apoptosis in pancreas
Insulin sensitivity in muscles	
Pancreatic insulin secretion	
Insulin biosynthesis in pancreas	
New β-cell formation	

Data source Armstrong et al. (119)

1.6.2. Hepatoprotective effects of GLP-1 analogs in NAFLD in clinical trials

Various studies have been performed to assess the direct effect GLP-1 analogs on liver and hepatocytes. Enhancement of liver function, and a decrease in liver fat content have been

confirmed by demonstration of presence of GLP-1 receptor in hepatocytes by Gupta et al. (117). The most commonly assessed GLP-1 analogs is liraglutide. Armstrong et al. conducted a study (120) to assess the effect of 48 weeks-long liraglutide (LIRA) treatment in patients with NASH (120). Results suggested that LIRA contributed to resolution of NASH, and also to a smaller extent reduced the progression to fibrosis rate (120). Other studies reported a greater decrease in AST and ALT levels together with reduction of liver fat content and body weight, in patients treated with LIRA compared to patients treated with other antidiabetic drugs (such as pioglitazone, metformin, gliclazide). This supported use of LIRA over the other agents in treatment of NAFLD (121-123). Another GLP-1 agonist with proven antisteatotic effect is exenatide. Compared to insulin and metformin, its effectiveness was greater in lowering AST, ALT, and gamma-glutamyl transferase (GGT), and also body weight (124, 125). More studies are needed to evaluate histological outcomes in NASH patients treated with exenatide. Dong et al. confirmed the possible beneficial effects of exenatide and LIRA in treatment of patients with biopsy proven NASH (126). Newer GLP-1 analog, semaglutide, showed a significant effect in body weight reduction, improved glycemic control, decreased ALT and other markers of inflammation, and cardiovascular risk in overweight and T2DM patients (127-131). Capehorn et al. compared the safety and efficacy of semaglutide vs LIRA in patients with T2DM, and showed a greater effect of semaglutide on reduction of body weight and HbA_{1c}, with higher rates form gastrointestinal adverse effect (128). However, more studies are needed to assess its effect on liver fat content and possible role in NAFLD treatment.

1.6.3. Hepatoprotective effects of GLP-1 analogs in NAFLD in animal and *in vitro* models

Li et al. demonstrated *in vivo* and *in vitro* the beneficial effects of exenatide in NAFLD animal model and related cell culture model (132). Exenatide significantly reduced the body weight, AST, and ALT, total cholesterol, low-density lipoprotein, and FAs in high fat diet (HFD)-induced obese rabbits (132). Also, exenatide significantly reversed the HFD-induced lipid accumulation and inflammatory changes that were accompanied by decreased fat mass and obesity associated gene (FTO) mRNA and protein expression according to histological analysis.

Møllerhøj et al. showed therapeutic benefits of semaglutide in NASH mice model (133). Semaglutide improved steatosis scores, reduced number of lipid-laden hepatocytes, the number of inflammatory loci, and the expression of galectin-3 (inflammation marker particularly produced by activated macrophages) (133).

Numerous effects in liver make LIRA a most promising GLP-1R agonist for NAFLD prevention and/or treatment. These include a decrease in lipid over-accumulation by upregulating autophagy, decrease in oxidative stress and apoptosis of liver cells, reduction in activation and proliferation of HSCs through RAGE/NOX2, adjustment of lipid metabolism via SHP1/AMPK/SREBF1 signalling pathway, reduction in lipotoxicity-induced oxidative stress, possibly by modulation of NRF2, decrease in expression of main elements involved in peroxisomal b-oxidation (*ACOX1*), lipogenesis (phospho-ACC), and lipid flux/storage (*PPARG*) (134-139). Considering the role of the *SREBF1* and *PPARG* signalling pathways in NAFLD and DIFLD development, and hepatoprotective action of LIRA, analysis of their expression, and expression of other signalling pathways connected to them (such as *ACSL1*) could help better understand their effects on hepatocytes (73, 138, 139).

2. HYPOTHESIS

GLP-1 analogs reduce liver injury in a cell model of drug-induced fatty liver disease.

3. RESEARCH OBJECTIVES

The main objectives of this study were:

1. To establish a human liver, Huh7, cell culture model of hepatocyte steatosis that occurs in drug-induced fatty liver disease (DIFLD) by incubation with amiodarone and tamoxifen.
2. To establish a human liver, Huh7, cell culture model of hepatocyte steatosis that occurs in non-alcoholic fatty liver disease (NAFLD) by incubation with fatty acids.
3. To measure the hepatotoxic effect of amiodarone and tamoxifen, and the protective effect of GLP-1 analogs in the DIFLD model by determining cell survival compared to the NAFLD model.
4. To measure the hepatotoxic effect of amiodarone and tamoxifen, and the protective effect of GLP-1 analogs in the DIFLD hepatocyte steatosis model by microscopic visualization and Oil-Red-O staining, compared to the NAFLD hepatocyte steatosis model.
5. By measuring triglyceride levels, evaluate the effects of amiodarone, tamoxifen, and GLP-1 analogs on fat accumulation in Huh7 cells, compared to the NAFLD hepatocyte steatosis model.
6. To determine the expression level of genes involved in the process of lipogenesis and mitochondrial dysfunction in the DIFLD hepatocyte steatosis model after treatment with amiodarone and tamoxifen and GLP-1 analogs using RT-PCR method.
7. To investigate the correlation of expression of genes involved in the process of lipogenesis and mitochondrial dysfunction with cell survival parameters and the amount of triglycerides and GSH in the DIFLD hepatocyte steatosis cell culture model.

4. MATERIAL AND METHODS

4.1. Study design

The study was designed as a randomized controlled trial. Experiments were conducted in two series. First series of experiments included twelve groups of cells: group A, Huh7 cells grown in DMEM as a negative control; groups B-D, Huh7 cells treated with increasing concentrations of LIRA (5, 10, and 20 nM), groups E cells treated with OA, groups F-H Huh7 cells treated with OA and increasing concentrations of LIRA, group I Huh7 cells treated with 20 μM AMD, groups J-L Huh7 cells treated with AMD and increasing concentrations of LIRA. Second series of experiments included 5 groups of cells: cells treated with 2 μM TAM, and Huh7 cells treated with TAM and increasing concentrations of LIRA.

4.2. Material

4.2.1. Chemicals

Amiodarone, sodium oleate, and Oil-Red-O were purchased from Sigma-Aldrich (St. Louis, MO, USA), tamoxifen was purchased from Acros Organics (New Jersey, USA), liraglutide (Victoza) was purchased from Novo Nordisk (Denmark).

4.2.2. Cell culture

Prof. George Y Wu, University of Connecticut Health Centre in Farmington, United States of America generously provided us with a Huh7 cell line. Huh7 cell line is an immortal cell line composed of epithelial-like tumorigenic cells and established from a well-differentiated hepatocyte-derived cellular carcinoma cell line (its origin is a liver tumor from a male patient). Cells were sub-cultivated in 10 cm dishes in Dulbecco's Modified Eagle's medium (DMEM) supplemented with 10% fetal bovine serum (FBS/ Thermo Fisher Scientific Cat. No. 16000036) and 1% penicillin/streptomycin solution (Thermo Fisher Scientific Inc., Waltham, MA, USA) at 37°C in a humidified atmosphere of 5% CO_2 v/v in air.

Thawing and culturing cells protocol:

1. Tubes with frozen cells were taken from a liquid nitrogen tank.
2. These tubes were defrosted for 2 minutes in the water bath heated up to 37°C.
3. The defrosted cell suspension was transported by sterile pipette into 9 ml of growth medium in the Falcon tube.
4. The cell suspension was centrifuged at room temperature at 140 x g for 4-minutes.
5. Supernatant was discarded and cells were resuspended in 3 ml of pipetted fresh medium.

6. 10 µl of cell suspension was mixed with the same volume of Erythrosin B color solution (ratio 1:1, viable cells remained colorless, protocol explained further in text), counted in the Neubauer chamber, cell concentration was calculated, and cell suspension was diluted to obtain the final concentration of 100 000 cells/ml.
7. Diluted cell suspension was transferred to 100 mm Petri dish.
8. The next day the growth medium was replaced with the same volume of a fresh medium.
9. Cells were grown to 75-85% confluence and passaged every 3-4 days.
10. After reaching the required confluent state, cells were detached from the surface using trypsin. First, cell medium was removed, then 3 ml of trypsin per Petri dish was added, afterwards cells were incubated in above described conditions in the incubator for 3 minutes.
11. 3 ml of a fresh growth medium was added to trypsin/cell suspension to block the enzyme, and everything was transferred to a sterile Falcon tube, centrifuged at room temperature at 140 x g for 4-minutes.
12. The supernatant was removed and the cell pellet was resuspended in 10 ml of a fresh medium and added to the new plates.
13. Cells were counted in the Neubauer chamber to obtain the final concentration of 150 000 cells/mL and cell suspension was transferred to the Petri dish.

4.2.3. Drugs and oleic acid preparation

Amiodarone hydrochloride and TAM were dissolved in dimethyl sulfoxide (DMSO) to 10 mM concentration, and stock solutions were stored at -20°C. Finally, AMD was prepared in five different concentrations (5 µM, 10 µM, 20 µM, 40 µM, 80 µM), TAM was prepared in four different concentrations (0,5 µM, 1 µM, 2 µM, 4 µM,). Oleic acid (OA) stock solution was prepared by dissolving sodium oleate powder in 6% bovine serum albumin (BSA) to 200 mM concentration and homogenized with an ultrasonic homogenizer (Bandelin Sonoplus 2070) for 15s. OA was diluted to the final concentration of 0,5 mM (working solution, WS). LIRA original stocks (concentration 6 mg/ml, 1,5996 mM) were kept at -20°C. For experiments, LIRA WS were prepared in three different concentrations (5 nM, 10 nM, 20 nM). To obtain the studied concentrations, all these agents were finally dissolved in DMEM without FBS.

4.3. Methods

4.3.1. NAFLD and DIFLD cell culture models

Huh7 cells were cultured as previously described and grown overnight in a 96-well plate at density $2x10^5$ cells/cm^2. Cells incubated only in medium without FBS were used as a negative control. Cells were exposed to increasing concentrations of OA, AMD, and TAM for 24 h for up to 72 h in triplicates, respectively. To determine the effect of drugs on cell viability an MTT (3-(4, 5-dimethylthiazolyl-2)-2, 5-diphenyltetrazolium bromide) assay was used and the results were read on a microplate reader (iMarkTM Microplate Absorbance Reader; Bio-Rad, Hercules, California, USA). The MTT assay is a colorimetric assay for evaluating cell metabolic activity and proliferation. Conversely, when metabolic events lead to apoptosis or necrosis, the reduction in cell viability can be determined by MTT. Metabolically active cells reduce the yellow tetrazolium MTT, in part by the action of dehydrogenase enzymes, to generate reducing equivalents such as NADPH and NADH (140). The resulting intracellular purple formazan can be solubilized, and the absorbance of this colored solution quantified by measuring at a certain wavelength (usually between 500 and 600 nm) by a spectrophotometer (140). MTT stock solution was prepared as follows: 100 mg of tetrazolium bromide powder (Cruz chemicals, Dallas, Texas, USA) was dissolved in 20 mL of 1×PBS, followed by sterilization of solution using 0,2 μm syringe PES filter (Nalgene ™ Thermo Fisher Scientific Waltham, Massachusetts, United States. Aliquots (1 mL) were frozen at -20 °C and protected from the UV light. At the end of the experiment 10 μl of MTT solution was added to each well resulting in a 0,5 mg/ml concentration of MTT. Cells were incubated for 4 hours in an incubator (above-mentioned conditions) resulting in the clearly visible purple precipitate. 100 μl of MTT solvent (0,04 M HCl in isopropanol) was pipetted into each well and by repeated pipetting in and out formazan purple crystals were dissolved (140). Absorbance was read at 595 nm on a microplate reader. Absorbance values that are lower compared to the control cells (set as 100%) signify a reduction in the rate of cell proliferation (expressed as a percentage of control). The optimal concentration IC_{20} (inhibitory concentration which induces 20 % cytotoxicity) and time period for further experiments were then selected as follows: 0,5 mM OA (for NAFLD model), 20 μM AMD, and 2 μM TAM (for DIFLD models), and time period of 24 h of incubation.

These results were also confirmed by the Erythrosin B color exclusion test and Neubauer Hemocytometer counting. According to previous protocol, the cells were grown overnight and treated with toxic drugs and oleic acid in 24-well plates. At the end of the experiment, cells were trypsinized and cell viability was determined using Erythrosin B color exclusion test and

Neubauer Hemocytometer counting. Live cells possess intact cell membranes that exclude certain dyes including Erythrosin B, whereas dead cells do not (141). A cell suspension (after trypsinization) was simply mixed with the dye (10 µl of cell suspension and 10 µl of dye), and pipetted on the hemocytometer. Cells were counted using a hemocytometer (a device that consists of a thick glass microscope slide with a rectangular indentation that creates a chamber) placed on the stage of the light microscope. Clear cytoplasm is present in viable cells whereas dead cells have a red cytoplasm. Finally, the concentration of viable and dead cells was calculated using this equation: total viable cells (ml)= total viable cells counted x dilution factor/number of squares x 10000 (cells/ml).
The results were expressed as a percentage relative to negative control (set as 100%) of at least three independent experiments.

4.3.2. Measurement of the Hepatoprotective Effect of LIRA in NAFLD and DIFLD Cell Culture Models

LIRA workings solutions were added as a co-treatment to the abovementioned NAFLD and DIFLD models. First, the cells were grown overnight in 96 well and 6- well plates at a density of $2x10^5$ cells/cm^2. The cell groups for the determination of the hepatoprotective effect of LIRA were designed as explained earlier in 4.1. Study design section. After 24 h of incubation, cell survival and viability were determined by MTT colorimetric assay and Erythrosin B color exclusion test as described above. Results were expressed as a percentage relative to the negative control of at least three independent experiments.

4.3.3. Visualization of fat accumulation

After incubating and treating cells in 24-well plates with cover slides, previously prepared following the protocol by Zjalic et al. (142) and coated with poly-D-lysine (Sigma Aldrich, St. Louis, MO, USA), as described above, medium was pipetted out, and 1 ml of 4 % paraformaldehyde (PFA, cooled at 4°C) per well was added. After fixing the cells for 30 - 45 min at 4 °C, fixative was removed and cells were rinsed twice with cooled phosphate buffered saline (PBS). PBS was removed and cells were allowed to air dry. Meantime, previously prepared Oil-Red-O stock (ORO, 0,5 % ORO stock consists of 0,5 g ORO diluted in 100 ml of 99% isopropanol, kept at 4 °C in aluminium foil) was used to prepare ORO WS. ORO was mixed at 6:4 ratio with distilled H_2O (dH_2O) and let stand for 10 min (WS is stable for no longer than 2 hours). ORO (ChemCruz, Huissen, The Netherlands) is a lysochrome (fat-soluble dye) diazo dye used for staining of neutral triglycerides and lipids in different tissue samples. It has the appearance of a red powder with maximum absorption at 518 (359) nm. 0,2 micron syringe

filter was used to add ORO to cells (1 ml/well). ORO was left at room temperature (RT) for 10 min, then removed from the wells. After rinsing two times with PBS, cells were mounted in the fluorescent mounting medium with 4',6'-diamidino-2-phenylindole (DAPI) (Abcam, Cambridge, UK). The cells were visualized using a microscope (Axioskop 2 MOT Inverted microscope, Carl Zeiss, Göttingen Germany) with an Olympus D70 camera, controlled through the computer program DP Manager 1.2.1.107 and DP Controller 1.2.1.108. Lipids appeared red and the nuclei appeared blue. ImageJ-Fiji software was used to count cell nuclei and measure integrated density relative to the cell count.

4.3.4. Measurement of triglyceride levels

The cells were incubated and treated as described above in 6-well plates, and on the second day of experiment the accumulation of triglycerides in cells was measured by Triglyceride GPO - PAP method (Glycerol 3 phosphate oxidase - 4-Amino-antipyrine, Greiner Diagnostic, Bahlingen, Germany). On the last day of experiment, medium was pipetted out of the wells, and 1 ml per well of TG GPO-PAP was added. Cell scraper was used to detach cells from the surface, and suspensions were transferred to 1,5 ml. All tubes were vigorously vortexed for at least 5 seconds, and then incubated at 37 ºC in the incubator for 15 minutes. Afterward, samples were centrifuged at 1000 g RT for 5 minutes. 200 µl per well of each supernatant was transferred to wells in 96-well plate. Standards were prepared as serial dilutions (original stock 200 mg/dl as first standard, 200 µl of this stock was transferred to first tube- S1, 100 µl was pipetted to other tube and mixed with 100 µl PBS (S2) until the final S6 (62,5 mg/dl). 5 µl of each standard was transferred to wells in 96-well plate, and mixed with 200 µl of TG GPO-PAP reagent. Finally, absorbance was read on a microplate reader (wavelength 492-550). Triglyceride standards were used in order to quantify absolute concentration of triglycerides. Results were expressed as absolute values (mg/dl).

4.3.5. Measurement of Cellular Glutathione (GSH) Concentration

GSH in its reduced form (90-95 % of total GSH) represents the major free thiol in most living cells. Its role is significant in various biological processes such as detoxification of xenobiotics, maintenance of the oxidation state of protein sulfhydryls, and removal of hydroperoxides (143). Glutathione disulfide (GSSG) is a product of oxidation of GSH. Therefore, intracellular GSH status represents an indicator of the overall health of a cell, and of its ability to resist toxic challenge (144). The cells were incubated and treated as described above in 6-well plates, and on the second day of experiment the level of total glutathione in 12 groups of cells was measured by ELISA using a commercially available Glutathione Assay Kit (Sigma-Aldrich, Saint Louis,

MO, SAD) according to manufacturer's instructions and as briefly described by our group earlier (145). At the end of the experiment, cells were scraped from the dish surface, and 2 ml of cells in medium were pipetted into 2 ml tubes. Afterward, cells were centrifuged at 140 x g for 7 minutes at 4 ºC to remove the precipitated protein. Supernatants of the samples were discarded and pellets were resuspended in 1 ml of ice-cold 1xPBS/tube, centrifuged at 600 x g for 5 minutes at 4 ºC and the supernatant was discarded. Volume of the pellet was then measured, and 3 volumes of the 5% SSA (5 % 5-Sulfosalicylic acid) solution were added to the packed cell pellet, each tube was vortexed for 5-10 s, freeze and thawed twice (frozen at -80 ºC for 5 minutes and thawed at 37 ºC for 6 min), and left for 5 minutes in the refrigerator. The extract was then centrifuged at 10 000 x g for 10 minutes, 50 µl of supernatant was transferred to the 0,2 ml microcentrifuge tubes, and stored at 2-8 ºC before the next step (if the assay could not be performed within 2 hours, the content was stored at -70 ºC for up to 7 days).

Working solutions were prepared as described below (the volumes for 48 reactions of 200 µl performed in 96 well plate):

1x Assay Buffer (AB)- 2,4 ml of 5x AB was diluted five-fold by addition of 9,6 ml of distilled water

Enzyme Solution- 3,8 µl of Glutathione Reductase was diluted with 1x AB to a final volume of 250 µl

NADPH Solution- 10 µl of NADPH Stock Solution (25 mg of NADPH was dissolved in 0,625 ml of distilled water) was added to 2,5 ml of 1x AB

Working Mixture (WM) - 228 µl of the Enzyme Solution, and 228 µl of DTNB Stock Solution (8mg of DTNB was dissolved with 5,33 ml of DMSO) was added to 8 ml of 1x AB, and mixed well.

Glutathione Standard Solutions- GSH Stock Solution (10mM) was 200-fold diluted to 50 µM solution in 5% SSA. This was Standard 1 (S1), and S2-S5 were prepared by serial dilutions of the 50 µM S1 glutathione Solution in 5% SSA, to the final concentrations as follows: S2- 2 µM, S3- 12,5 µM, S4- 6,25 µM, S5 3,125 µM.

Finally, 5 µl of 5% SSA, 5 µl of sample/standard, and 150 µl of WM were added to each well on the 96-well plate (blank consisted of 150 µl WM and 10 µl of 5% SSA), incubated at RT for 5 minutes, and then 50 µl of NADPH Solution was added to each well and mixed by pipetting up and down.

Response is measured as intensity of yellow product, 5-thio-2-nitrobenzoic acid (TNB), which is a result of following reactions:

2 GSH+DTNB→GSSG + 2 TNB

GSSG+NADPH+H^+→ (Glutathione reductase) 2 GSH + $NADP^+$

The combined reaction:

DTNB+H^++NADPH→(Glutathione reductase/GSSG/GSH) **2 TNB** + $NADP^+$

Absorbance was measured at 412 nm using a microplate reader (iMarkTM Microplate Absorbance Reader; Bio-Rad, Hercules, California, USA). Results were expressed as percentage compared to untreated controls.

4.3.6. Total RNA isolation and Reverse Transcription Polymerase Chain Reaction (RT-PCR) analysis

To evaluate the expression of various genes (*ACTB, SREBF1, CEBPA, PPARG, ACSL1*), total RNA from cells, prepared as previously described in 6-well plates, was isolated on the third day of experiment using NucleoZOL (Macherey-Nagel, Valencienner Str. 11, 52355 Düren, Germany) according to the manufacturer's protocol. Firstly, cells were homogenized with 500 µl NucleoZOL per well. Afterward 200 µl of DNA-RNAse free water (DEPC) was added to the lysate, mixed vigorously for 15s, incubated for 5 min at RT, and centrifuged for 15 min at 12000 g in order to precipitate contaminants. 500 µl of the supernatant was then transferred to a new tube, mixed with 500 µl of 100% isopropranol, incubated for 10 min at RT, and centrifuged for 10 min at 12000g in order to precipitate total RNA. Supernatant was discarded, and 500 µl of 75% ethanol was added to the pellet, centrifuged for 3 min at 8000 g, and supernatant was discarded again. This washing procedure was repeated, and finally RNA pellets were dissolved in 30 µl of DEPC-water by vortexing at RT for 3 min. RNA concentration and purity of samples were determined by measuring absorbance on a NanoPhotometer® P-Class P330-30 spectrophotometer (Implen GmbH, Munich, Germany) at wavelengths of 260 nm and 280 nm. cDNA strand was synthesized using a commercially available kit (High Capacity cDNA Reverse Transcription Kit, Applied Biosystems, Thermo Fisher Scientific Inc., Waltham, MA, USA) according to the manufacturer's instructions in reaction mixtures with a total volume of 20 µl on a DNA Engine® Thermal Cycler device (Bio-Rad, Hercules, California, USA). The resulting cDNA was stored at -20 °C until preparation for PCR. The reaction mixtures for cDNA and PCR synthesis are listed in Table 4.1., and the PCR reaction

conditions are listed in Table 4.2. A commercially available kit (Taq PCR Core Kit, Qiagen, Hilden, Germany) was used to amplify the obtained cDNA using a PCR device. The synthesized cDNA was amplified using specific primer sequences as shown in Table 4.3. As an internal control to determine the possible presence of different cDNA concentrations *ACTB* was used. PCR results were visualized on a 1,7 % agarose gel stained with Diamond™ Nucleic Acid Dye (Promega, Madison, WI, USA) according to the manufacturer's instructions, visualized by Gel Imaging System (ChemiDocTM Imaging System, Bio-Rad, Hercules, California, USA), and semi quantified by ImageJ software (version 5.2.1. build 11, BioRad, Hercules, CA, USA) using QuantIF ImageJ macro (normalized to the *ACTB* mRNA levels). Results are shown as percentages compared to the negative control of at least three independent experiments.

Table 4. 1. Reaction mixtures for Reverse Transcription and PCR (total volume 20 µl)

Reverse Transcription		**PCR**	
Component	Volume per sample (µl)	Component	Volume per sample (µl)
10 RT Buffer	2	10X PCR Buffer (Qiagen+1.5 mM Mg)	2
25x dNTP Mix	0,8	5’ oligo (10 µM)	0,5
10x RT Random Primers	2	3’ oligo (10 µM)	0,5
Multiscribe RT	1	4 dNTP mix (Qiagen 10 mM each	0,4
Nuclease-free Water	4,2	Taq polymerase (Qiagen 5 U/µl)	0,1
		Nuclease-free Water	15,5

Table 4. 2. PCR conditions for amplification of various genes.

Gene	**denaturation**	**annealing**	**elongation**

ACTB	94 °C for 3 min	56.7 °C for 45 s	72 °C for 1 min in 30 cycles
ACSL1	94 °C for 3 min	61 °C for 45 s	72 °C for 1 min in 30 cycles
CEBPA	94 °C for 3 min	61 °C for 45 s	72 °C for 1 min in 30 cycles
PPARG	94 °C for 3 min	61 °C for 45 s	72 °C for 1 min in 30 cycles
SREBF1	94 °C for 3 min	61 °C for 45 s	72 °C for 1 min in 30 cycles

ACSL1- Acyl-CoA Synthetase Long Chain Family Member 1, *CEBPA*- CCAAT/enhancer-binding protein α, *PPARG*- peroxisome proliferator-activated receptor gamma, *SREBF1*- sterol regulatory element binding transcription factor 1c

Table 4. 3. Primer sequences used for RT (Reverse transcription)-PCR.

Gene	**Primer sequences (5'-3')**
ACTB	Forward GCACCACACCTTCTACAATG Reverse TGCTTGCTGATCCACATCTG
ACSL1	Forward GGAGTGGGCTGCAGTGAC Reverse GGGCTTGCATTGTCCTGT
CEBPA	Forward CGCCTTCAACGACGAGTTCCTG Reverse CGCCTTGGCCTTCTCCTGCT
PPARG	Forward ACCAAAGTGCAATCAAAGTGGA Reverse ATGAGGGAGTTGGAAGGCTCT
SREBF1	Forward CGGAACCATCTTGGCAACAGT Reverse CGCTTCTCAATGGCGTTGT

ACTB- actin beta, *ACSL1*- Acyl-CoA Synthetase Long Chain Family Member 1, *CEBPA*- CCAAT/enhancer-binding protein α, *PPARG*- peroxisome proliferator-activated receptor gamma, *SREBF1*- sterol regulatory element binding transcription factor 1c. (69, 146)

4.3.7. Statistical analysis

The statistical program Statistica 12 (Tibco, Palo Alto, California USA) was used for statistical analyses. Statistical analyses were performed using One-way ANOVA with Post-hoc Tukey HSD, and Two-way ANOVA. p-values of $p < 0,05$, $p < 0,01$, and $p < 0,001$ were considered statistically significant. When the post-hoc test required, the Bonferroni correction was performed. Normality of data distribution was determined with Shapiro-Wilk test. T-test was used to determine the significance of the difference between the two samples in the case of a normal distribution of results in the population. The option of t-test type depended on the size and whether the samples were dependent or independent. The conclusion about the differences between the two independent continuous random variables distributions was based on the Mann-Whitney-Wilcoxon test if the distribution of the results was not normal. In the case of more than two samples, and depending on the nature of the results, parametric or nonparametric analysis of variance (ANOVA) was used. Friedman test was used for multiple dependent samples and the Kruskal-Wallis test was used as a nonparametric analysis for multiple independent samples. Statistics applies to all of these experiments. A sample in minimal biological triplicate was used for each statistical analysis.

5. RESULTS

5.1. Establishment of the Cell Culture Model of DIFLD and NAFLD, and Assessment of the Effect of Oleic Acid, Amiodarone, and Tamoxifen on the Cell Viability

The toxic effect of OA, AMD and TAM on the viability of Huh7 cells was investigated using the MTT assay after treatment with two different concentrations of OA (0,5, and 1 mM), five different AMD concentrations (5, 10, 20, 40 and 80 μM), four different TAM concentrations (0,5, 1, 2, 4 μM) and at different time periods (24 h, 48 h, 72 h). Each experiment was repeated at least three times to ensure consistency of results. IC_{20} were 0,5 mM OA, 20 μM AMD and 2 μM TAM at 24 h incubation. Cells treated with higher concentrations of AMD experienced a greater decrease in cell viability with only 30% viable cells compared to the negative control as determined by the MTT assay shown in Figure 5.1. ($p < 0,001$). Incubation of the cells for a longer period of time also resulted in a significant decrease in cell viability at lower AMD concentrations, as shown in Figure 5.1 ($p < 0,001$). These results were mostly confirmed with Erythrosin B exclusion test where cell survival decreased with AMD treatment in dose and time dependent manner as shown in Figure 5.3. ($p < 0,001$), whereas the effect of OA on cell survival was insignificant comparing to the one observed with MTT assay.

Higher concentrations of TAM did not have a significantly greater effect on cell viability, but a longer incubation period of 48 hours resulted in significant reduction in cell viability compared to the negative control, as shown in Figure 5.2. ($p < 0,001$). These results were confirmed by Erythrosin B exclusion test (Figure 5.4.). According to the MTT results, the concentrations of 0,5 mM OA, 20 μM AMD and 2 μM TAM at 24 h exposure time were selected as Huh7 model for NAS and DIS for all subsequent experiments.

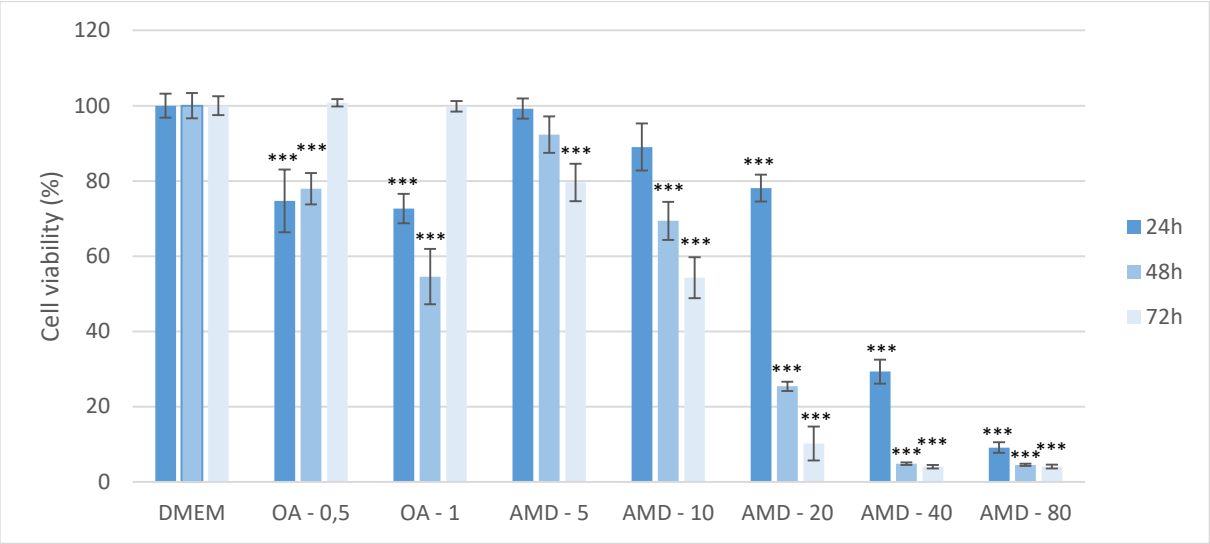


Figure 5. 1. Determination of cell viability by MTT assay after exposure to varying amiodarone (AMD) and oleic acid (OA) concentrations and varying time periods in the Huh7 cell line. MTT measurements were done by absorption spectrophotometry at 595 nm. Results are shown as a percentage relative to the negative control from at least three independent experiments. Two-way ANOVA Time period F (2,71) = 88,8; $p = 7{,}41 \times 10^{-17}$, Treatment F (7,71) = 741,1; $p = 1{,}23 \times 10^{-46}$; post-hoc Tukey HSD. Bars assigned with asterisks are statistically significantly different (*** $p < 0.001$) compared to the negative control. Dulbecco's Modified Eagle's Medium (DMEM), oleic acid (OA/mM), amiodarone (AMD/µM)

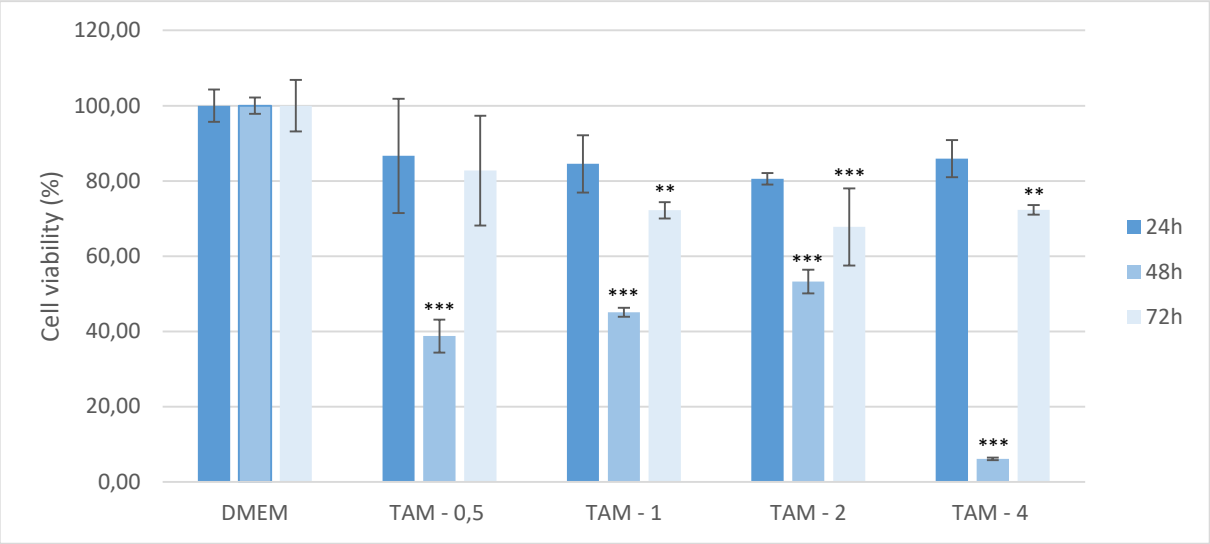
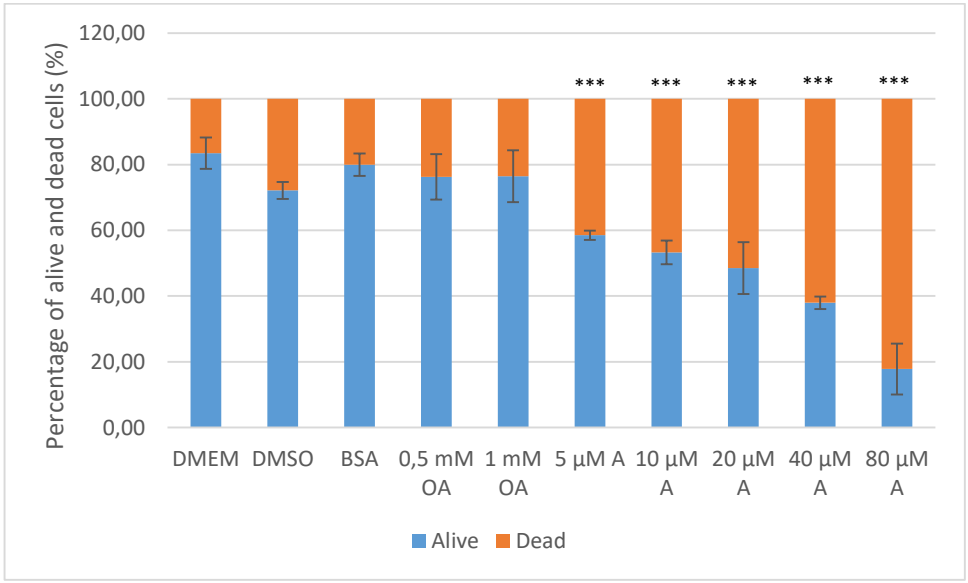
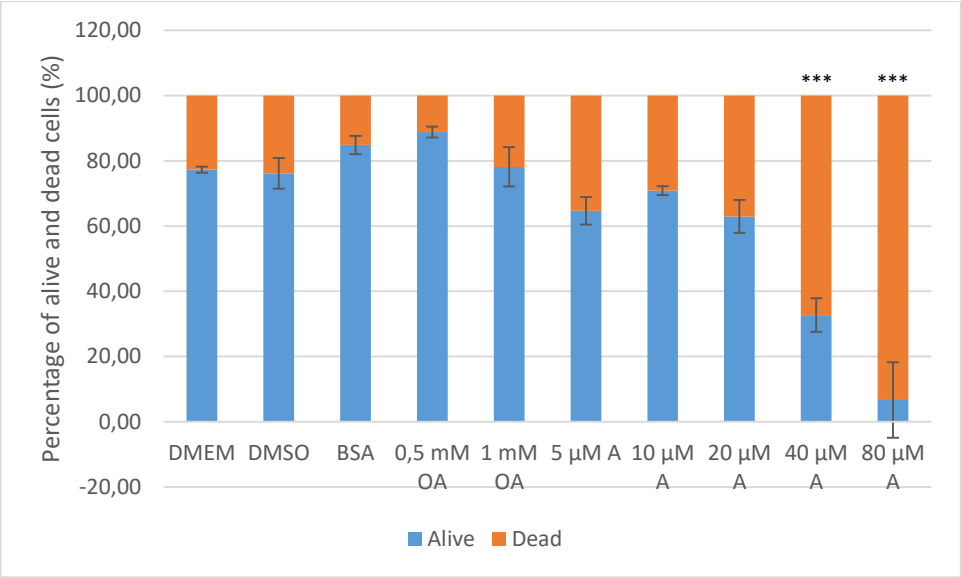


Figure 5. 2. Determination of cell viability by MTT assay after exposure to varying tamoxifen (TAM) concentrations and varying time periods in the Huh7 cell line.

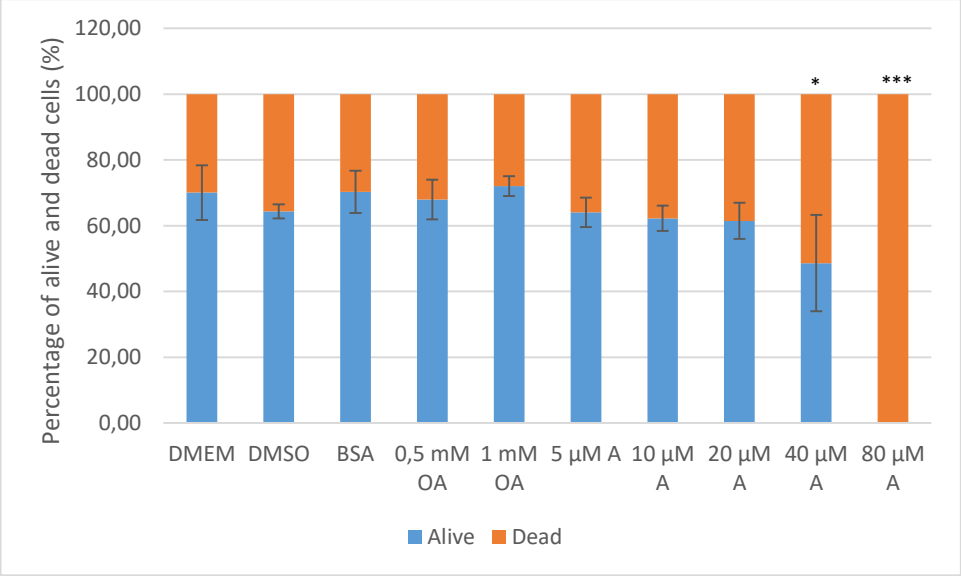
MTT measurements were done by absorption spectrophotometry at 595 nm. Results are shown as a percentage relative to the negative control from at least three independent experiments. Two-way ANOVA Time period F (2,44) = 127; $p = 2{,}27 \times 10^{-15}$, Treatment F (4,44) = 51,64; $p = 4{,}98 \times 10^{-13}$; post-hoc Tukey HSD. Bars assigned with asterisks are statistically significantly different (** $p < 0{,}01$, *** $p < 0{,}001$) compared to the negative control. Dulbecco's Modified Eagle's Medium (DMEM), tamoxifen (TAM/µM)



(a)



(b)



(c)

Figure 5. 3. Cell survival after exposure of cells to varying amiodarone (AMD) and oleic acid (OA) concentrations and varying time periods in the Huh7 cell line.

Determined by the Erythrosin B color exclusion test 24, 48, and 72 h after treatment; significance was analyzed on data regarding dead cells and compared to the negative DMEM control. Figure 5.3.a. Cell survival after 24 h of exposure to AMD and OA. One-way ANOVA $F(9,29) = 46{,}79$, $p = 1{,}74 \times 10^{-11}$ with Tukey HSD post-hoc test; ***$p < 0{,}001$. The data shown are representative of at least three independent experiments. Figure 5.3.b. Cell survival after 48 h of exposure to AMD and OA. One-way ANOVA $F(9,29) = 71{,}56$, $p = 3{,}05 \times 10^{-13}$ with post-hoc Tukey HSD test; ***$p < 0{,}001$. The data shown are representative of at least three independent

experiments. Figure 5.3.c. Cell survival after 72 h of exposure to AMD and OA. One-way ANOVA F (9,29) =31,48, $p=6,48\times10^{-10}$ with post-hoc Tukey HSD test; *p<0,05 ***p<0,001. The data shown are representative of at least three independent experiments. Dulbecco's Modified Eagle's Medium (DMEM), dimethyl sulfoxide (DMSO), bovine albumin serum (BSA), oleic acid (OA/mM), amiodarone (AMD/µM)

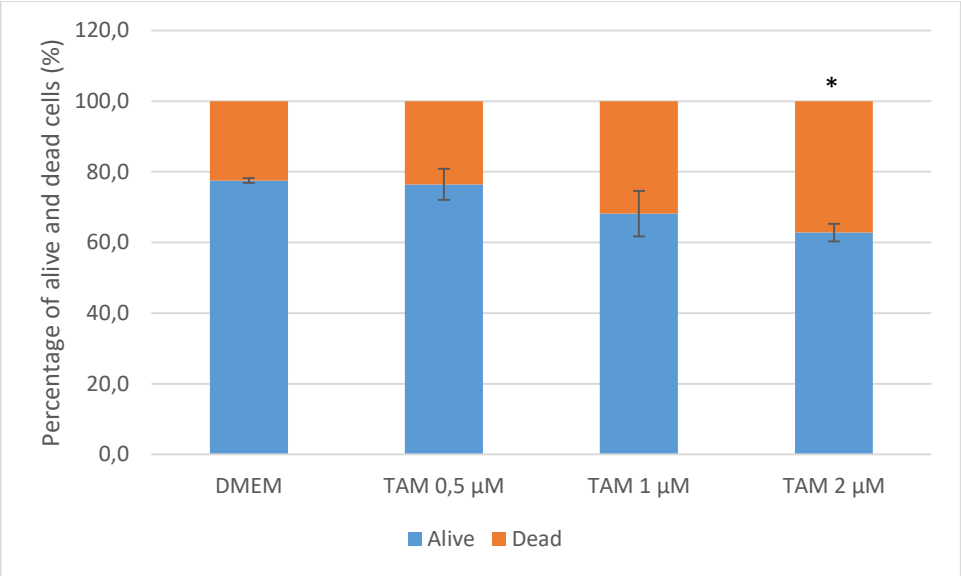


Figure 5. 4. Cell survival after exposure of cells to varying tamoxifen (TAM) concentrations in the Huh7 cell line.

Determined by the Erythrosin B color exclusion test 24 h after treatment; significance was analyzed on data regarding dead cells compared to the negative DMEM control. One-way ANOVA F (3,11) =8,769, $p= 6,56x10^{-03}$ with post-hoc test Tukey HSD; *p<0,05. The data shown are representative of at least three independent experiments. Dulbecco's Modified Eagle's Medium (DMEM), tamoxifen (TAM/µM)

5.2. Measurement of the Effect of Liraglutide in NAFLD and DIFLD Cell Culture Models on the Cell Viability

To evaluate protective effect of LIRA in NAFLD and DIFLD cell culture models, three different concentrations of LIRA (5, 10, and 20 nM) were used as shown in Figures 3.a. and 3.b. Cell viability was determined, and compared to negative control, and to cells treated with OA, AMD, and TAM. In the cells treated with OA (NAFLD model), 5 nM LIRA significantly increased cell viability ($p < 0,01$), whereas higher LIRA concentrations had the opposite effect. All three concentrations of LIRA increased cell viability in the DIFLD models (cells treated with AMD and TAM) but without statistical significance, as shown in Figures 5.5. and 5.6. These results were confirmed with Erythrosin exclusion test, but in AMD DIFLD

significant increase in cell viability with LIRA co-treatment was observed ($p < 0,05$, $p < 0,01$) (Figure 5.7. and 5.8.).

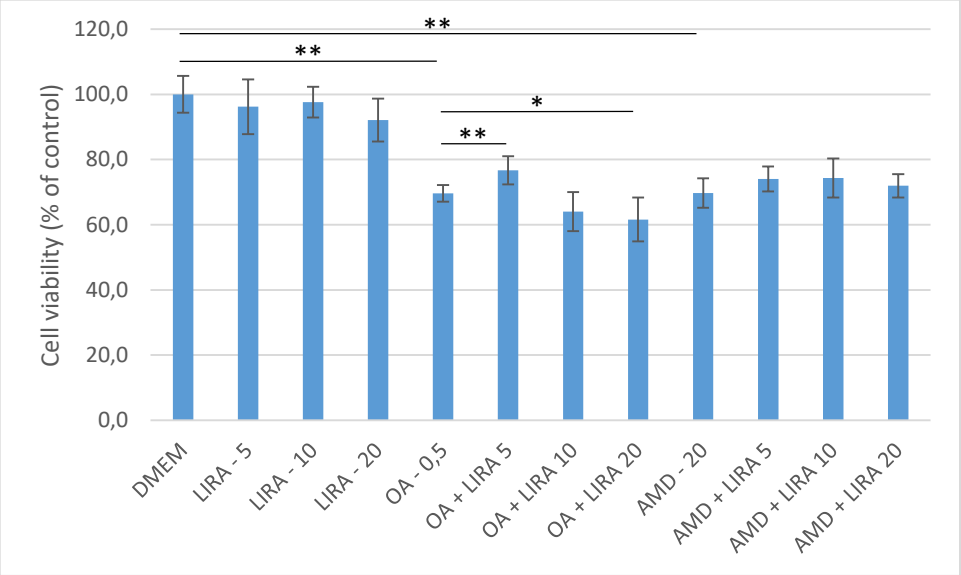


Figure 5. 5. Determination of cell viability by MTT assay after exposure of Huh7 cells to OA, AMD and various LIRA concentrations for 24 h.

MTT measurements were done by absorption spectrophotometry at 595 nm. Results are shown as a percentage relative to the negative control of at least three independent experiments. One-way ANOVA $F(11,71) = 37,61$; $p = 8,38 \times 10^{-23}$; Mann-Whitney pairwise. Bars assigned with asterisks are statistically significantly different (*$p < 0,05$, **$p < 0,01$). Dulbecco's Modified Eagle's Medium (DMEM) as a negative control, LIRA (L/nM), oleic acid (OA/mM), amiodarone (AMD/µM).

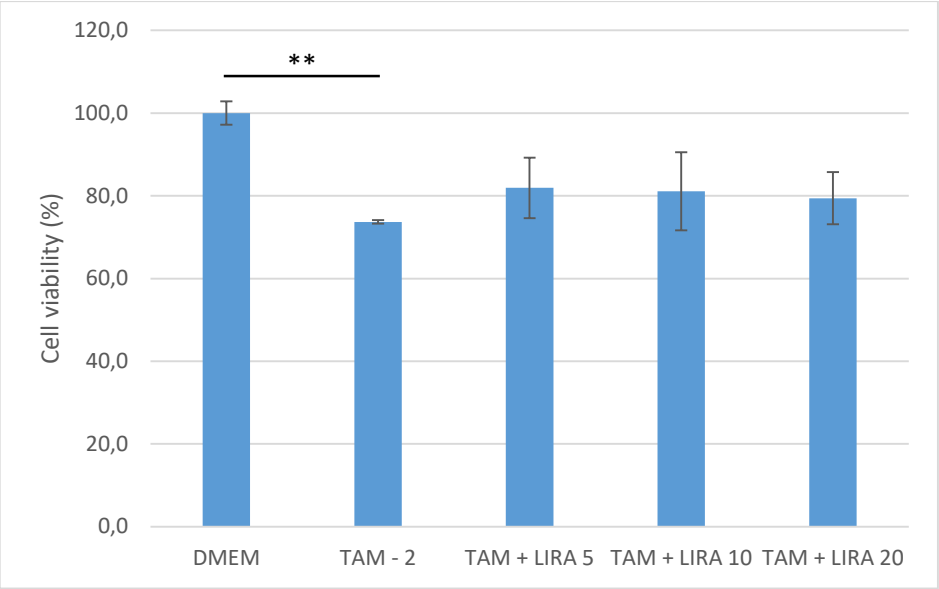


Figure 5. 6. Determination of cell viability by MTT assay after exposure of Huh7 cells to TAM and various LIRA concentrations for 24h.

MTT measurements were done by absorption spectrophotometry at 595 nm. Results are shown as a percentage relative to the negative control of at least three independent experiments. One-way ANOVA F (4,14) = 7,73; p = $4{,}164 \times 10^{-03}$; post-hoc Tukey HSD. Bars assigned with asterisks are statistically significantly different (**p < 0,01). Dulbecco's Modified Eagle's Medium (DMEM) as a negative control, liraglutide (LIRA/nM), tamoxifen (TAM/µM)

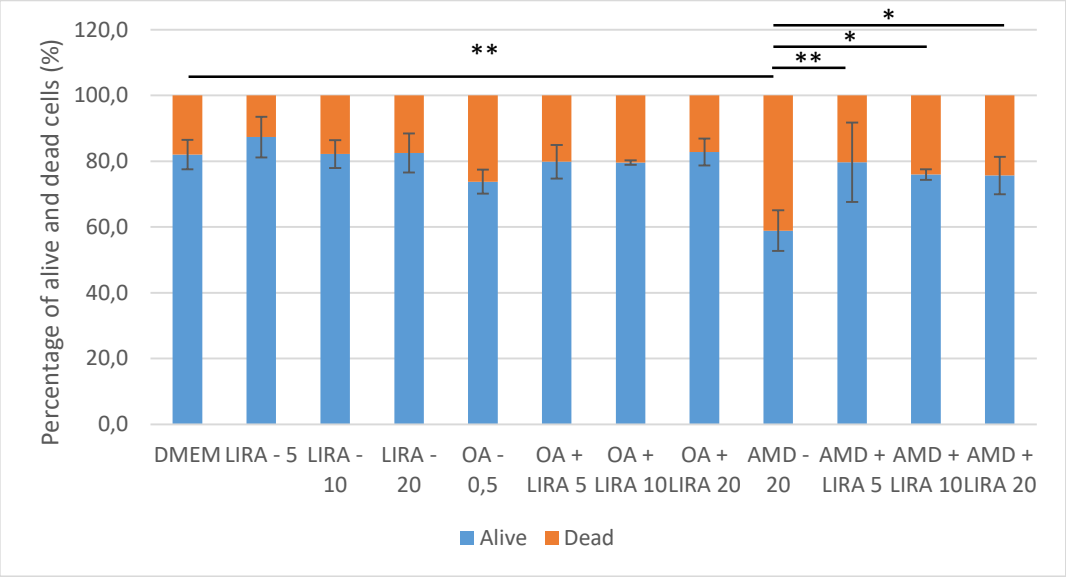


Figure 5. 7. Cell survival after exposure of Huh7 cells to OA, AMD and various LIRA concentrations for 24 h.

Determined by the Erythrosin B color exclusion test 24 h after treatment; significance was analyzed on data regarding dead cells. One-way ANOVA F (1,35) =4,771, $p=0{,}67 \times 10^{-03}$; post-

hoc Tukey HSD test; *p<0,05, **p<0,01. The data shown are representative of at least three independent experiments. Dulbecco's Modified Eagle's Medium (DMEM), liraglutide (LIRA/nM), oleic acid (OA/mM), amiodarone (AMD/µM)

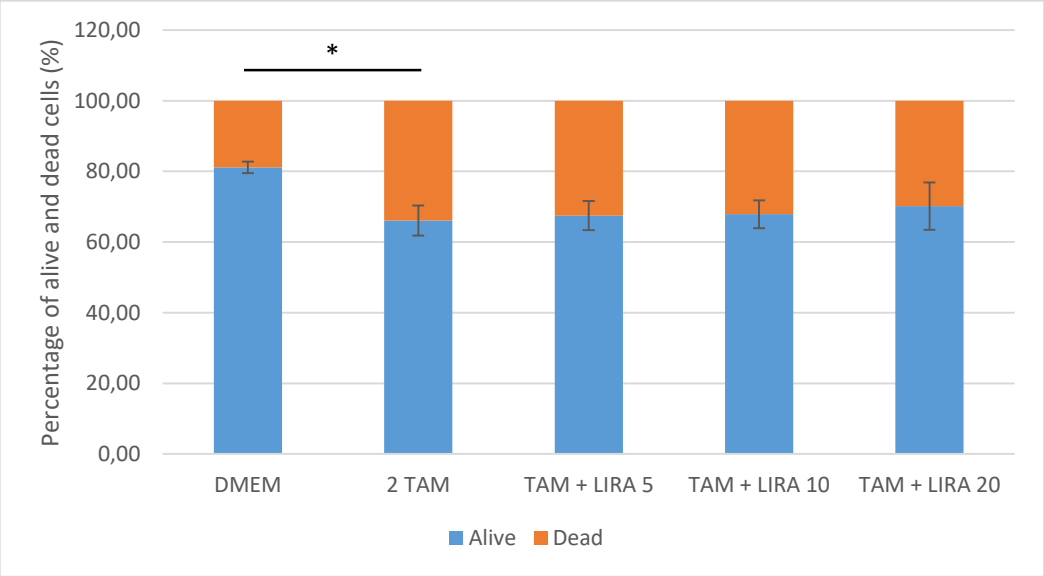


Figure 5. 8. Cell survival after exposure of Huh7 cells to TAM and various LIRA concentrations for 24 h.

Determined by the Erythrosin B color exclusion test 24 h after treatment; significance was analyzed on data regarding dead cells. One-way ANOVA F (4,14) = 5,703, $p=11,77x10^{-03}$ with post-hoc Tukey HSD test; *p<0,05. The data shown are representative of at least three independent experiments. Dulbecco's Modified Eagle's Medium (DMEM), liraglutide (LIRA/nM), tamoxifen (TAM/µM)

5.3. Visualization and Quantification of lipid accumulation in NAFLD and DIFLD cell culture models, cotreated with different LIRA concentrations

Accumulation of lipid droplets in OA and AMD models was demonstrated by ORO staining (Figure 5.9). Incubation of Huh7 cells with OA and AMD induced a statistically significant increase in lipid accumulation as shown in Figure 5.10. ($p < 0,05$, $p < 0,01$). Both OA and AMD increased the number of lipid droplets per cell, with 25-fold increase in OA treated cells ($p < 0,05$), and a 100-fold increase observed in AMD treated cells ($p < 0,01$) compared to negative control as shown in Figure 5.11. Microsteatosis was found as a predominant feature of AMD induced DIFLD, with nuclei positioned in the center of the cells, whereas lipid droplets in OA where almost two-fold larger compared to negative control ($p < 0,001$), indicating macrosteatosis occurrence (Figure 5.12.). Co-treatment with LIRA reduced the lipid

accumulation in both NAFLD and DIFLD models ($p < 0,01$, $p < 0,05$). LIRA also significantly reduced the number of lipid droplets in AMD DIFLD by a half ($p < 0,05$).

Accumulation of lipid droplets in TAM DIFLD models was demonstrated by ORO staining in Figure 5.13). TAM significantly increased lipid accumulation measured by integrated density of ORO staining per cell, in a 5-fold manner compared to negative DMEM control ($p < 0,001$), whereas LIRA slightly reversed this effect (Figure 5.14). TAM also increased number of lipid droplets per cell significantly, while LIRA reversed this effect ($p < 0,05$, $p < 0,001$) as seen in Figure 5.15. On the other hand, average size of lipid droplets was smaller with TAM, and LIRA increased it ($p < 0,001$) (Figure 5.16).

Microscopic images of these cell culture models, taken by author, confirm these effects (Figure 5.9. and 5.13.).

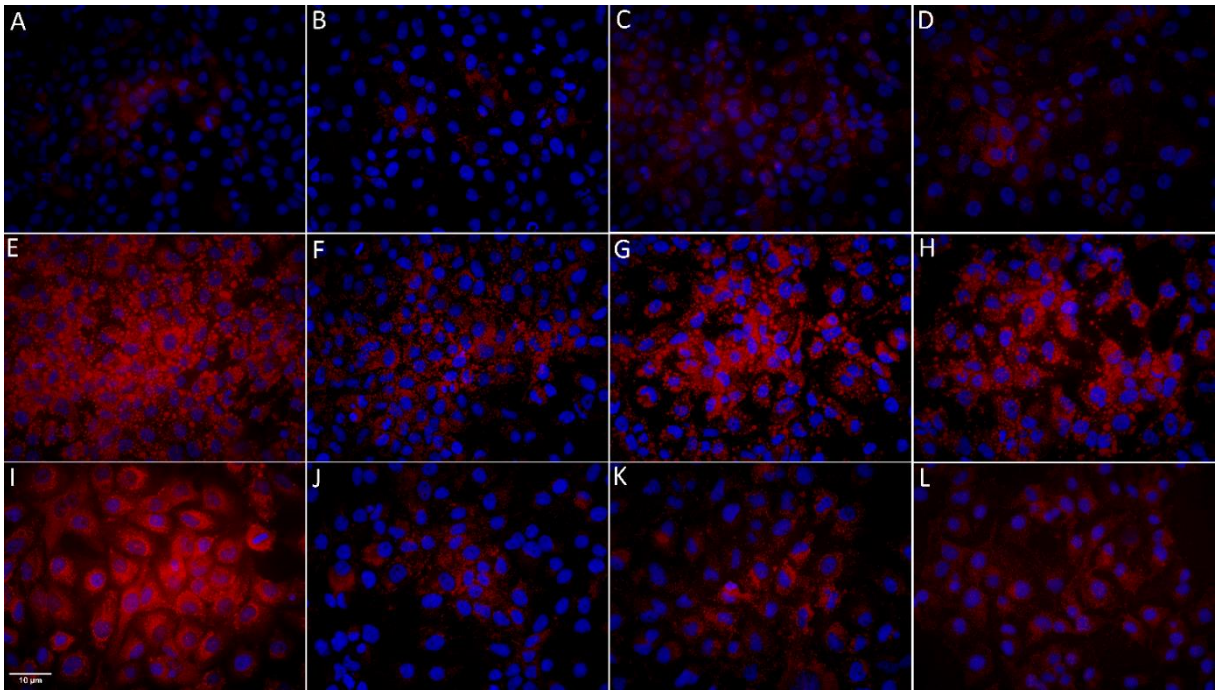


Figure 5. 9. Visualization of lipid accumulation with Oil-Red-O dye.

Lipid accumulation in Huh7 cells was visualized with Oil-Red-O dye, while DAPI (blue color) was used to stain nuclei. A- DMEM (negative control), B- 5 nM LIRA, C- 10 nM LIRA, D- 20 nM LIRA, E- 0,5 mM OA (positive control), F- 0,5 mM OA and 5 nM LIRA, G- 0,5 mM OA and 10 nM LIRA, H- 0,5 mM OA and 20 nM LIRA, I- 20 μM AMD, J- 20 μM AMD and 5 nM LIRA, 20 μM AMD and 10 nM LIRA K- 20 μM AMD and 20 nM LIRA. Size bar represents 10 μm. Dulbecco's Modified Eagle's Medium (DMEM), liraglutide (LIRA/nM), oleic acid (OA/mM), amiodarone (AMD/μM)

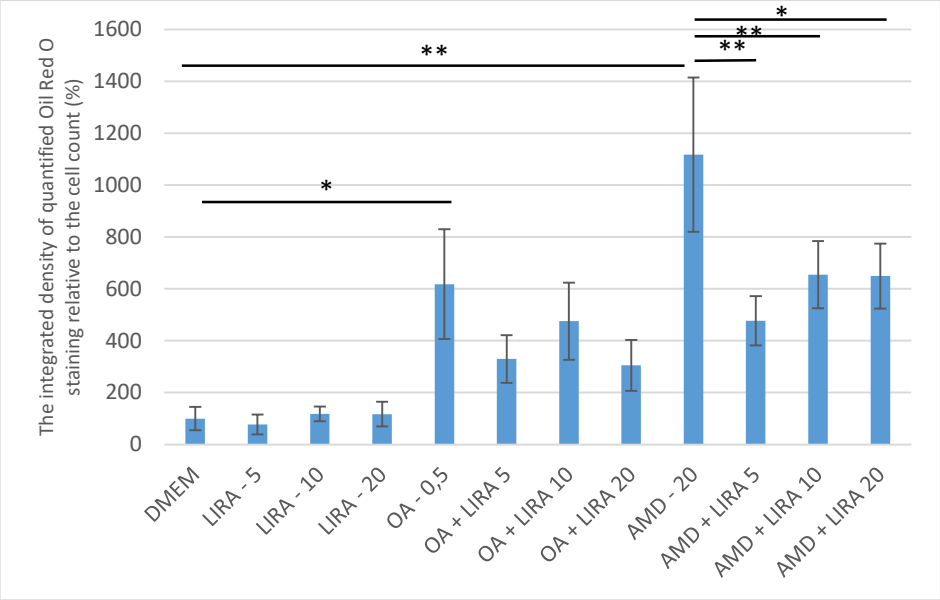


Figure 5. 10. Levels of lipids stained with Oil-Red-O dye in the Huh7 cells treated with OA, AMD, and LIRA.

The data represent the integrated density of red color relative to the cell count. A higher number equals a more intense stain. Results are shown as a percentage relative to the negative control. One-way ANOVA F (11, 130) = 66,2; p= $2{,}54 \times 10^{-45}$; Mann-Whitney U (Bonferroni-corrected p-value). Bars assigned with asterisks are statistically significantly different (* $p < 0{,}05$, ** $p < 0{,}01$). The data are shown as the means ± SD (standard deviation) from at least three independent experiments. Dulbecco's Modified Eagle's Medium (DMEM), liraglutide (LIRA/nM), oleic acid (OA/mM), amiodarone (AMD/µM)

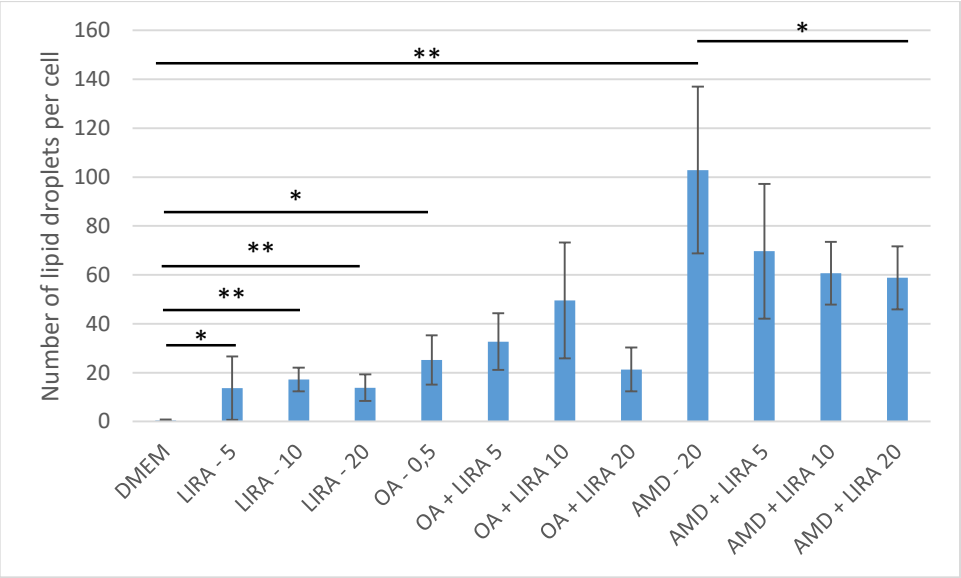


Figure 5. 11. Number of lipids droplets per cell after analyzing the images of Oil-Red-O stained Huh7 cells treated with OA, AMD, and LIRA.

The data represent the number of lipid droplets per cell. Results are shown as absolute values. One-way ANOVA F (11, 128) = 32,2; p= 2,4 × 10^{-30}; Mann-Whitney U (Bonferroni-corrected p-value). Bars assigned with asterisks are statistically significantly different (* p < 0,05, ** p < 0,01). The data are shown as the means ± SD (standard deviation) from at least three independent experiments. Dulbecco's Modified Eagle's Medium (DMEM), liraglutide (LIRA/nM), oleic acid (OA/mM), amiodarone (AMD/μM)

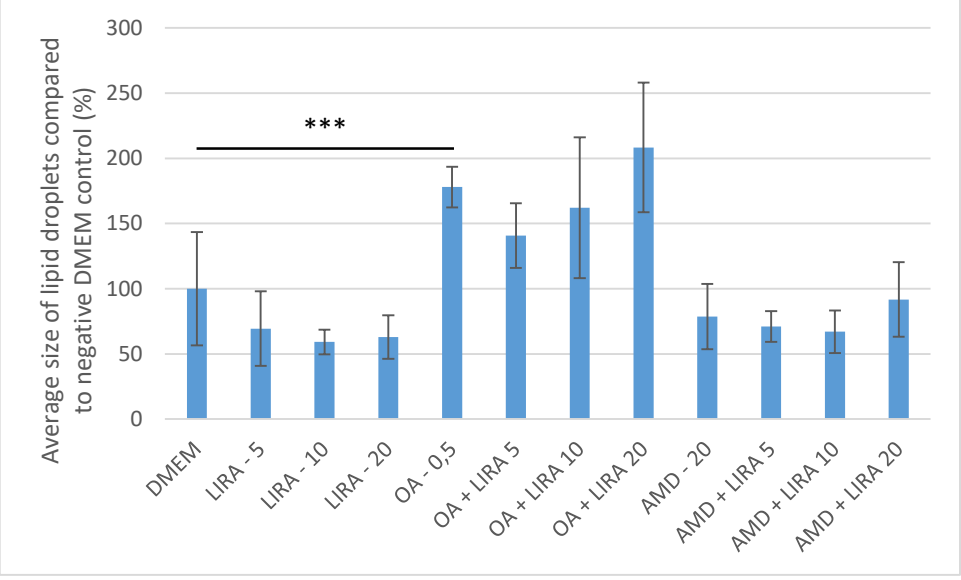


Figure 5. 12. Average size of lipid droplets after analyzing images of the Oil-Red-O stained Huh7 cells treated with OA, AMD, and LIRA.

Data represent the size of lipid droplets compared to negative DMEM control. One-way ANOVA F (11, 128) = 31,59; p= 5,48 × 10^{-30}; post-hoc Tukey HSD. Bars assigned with asterisks are statistically significantly different (*** p < 0,001). The data are shown as the means ± SD (standard deviation) from at least three independent experiments. Dulbecco's Modified Eagle's Medium (DMEM), liraglutide (LIRA/nM), oleic acid (OA/mM), amiodarone (AMD/µM)

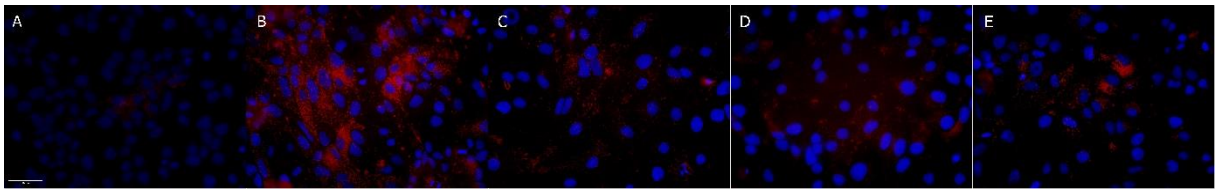


Figure 5. 13. Visualization of lipid accumulation with Oil-Red-O dye.

Lipid accumulation in Huh7 cells was visualized with Oil-Red-O dye, while DAPI (blue color) was used to stain nuclei. A- DMEM (negative control), B- 2 µM TAM, C- 2 µM TAM and 5 nM LIRA, D- 2 µM TAM and 10 nM LIRA, E- 2 µM TAM and 20 nM LIRA. Size bar represents 10 µm. Dulbecco's Modified Eagle's Medium (DMEM), liraglutide (LIRA/nM), tamoxifen (TAM/µM)

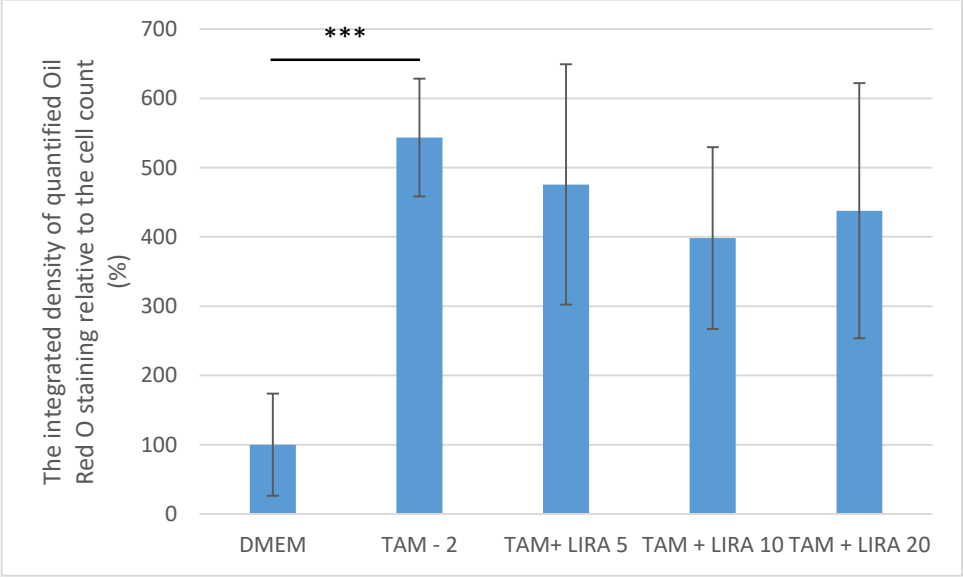


Figure 5. 14. Levels of lipids stained with Oil-Red-O dye in the Huh7 cells treated with TAM and LIRA.

The data represent the integrated density of red color relative to the cell count. A higher number equals a more intense stain. Results are shown as a percentage relative to the negative control. One-way ANOVA F (4, 49) = 12,79; p= 4,94 × 10^{-07}; post-hoc Tukey HSD. Bars assigned with

asterisks are statistically significantly different (*** $p < 0{,}001$). The data are shown as the means ± SD (standard deviation) from at least three independent experiments. Dulbecco's Modified Eagle's Medium (DMEM), liraglutide (LIRA/nM), tamoxifen (TAM/µM)

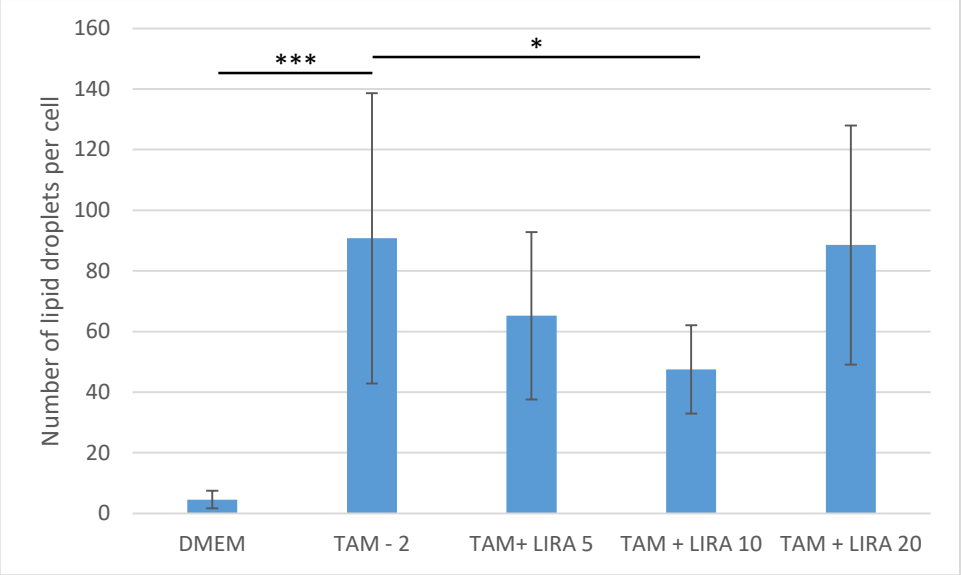


Figure 5. 15. Number of lipids droplets per cell after analyzing images of Oil-Red-O stained Huh7 cells treated with TAM and LIRA.

The data represent the number of lipid droplets per cell. Results are shown as absolute values. One-way ANOVA $F(4, 49) = 11{,}25$; $p = 2{,}27 \times 10^{-06}$ post-hoc Tukey HSD. Bars assigned with asterisks are statistically significantly different (* $p < 0{,}05$, *** $p < 0{,}001$). The data are shown as the means ± SD (standard deviation) from at least three independent experiments. Dulbecco's Modified Eagle's Medium (DMEM), liraglutide (LIRA/nM), tamoxifen (TAM/µM)

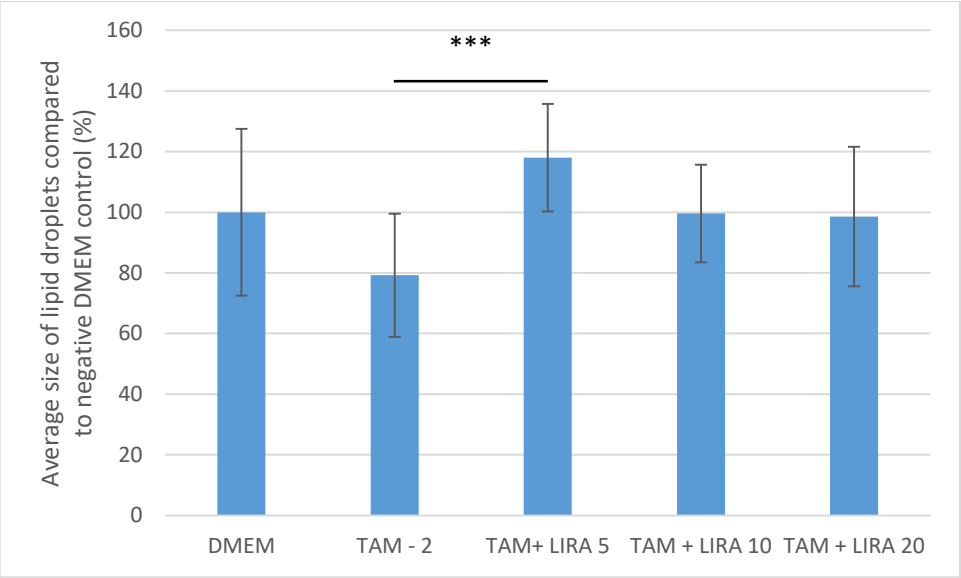


Figure 5. 16. Average size of lipid droplets after analyzing images of Oil-Red-O stained Huh7 cells treated with TAM and LIRA.

The data represent the size of lipid droplets compared to negative DMEM control. One-way ANOVA F (4,49) = 4,557; p= $3{,}555 \times 10^{-03}$; post-hoc Tukey HSD. Bars assigned with asterisks are statistically significantly different (*** $p < 0{,}001$). The data are shown as the means ± SD (standard deviation) from at least three independent experiments. Dulbecco's Modified Eagle's Medium (DMEM), liraglutide (LIRA/nM), tamoxifen (TAM/μM)

5.4. Measurement of triglyceride content in NAFLD and DIFLD cell culture models, and/or cotreated with different LIRA concentrations

AMD and OA increased significantly triglyceride content in Huh7 cells ($p < 0{,}001$), as did TAM, but to a smaller extent ($p < 0{,}05$) as shown in Figures 5.17. and 5.18. LIRA reduced the triglyceride accumulation in all models in all three concentrations, but to the greatest extent in NAFLD ($p < 0{,}001$).

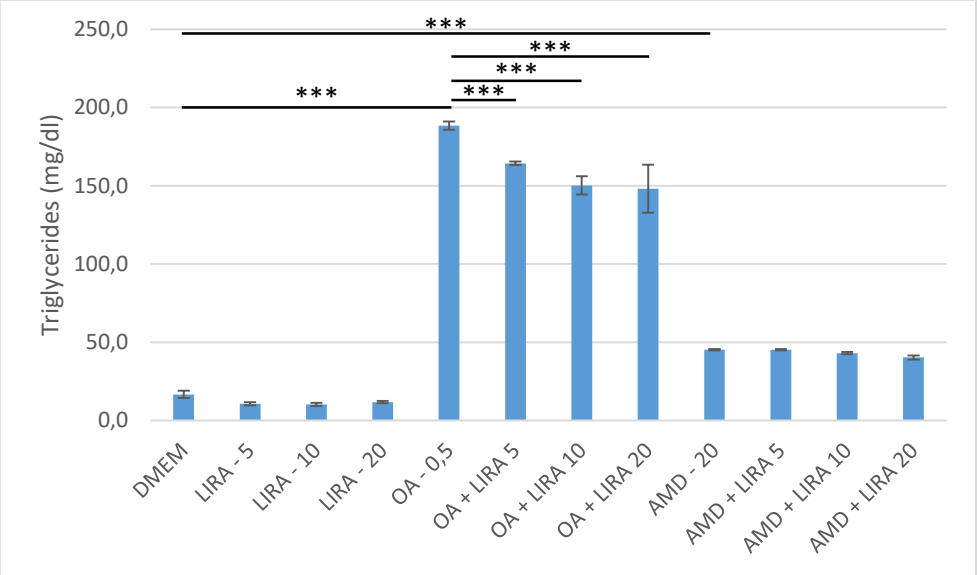


Figure 5. 17. Triglyceride content in DIFLD and NAFLD cell culture models incubated with varying concentrations of LIRA.

The data represent concentrations of triglycerides in cell samples. Results are shown as absolute values. One-way ANOVA F (11, 35) = 579,2; p= 2,62 × 10^{-26}; post- hoc Tukey HSD. Bars assigned with asterisks are statistically significantly different (*** p < 0,001). The data are shown as the means ± SD (standard deviation) from at least three independent experiments. Dulbecco's Modified Eagle's Medium (DMEM), liraglutide (LIRA/nM), oleic acid (OA/mM), amiodarone (AMD/μM)

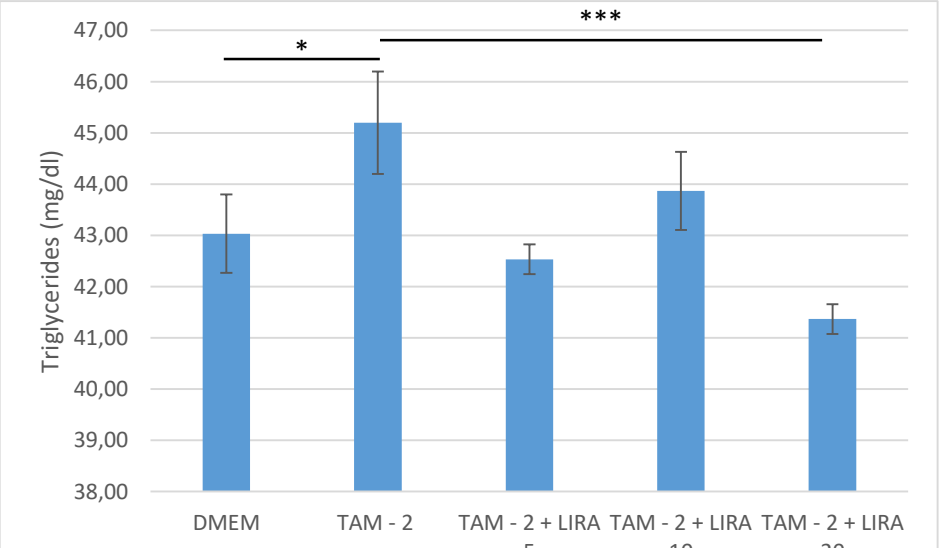


Figure 5. 18. Triglyceride content in TAM NAFLD cell culture model, incubated with varyin concentrations of LIRA.

Data represent concentrations of triglycerides in cell samples. Results are shown as absolute values. One-way ANOVA F (4, 44) = 8,713; p= 3,72 × 10^{-05}; post-hoc Tukey HSD. Bars assigned with asterisks are statistically significantly different (* p < 0,05, *** p < 0,001). The data are shown as the means ± SD (standard deviation) from at least three independent experiments. Dulbecco's Modified Eagle's Medium (DMEM), liraglutide (LIRA/nM), oleic acid (OA/mM), amiodarone (AMD/μM)

5.5. Assessment of the Effect of LIRA on GSH concentration in hepatocyte steatosis NAFLD and DIFLD cell culture models

GSH levels were reduced in all three models of steatosis (Figure 5.19 and 5.20). Amiodarone and tamoxifen reduced it to 80% compared to DMEM negative control (p < 0,01, p < 0,05), while effect of OA was smaller. There was no significant difference in GSH concentrations with LIRA co-treatment.

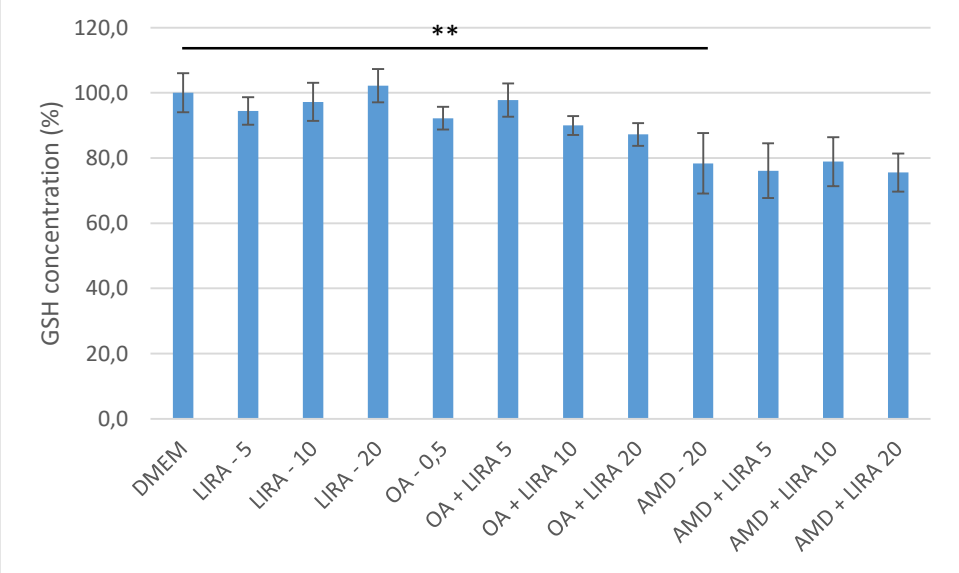


Figure 5. 19. GSH levels in the hepatocyte steatosis NAFLD and AMD DIFLD Huh7 cell culture models.

GSH measurements were done by absorption spectrophotometry at 415 nm. Results are shown as a percentage relative to the negative control of at least three independent experiments. One-way ANOVA F (11, 35) =8,171, p=9,93×10^{-06}. post-hoc Tukey HSD test. Bars assigned with asterisks are statistically significantly different (**p < 0,01). Dulbecco's Modified Eagle's Medium (DMEM) as a negative control, LIRA (L/nM), oleic acid (OA/mM), amiodarone (AMD/μM)

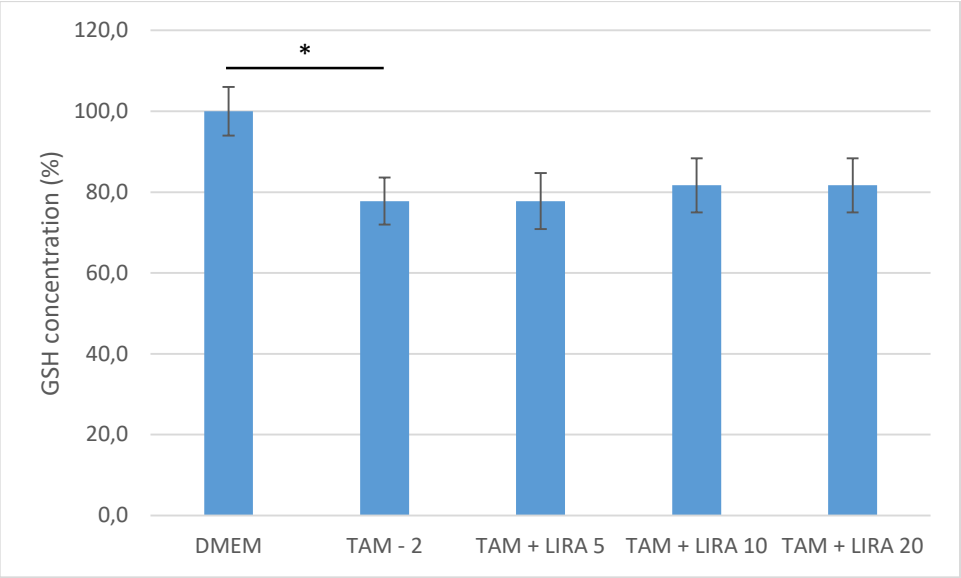
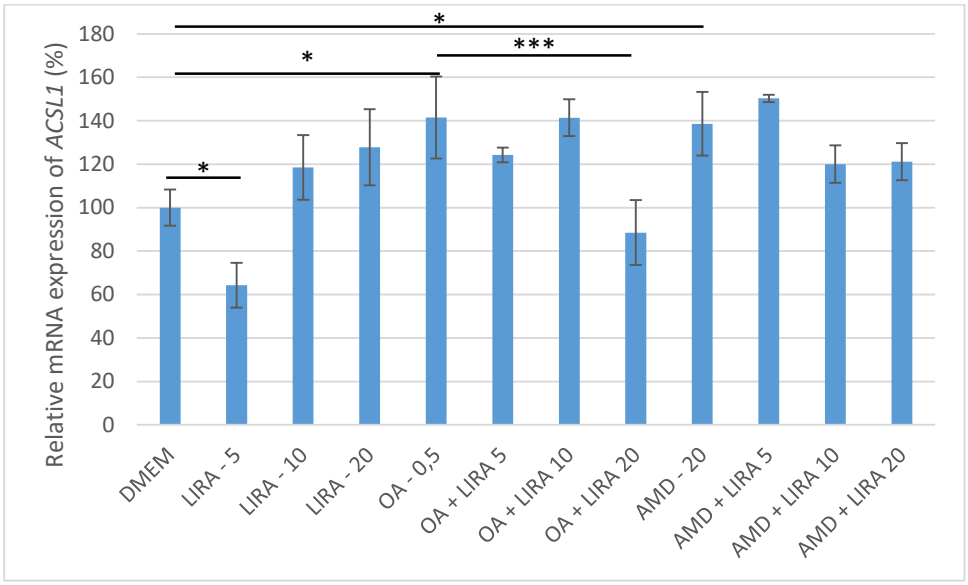


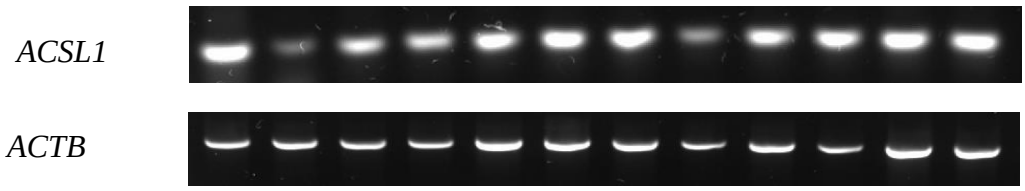
Figure 5. 20. GSH levels in the hepatocyte steatosis TAM DIFLD Huh7 cell culture model. GSH measurements were done by absorption spectrophotometry at 415 nm. Results are shown as a percentage relative to the negative control of at least three independent experiments. One-way ANOVA F (4, 14) =6,211, p=8,84x10^{-03}. post-hoc Tukey HSD test. Bars assigned with asterisks are statistically significantly different (*p < 0,05). Dulbecco's modified Eagle's medium (DMEM) as a negative control, LIRA (L/nM), tamoxifen (TAM/µM)

5.6. Evaluation of the effect of LIRA on various gene expression in hepatocyte steatosis NAFLD and DIFLD cell culture models

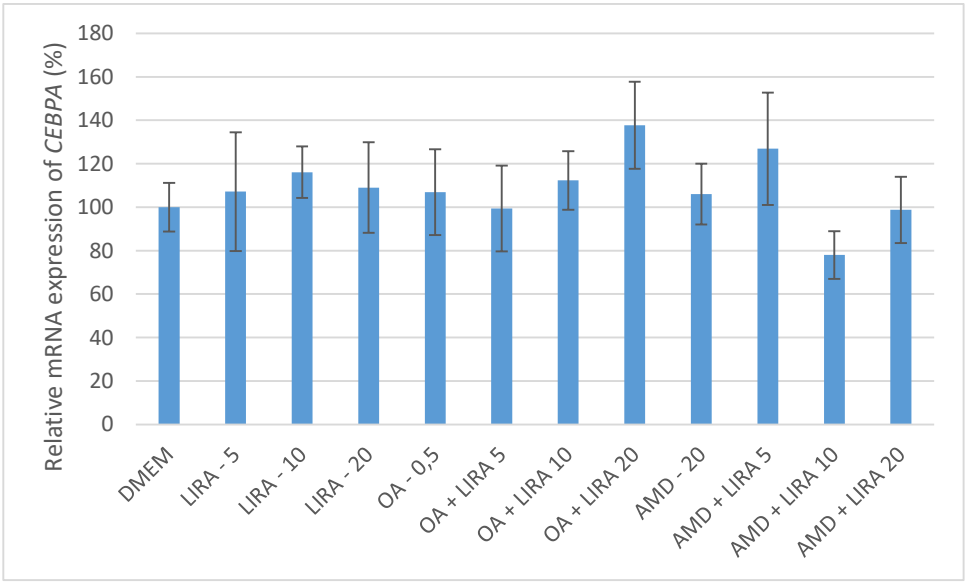
To determine the effects of LIRA in hepatocyte steatosis NAFLD and DIFLD models on mRNA levels of *ACSL1*, *CEBPA*, *PPARG*, and *SREBF1* RT-PCT was performed. In both OA and AMD models, *ACSL1* gene expression was upregulated, whereas LIRA co-treatment decreased *ACSL1* levels, but only in OA model with statistical significance (p < 0,001), as shown in Figure 5.21.a. *CEBPA* was downregulated with the lowest LIRA treatment in the NAFLD model, Higher LIRA concentrations achieved downregulation in the DIFLD model, but all without statistical significance, as shown in Figure 5.21.b. The effect of LIRA on *PPARG* gene expression is shown in Figure 5.21.c. OA increased *PPARG* mRNA levels, whereas 5 nM and 20 nM LIRA reversed this effect. In the AMD DIFLD model, *PPARG* gene expression was upregulated and 10 nM LIRA reversed this effect, but without statistical significance. In both models a slight increase in *SREBF1* expression was observed (Figure 5.21.d.), whereas 5 nM LIRA significantly downregulated its expression in NAFLD model (p < 0,05), and 10 nM LIRA in DIFLD model (p < 0,01).

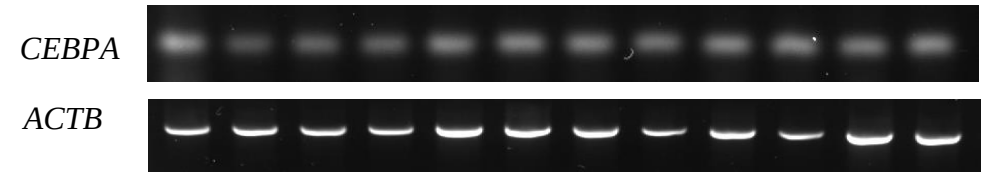
In second series of experiments with hepatocyte steatosis TAM DIFLD model, increased expression of all genes occurred with TAM treatment except a decrease in *PPARG* gene expression as demonstrated in Figures 5.22.a, 5.22.b, 5.22.c, and 5.22.d ($p < 0.05$, $p < 0.001$). LIRA co-treatment decreased expression of *ACSL1* and *SREBF1* genes, while the effect on *CEBPA* and *PPARG* was opposite ($p < 0.01$, $p < 0.001$).



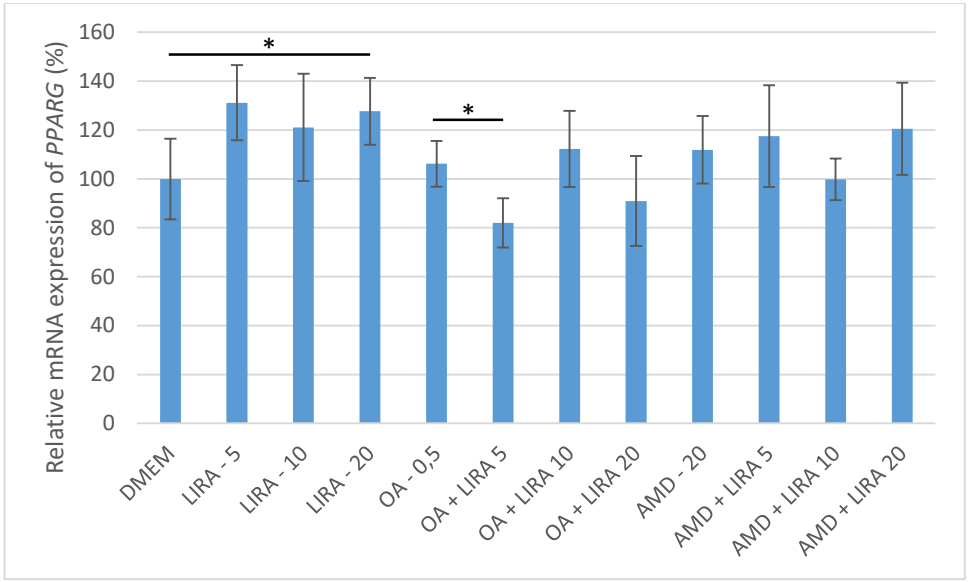


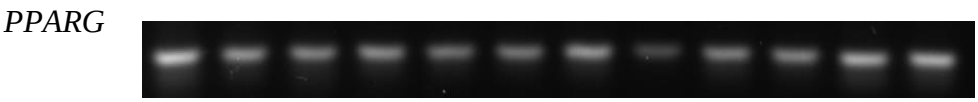
(a)



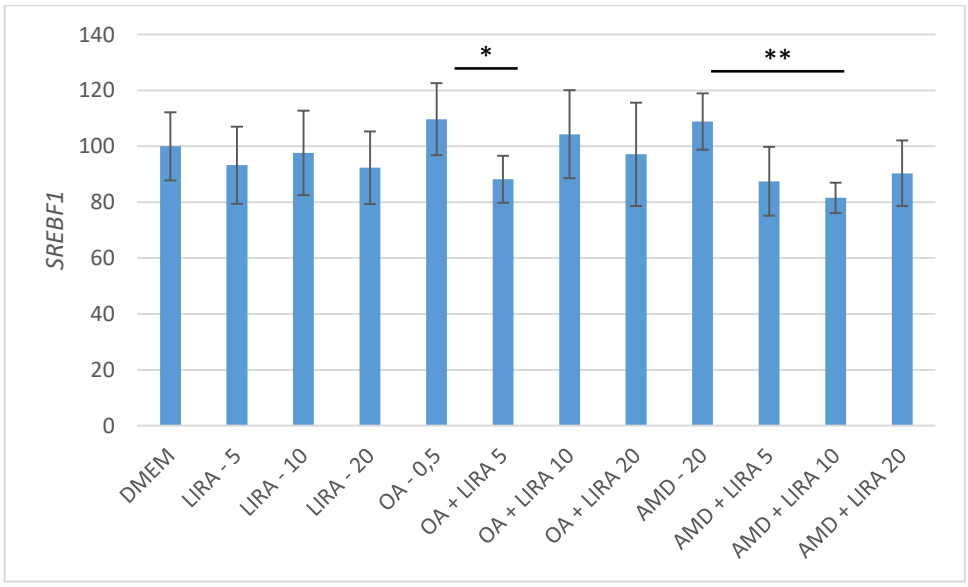

CEBPA
ACTB

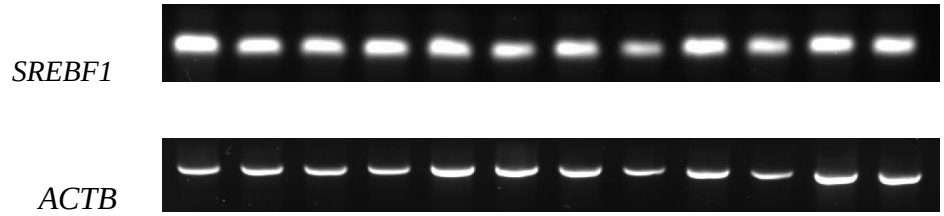
(b)


Relative mRNA expression of PPARG (%)
160
140
120
100
80
60
40
20
0
*
*
DMEM
LIRA - 5
LIRA - 10
LIRA - 20
OA - 0,5
OA + LIRA 5
OA + LIRA 10
OA + LIRA 20
AMD - 20
AMD + LIRA 5
AMD + LIRA 10
AMD + LIRA 20


PPARG
ACTB

(c)


SREBF1
140
120
100
80
60
40
20
0
*
**
DMEM
LIRA - 5
LIRA - 10
LIRA - 20
OA - 0,5
OA + LIRA 5
OA + LIRA 10
OA + LIRA 20
AMD - 20
AMD + LIRA 5
AMD + LIRA 10
AMD + LIRA 20

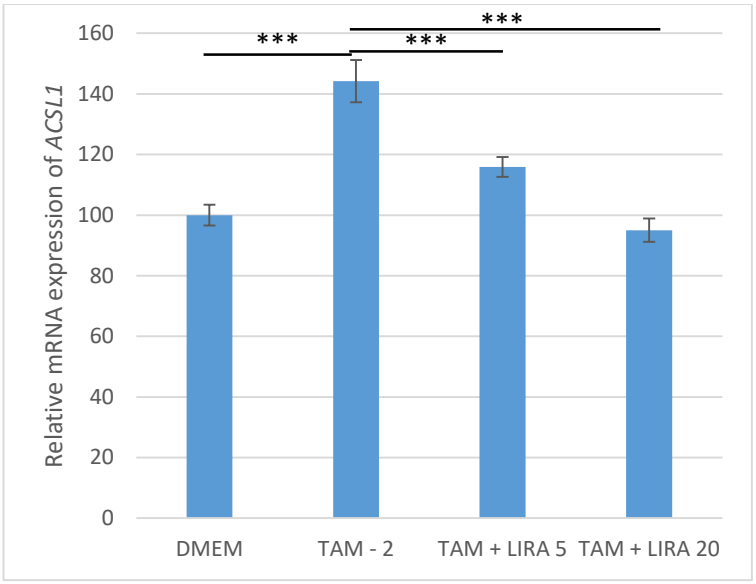


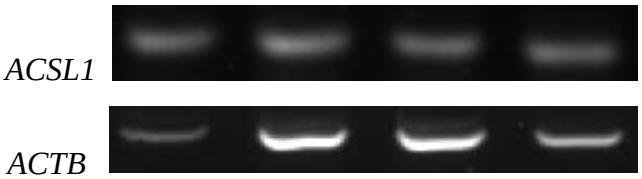
(d)

Figure 5. 21. Expression of *ACSL1, CEBPA, PPARG,* and *SREBF1* in hepatocyte steatosis cell culture models of NAFLD and AMD DIFLD.

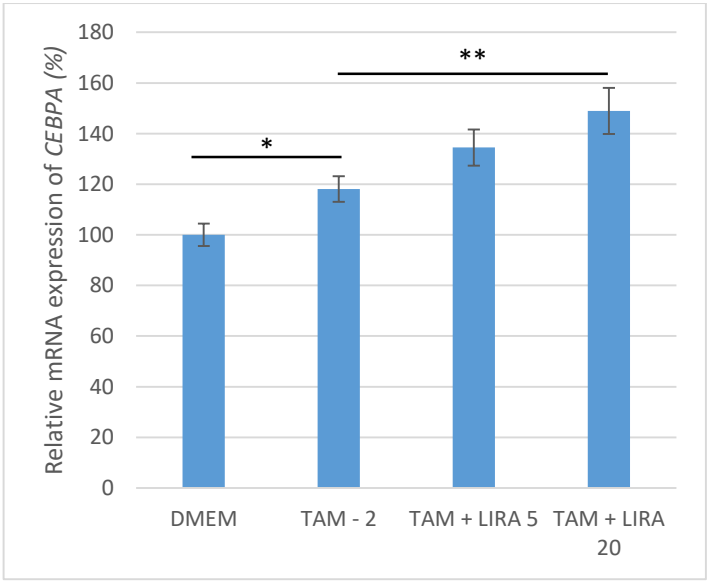
(a) *ACSL1* gene expression in the treated Huh7 cell line. Data represents a percentage relative to negative control (DMEM), of at least three independent experiments. One-way ANOVA F (11, 35) = 12,8 p = $1{,}63x10^{-07}$; post-hoc Tukey HSD test; * p < 0,05, *** p < 0,001. RT-PCR was used for the gene expression analysis, and Image Lab 6.0.1 build 34 Bio-Rad Laboratories was used to semi-quantify the results (normalized to the *ACTB* mRNA levels). The values are represented as means ±SD. Representative figure of Southern blot analysis of *ACSL1* gene expression compared to *ACTB* expression. (b) *CEBPA* gene expression in the treated Huh7 cell line. Data represents a percentage relative to negative control (DMEM), of at least three independent experiments. One-way ANOVA F (11, 47) = 2,661, p = $13{,}17x10^{-03}$; post hoc Tukey HSD test. RT-PCR was used for the gene expression analysis, and Image Lab 6.0.1 build 34 Bio-Rad Laboratories was used to semi-quantify the results (normalized to the *ACTB* mRNA levels). The values are represented as means ±SD. Representative figure of Southern blot analysis of *C/EBPα* expression compared to *ACTB* expression. (c) *PPARG* gene expression in the treated Huh7 cell line. Data represents a percentage relative to negative control (DMEM), of at least three independent experiments. One-way ANOVA F (11, 59) = 4,415, p = $1{,}42x10^{-04}$; Mann-Whitney U test * p < 0,05. RT-PCR was used for the gene expression analysis, and Image Lab 6.0.1 build 34 Bio-Rad Laboratories was used to semi-quantify the results (normalized to the *ACTB* mRNA levels). The values are represented as means ± SD. Representative figure of Southern blot analysis of *PPARG* expression compared to *ACTB* expression. (d) *SREBF1* gene expression in the treated Huh7 cell line. Data represents a percentage relative to negative control (DMEM), of at least three independent experiments. One-way ANOVA F (11, 59) = 4,241, p = $2{,}12x10^{-04}$; post hoc Tukey HSD test; * p < 0,05, ** p < 0,01. RT-PCR was used for the gene expression analysis, and Image Lab 6.0.1 build 34 Bio-Rad Laboratories was used to semi-quantify the results (normalized to the *ACTB* mRNA levels). The values are represented as means ± SD. Representative figure of Southern blot analysis of *SREBF1* expression compared to *ACTB* expression. Dulbecco's Modified Eagle's

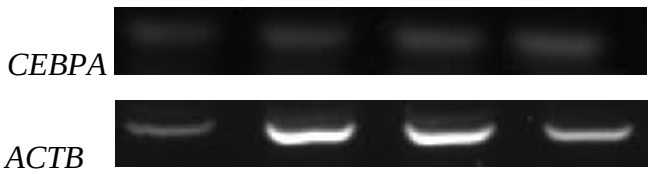
Medium (DMEM), LIRA (LIRA/nM), oleic acid (OA/mM), amiodarone (AMD/µM), Acyl-CoA Synthetase Long Chain Family Member 1 (*ACSL1*), CCAAT/enhancer-binding protein α (*CEBPA*), peroxisome proliferator-activated receptor gamma (*PPARG*), sterol regulatory element binding transcription factor 1c (*SREBF1*)



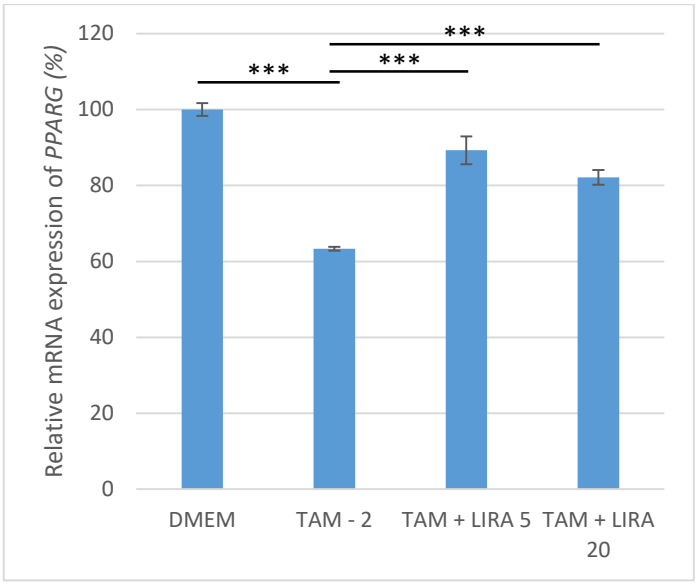


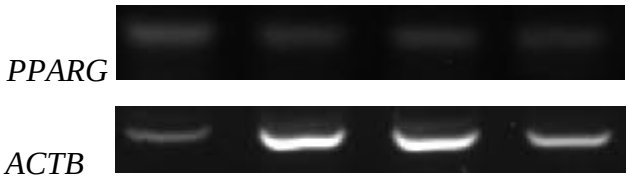
(a)



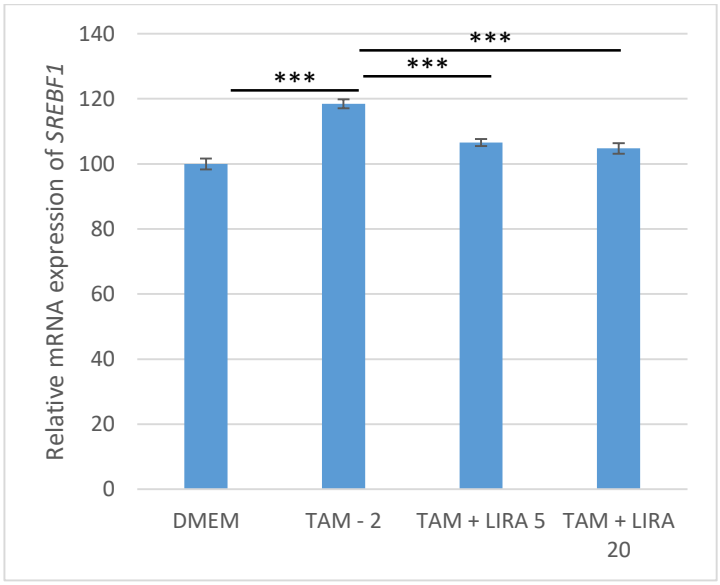


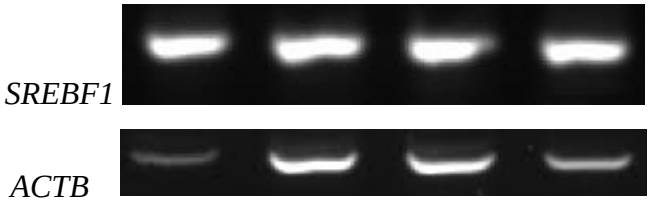
(b)





(c)





(d)

Figure 5. 22. Expression of *ACSL1*, *CEBPA*, *PPARG*, and *SREBF1* in hepatocyte steatosis cell culture models of TAM DIFLD.

(a) *ACSL1* gene expression in the treated Huh7 cell line. Data represents a percentage relative to negative control (DMEM), of at least three independent experiments. One-way ANOVA F (3, 11) = 68,59 p = $4{,}75 \times 10^{-06}$; post hoc Tukey HSD test; *** p < 0,001. RT-PCR was used for the gene expression analysis, and Image Lab 6.0.1 build 34 Bio-Rad Laboratories was used to semi-quantify the results (normalized to the *ACTB* mRNA levels). The values are represented as means ±SD. Representative figure of Southern blot analysis of *ACSL1* expression compared to *ACTB* expression. (b) *CEBPA* gene expression in the treated Huh7 cell line. Data represents a percentage relative to negative control (DMEM), of at least three independent experiments. One-way ANOVA F (3, 11) = 29,85, p = $1{,}08 \times 10^{-04}$; post hoc Tukey HSD test; * p < 0,05 ** p < 0,01. RT-PCR was used for the gene expression analysis, and Image Lab 6.0.1 build 34 Bio-Rad Laboratories was used to semi-quantify the results (normalized to the *ACTB* mRNA levels). The values are represented as means ± SD. Representative figure of Southern blot analysis of) *CEBPA* expression compared to *ACTB* expression. (c) *PPARG* gene expression in the treated Huh7 cell line. Data represents a percentage relative to negative control (DMEM), of at least three independent experiments. One-way ANOVA F (3, 11) = 141,4, p = $2{,}87 \times 10^{-07}$, post hoc Tukey HSD test; *** p < 0,001. RT-PCR was used for the gene expression analysis, and Image Lab 6.0.1 build 34 Bio-Rad Laboratories was used to semi-quantify the results (normalized to the *ACTB* mRNA levels). The values are represented as means ± SD. Representative figure of Southern blot analysis of *PPARG* expression compared to *ACTB* expression. (d) *SREBF1* gene expression in the treated Huh7 cell line. Data represents a percentage relative to negative control (DMEM), of at least three independent experiments. One-way ANOVA F (3, 11) = 85,78, p = $2{,}01 \times 10^{-06}$; post hoc Tukey HSD test; *** p < 0,001. RT-PCR was used for the gene expression analysis, and Image Lab 6.0.1 build 34 Bio-Rad Laboratories was used to semi-quantify the results (normalized to the *ACTB* mRNA levels). The values are represented as means ± SD. Representative figure of Southern blot analysis of *SREBF1* expression compared to *ACTB* expression. Dulbecco's Modified Eagle's Medium (DMEM), LIRA (LIRA/nM), oleic acid (OA/mM), amiodarone (AMD/μM), Acyl-CoA Synthetase Long Chainn Family Member 1 (*ACSL1*), CCAAT/enhancer-binding protein α (*CEBPA*), peroxisome proliferator-activated receptor gamma (*PPARG*), sterol regulatory element binding transcription factor 1c (*SREBF1*)

6. DISCUSSION

Various *in vitro* models for NAFLD have so far been developed, most commonly by adding palmitic acid and/or OA to different cell cultures. We used an Huh7 cell line and OA in our current research which revealed a significant reduction in cell viability (20%) after treatment of Huh7 cells with 0,5 mM OA for 24 h and 48 h. In contrast, Ricchi et al. found that OA had no effect on cell viability (116). In our current study, after 72 hours of treatment, the observed toxic effect vanished. One explanation is that OA was only added at the start of this experiment, giving cells time to recover.

AMD was chosen as a key compound for the induction of DIFLD after a thorough literature search. It has been demonstrated to have a hepatosteatotic effect, and clinical use of it is widespread. AMD has not been demonstrated to have an extrahepatic effect that could significantly contribute to its hepatosteatotic activity, in contrast to some other drugs that cause hepatosteatosis. AMD is therefore suitable for cell culture studies because it directly affects hepatic cells, and achieves hepatosteatotic effect (147). A concentration of 20 μM and an incubation time of 24 h were chosen after treating cells with various AMD concentrations for various amounts of time due to the significant effects on cell viability, but not in such manner to cause apoptosis to a greater extent (that occurs with higher AMD concentrations, and longer incubation times). The same settings for treatment have been used in earlier studies (67).

In the second series of experiments, TAM was used as a key compound for DIFLD establishment and evaluation. MTT analysis after 24 h revealed IC_{20} of TAM to be 2 μM, while 48 h incubation period significantly reduced cell viability to 50 %, or even less than 10% (with 4 μM) compared to control. Therefore, cells treated with 2 μM TAM for 24 h were chosen for TAM DIFLD model, although other studies used even 10 and 20 μM TAM (69).

When we compared the NAFLD and DIFLD models, we saw that the effects on cell viability were similar, but that OA induced triglyceride accumulation more than AMD or TAM. AMD had a greater impact on lipid accumulation/cell in general, as demonstrated by ORO staining. In HepG2 cells treated with AMD for 24 h, Zhou et al. observed a significant three-fold increase in the number of lipid droplets per cell, while in current our study 100-fold increase comparing to negative control occurred due to AMD 24 h treatment (147, 148). Average size of lipid droplets was increased with AMD treatment in the Zhou et al. study, whereas in our current study it was just slightly decreased (148). Comparing the integrated density of quantified ORO staining to the number of cells in the study, a tenfold increase over the negative control was found. As one of the primary characteristics of AMD DIFLD, triglyceride accumulation was

shown by Vitins et al., but only after longer incubation times. Following a 24 hour treatment period, only a slight increase was seen (149). Triglycerides were three times higher in AMD DIFLD in our current study according to ORO staining with a much greater increase in lipid accumulation. It is possible that AMD also caused an accumulation of other lipids in the liver. Accordingly, phosphatidylcholine accumulation was found after AMD treatment in one *in vivo* study (149, 150). On the other hand, similar to earlier studies, triglyceride accumulation was significantly increased in an OA NAFLD model (116).

DIFLD model with TAM also had an increase in triglyceride levels, similar to the AMD model, and to previous *in vitro* studies (69). However, in the current study, an increase in overall lipid accumulation and steatosis shown by ORO staining was greater which is similar to those of previous studies, indicating accumulation of other lipids as well (151). This increase occurred due to rise in the number of lipid droplets in 8-fold manner compared to control. The result was slightly less than the AMD-induced increase in the number of lipid droplets, but 2 times more than in OA NAFLD model.

The various models also had different histological patterns. According to earlier studies, AMD and TAM DIFLD in our study manifested as microsteatosis. (19, 42, 67, 116, 152). Whereas NAFLD presented with larger vesicles (macrosteatosis) and is typically found as macrovesicular steatosis, although Tandra et al. demonstrated that microvesicular steatosis was also present in roughly 10% of biopsies from patients with NAFLD (153, 154). Our current study supports these findings, considering that average size of lipid droplets was three-fold greater in OA NAFLD model, comparing to AMD and TAM DIFLD model, that appeared with lipid droplets even smaller than negative DMEM control.

Levels of GSH, a molecule that has an important role in detoxification in liver, can be reduced due to drug consumption and increase in ROS (63). A depletion of GSH was observed also in NAFLD (155). Similarly, in our current study, both AMD and TAM significantly reduced GSH levels to 80% comparing to negative control. This indicates that oxidative stress caused by these agents contributes to their hepatotoxic effect. OA NAFLD model showed just a slight decrease in GSH levels.

The expression of the gene for *ACSL1*, a protein that transforms free long-chain fatty acids into fatty acyl-CoA esters, increased in all three fatty liver models by 40% comparing to control. Although this increase has been shown in numerous prior studies using NAFLD models, this is the first report of an AMD- and TAM-induced increase in *ACSL1* in liver (73). Therefore,

upregulation of *ACSL1*, which has been linked to both a decrease in fatty acid -oxidation and an increase in lipogenesis in the liver, is at least partially responsible for the increased triglyceride accumulation seen in our models. (71, 72). This effect was achieved through *PPARG* signalling pathway according to Li et al. (71). *PPARG* expression was found to be significantly upregulated in NAFLD and AMD DIFLD models, while in a TAM model it was significantly downregulated. This is opposite to results of a previous *in vitro* study on a TAM DIFLD model (69). Additionally, earlier research has shown an increase in liver *PPARG* expression in NAFLD model (138, 156, 157). This may point to a potential steatotic role for *PPARG* in the liver in the formation of lipid droplets and triglyceride accumulation in OA and AMD models of fatty liver (78, 87). Considering the complicated role of *PPARG* (possible anti-fibrotic activity) in the liver, the downregulation observed in TAM could also indicate a higher possibility for fibrosis development. In the NAFLD and DIFLD models, an increase in *CEBPA* and *SREBF1* gene expression was seen, confirming their function in promoting fatty changes (73, 74). The greatest *CEBPA* upregulation by 20% over control, was observed in TAM DIFLD, although Zhao et al. demonstrated a slight downregulation of *CEBPA* following TAM treatment. TAM DIFLD model showed also the greatest increase in *SREBF1* expression, but to a much lesser extent comparing to Zhao et al. model (69).

After assessing various studies, which stated that the maximum clinical dose of LIRA given to patients was 3 mg per day (this number was increased to a person weighing 85 kg, yielding a dose of 11.3 nmol/kg), we chose to use 5, 10, and 20 nM LIRA for the experiments because, in our model concentrations higher than 20 nM significantly reduced cell viability (although some studies used even 100 nM and 500 nM) (134, 135). The selected LIRA doses used in the current study may have had a hypoglycemic effect when administered to cells. But only in response to increases in blood glucose levels does LIRA cause an increase in insulin secretion while inhibiting glucagon. As a result, there should be little chance of developing hypoglycemia. Although, the lowest LIRA concentration used in our study, 5 nM, had a slightly positive effect on cell viability, higher concentrations decreased cell viability. Erythrosin B exclusion test showed similar results regarding cell survival. But, in the AMD model all three LIRA concentrations significantly increased cell survival. In line with other studies, LIRA generally decreased lipid accumulation in the NAFLD model and had an even stronger impact in the AMD DIFLD model. (136, 158). We were unable to find a study that similarly demonstrated the antisteatotic effects of LIRA in the DIFLD model. In NAFLD model, however, LIRA also decreased the size of lipid droplets, indicating a reverse effect on macrosteatosis which was

supported by the significant drop in triglyceride content (triglycerides are thought to be the main contributor to lipid droplet enlargement) (159, 160). On the contrary, the antisteatotic effect of LIRA in DIFLD models was mainly reflected by a reduction in the number of lipid droplets. Also, a significant decrease in triglyceride content in TAM DIFLD model treated with 20 nM LIRA was observed.

GSH concentrations in all three models remained unchanged or just slightly elevated with LIRA co-treatment, although previous research reported significant increase in GSH activity achieved by LIRA (161, 162)

All concentrations of LIRA, with the exception of 5 nM LIRA in the DIFLD model, resulted in downregulation of *ACSL1* in all three models, with greatest downregulation observed in TAM model. This indicated that the antitosteatotic effects of LIRA were partly brought on by interfering with the *ACSL1* signaling pathway and lowering triglyceride synthesis. Vildagliptin, another drug that amplifies the effects of the GLP-1R, was shown by Flock et al. to have a comparable effect (163).

Similar to earlier *in vivo* studies, LIRA increased *PPARG* in cells that were incubated only in a low-glucose medium indicating that it is in charge of regulating the lipid balance in hepatocytes. (138). Decara et al. showed that LIRA upregulated lipogenesis-related *PPARG* genes in lean rats whereas in high-fat diet-induced obesity rats, LIRA reduction of lipid accumulation was caused by a reduction in *PPARG* liver expression (138). Accordingly, LIRA mainly decreased *PPARG* expression in our current study when it was added to the NAFLD and DIFLD models. It is also noteworthy that this effect was not dose-dependent and that it could even have been opposite at some LIRA concentrations. The varied functions of *PPARG* in the liver may help to explain this outcome. Numerous studies showed that liver *PPARG* activation has an antifibrotic effect. (79, 164, 165). *PPARG* is required for the inactivation of human hepatic stellate cells (HSCs) and the reversal of liver fibrosis in mice, according to research by Ni et al. and Liu et al. (79, 164). Additionally, *PPARG* prevented the proliferation of HSCs and reduced the production of extracellular matrix by inhibiting the activation of the TGF-1/Smad signalling pathway (78, 79, 166). Finally, *PPARG* agonism increased the sensitivity of muscle, liver, and adipose tissue to insulin. This effect likely overcame *PPARG* negative effects on fat accumulation in hepatocytes and led to a reduction in liver fat which was confirmed in various clinical studies (167-169). Decara et al. demonstrated that in the adipose tissue of HFD-induced obesity-prone rats, LIRA slightly upregulated *PPARG* (138, 139).

In our current study, the impact of LIRA on *CEBPA* gene expression varied, but lacked statistical significance. LIRA cotreatment had a different impact on the hepatocyte steatosis NAFLD and DIFLD models, with the hepatocyte steatosis AMD DIFLD model showing the greatest decrease in *CEBPA* mRNA levels while in hepatocyte steatosis NAFLD and TAM DIFLD model *CEBPA* expression was mostly increased with LIRA co-treatment. Guzman et al. showed that *CEBPA* repressed liver fatty acid binding protein (FABP1) which is in charge of regulating FFAs trafficking and partition as well as preventing the lipotoxicity of FFAs (74). In both human NAFLD and NAFLD in animal models, *CEBPA* was either induced or remained the same (74). However, numerous studies revealed that *CEBPA* also had an antifibrotic effect in the liver which is achieved by inducing HSC apoptosis (75, 170-172). Although numerous studies have demonstrated that LIRA downregulates *CEBPA* expression in adipose tissue when given for longer periods of time, more studies have yet to investigate these effects in the liver (173, 174). Additionally, more research is required to assess role of *CEBPA* in the liver.

In the current study, LIRA co-treatment significantly reduced the expression of *SREBF1* in all three models, confirming the function of the *SREBF1* gene pathway in the antisteatotic effect of LIRA. Wang et al. demonstrated the impact of LIRA on AMPK/SREBP1 pathway-mediated reduction in lipid content in the liver (136). *AMPK* controls the long-term adaptation of lipid metabolism in liver by downregulation of *SREBF1*. Therefore, upregulation of *SREBF1* leads to disturbance in lipid metabolism and accumulation of fat in liver (136).

Our study's primary limitation is the simplification of the NAFLD and DIFLD models established with the Huh7 cell line. However, these *in vitro* models have the benefit of allowing researchers to evaluate the direct impact of LIRA on hepatocytes.

LIRA has demonstrated its hepatoprotective and antisteatotic effects in NAFLD and DIFLD cell culture models established with Huh7 cell line. These effects are attained by reducing the gene expression of several factors (*ACSL1, CEBPA, PPARG*, and *SREBF1*) that contribute to lipid synthesis. Some of these gene pathways' functions in the liver have not yet been fully understood. Overall, our research indicates that LIRA may be crucial in the management of not only NAFLD, but also DIFLD. However, additional research is required to confirm the hepatoprotective function of LIRA in various fatty liver models and to define the precise role of the various gene pathways in the development of fatty liver disease, not only in hepatocytes but also in other liver cells.

7. CONCLUSIONS

Based on this study results, the following conclusions can be drawn:

- Cell viability is decreased in all three models of hepatocyte steatosis – OA-induced NAFLD, AMD-induced DIFLD, and TAM-induced DIFLD. LIRA in lower concentrations slightly increased cell viability in all models.
- Increased lipid accumulation occurred in all three models, with greatest accumulation observed in AMD DIFLD, due to the increase in number of lipid droplets, while OA NAFLD showed greatest increase in average size of lipid droplets, indicating macrosteatosis occurrence. On the contrary both DIFLD models showed microsteatotic changes. LIRA generally significantly reduced lipid accumulation.
- Levels of triglycerides were increased in all models, with greatest increase observed in OA NAFLD, which corresponds to macrosteatotic changes in this model. LIRA reduced significantly triglyceride levels in all hepatocyte steatosis models.
- GSH concentration was significantly reduced in DIFLD models, but not in NAFLD model. LIRA exerted little or no effect on levels of GSH.
- Expression of *ACSL1*, *CEBPA*, *PPARG*, and *SREBF1* gene pathways, which are all involved in lipogenesis was generally increased in all models, except for *PPARG* in TAM DIFLD model. LIRA generally downregulated these gene pathways, with greatest effect observed in *SREBF1* expression. However, *PPARG* and *CEBPA* were even upregulated in some cell groups (negative control, TAM DIFLD), indicating a complex role of these pathways in the liver.
- LIRA co-treatment ameliorates steatosis in hepatocyte steatosis NAFLD and DIFLD models established with Huh7 cell culture by downregulating the expression of lipogenic pathways.

8. SUMMARY

Background and aims: Drug-induced fatty liver disease (DIFLD) has become a common cause of non-alcoholic fatty liver disease (NAFLD) due to the aging of the population and the prevalence of polypharmacy in the elderly. It is possible for NAFLD and DIFLD to coexist which makes it even more crucial to be able to differentiate them. Our aim was to investigate hepatocyte steatosis NAFLD and DIFLD cell culture models and ascertain the effects of liraglutide in those models.

Materials and Methods: To create models of hepatocyte steatosis NAFLD and DIFLD, Huh7 cells were treated with oleic acid, amiodarone, or tamoxifen. Liraglutide was administered to the cells, and MTT was used to measure cell viability, while Erythrosin B color exclusion test was used to confirm results for cell survival. Oil-Red-O staining and a triglyceride assay were used to measure lipid accumulation, GSH assay kit was used for the measurement of GSH concentrations in all three models, and RT-PCR was used to measure intracellular signals involved in hepatosteatosis.

Results: The concentrations of oleic acid, amiodarone, and tamoxifen that achieved 80% cell viability comparing to the negative control were used in subsequent experiments to establish the NAFLD and DIFLD models. Those were 0.5 mM oleic acid, 20 μM amiodarone, and 2 μM tamoxifen, respectively. Liraglutide improved cell viability in all models ($p < 0,01$). All models showed increased lipid accumulation, with DIFLD showing a microsteatotic pattern and NAFLD showing a macrosteatotic pattern, the latter of which corresponds to greater triglyceride accumulation. These steatotic changes were lessened by liraglutide ($p < 0,001$). GSH levels were reduced in all three models of steatosis. Amiodarone and tamoxifen reduced it to 80% compared to DMEM negative control ($p < 0,01$, $p < 0,05$), while effect of OA was smaller. There was no significant difference in GSH concentrations with liraglutide co-treatment. In the hepatocyte steatosis NAFLD and DIFLD models, liraglutide decreased the expression of the lipogenic *ACSL1*, *PPARG*, and *SREBF1* pathways ($p < 0,01$).

Conclusion: In hepatocyte steatosis NAFLD and DIFLD models established with Huh7 cell culture, liraglutide reduced hepatocyte steatosis through downregulation of lipogenic *ACSL1*, *PPARG*, and *SREBF1* pathways.

Keywords: Liraglutide; Non-alcoholic fatty liver disease; Tamoxifen; Amiodarone; Drug Induced Liver Injury; Cell-culture

Utjecaj analoga peptida 1 sličnog glukagonu na mehanizme nastanka lijekovima izazvanog jetrenog oštećenja u staničnim kulturama

9. SAŽETAK

Uvod i ciljevi istraživanja: Masna promjena jetre izazvana lijekovima (DIFLD) postala je čest uzrok nealkoholne masne promjene jetre (NAFLD). zbog starenja stanovništva i raširenosti polifarmacije u starijih osoba. Moguće je da NAFLD i DIFLD koegzistiraju, što čini njihovo razlikovanje još važnijim. Naš je cilj bio istražiti modele NAFLD i DIFLD steatoze hepatocita u staničnoj kulturi i utvrditi učinke liraglutida u tim modelima.

Materijali i metode: Za izradu modela steatoze hepatocita NAFLD i DIFLD, Huh7 stanice su tretirane oleinskom kiselinom, amiodaronom ili tamoksifenom. Liraglutid je dodan kao kotretman u stanice, a MTT je korišten za mjerenje viabilnosti stanica, dok je test isključenja eritrozin B bojom korišten za potvrdu rezultata za preživljavanje stanica. Oil-Red-O bojenje i test triglicerida korišteni su za mjerenje nakupljanja lipida, GSH kit korišten je za mjerenje koncentracija GSH u sva tri modela, a RT-PCR je korišten za mjerenje intracelularnih signala uključenih u hepatosteatozu.

Rezultati: Koncentracije oleinske kiseline, amiodarona i tamoksifena koje su postigle 80% vijabilnosti stanica u usporedbi s negativnom kontrolom korištene su u narednim eksperimentima za uspostavljanje NAFLD i DIFLD modela. Te su koncentracije bile: 0,5 mM oleinske kiseline, 20 μM amiodarona, odnosno 2 μM tamoksifena. Liraglutid je poboljšao vijabilnost stanica u svim modelima ($p < 0,01$). Svi modeli pokazali su povećanu akumulaciju lipida, pri čemu je DIFLD pokazao mikrosteatotsku sliku, a NAFLD makrosteatotsku sliku, od kojih potonji odgovara većoj akumulaciji triglicerida. Liraglutid je smanjio ove steatotične promjene ($p < 0,001$). Razine GSH bile su smanjene u sva tri modela steatoze. Amiodaron i tamoksifen smanjili su ga na 80% u usporedbi s DMEM negativnom kontrolom ($p < 0,01$, $p < 0,05$), dok je učinak OA bio manji. Nije bilo značajne razlike u koncentracijama GSH s kotretmanom LIRA-om. U NAFLD i DIFLD modelu steatoze hepatocita, liraglutid je smanjio ekspresiju lipogenih puteva *ACSL1, PPARG* i *SREBF1* ($p < 0,01$).

Zaključak: U NAFLD i DIFLD modelima steatoze hepatocita uspostavljenim s Huh7 staničnom kulturom, liraglutid je smanjio steatozu hepatocita kroz regulaciju lipogenih puteva *ACSL1, PPARG* i *SREBF1*.

Ključne riječi: Liraglutid; Nealkoholna masna promjena jetre; Tamoksifen; Amiodaron; Lijekovima uzrokovano oštećenje jetre; Stanična kultura

10. REFERENCES

1. Zhou Y, Wang J, Zhang D, Liu J, Wu Q, Chen J, et al. Mechanism of drug-induced liver injury and hepatoprotective effects of natural drugs. Chin Med. 2021;16(1):135.
2. European Association for the Study of the Liver. EASL Clinical Practice Guidelines: Drug-induced liver injury. J Hepatol. 2019;70(6):1222-61.
3. Ntamo Y, Ziqubu K, Chellan N, Nkambule BB, Nyambuya TM, Mazibuko-Mbeje SE, et al. Drug-Induced Liver Injury: Clinical Evidence of N-Acetyl Cysteine Protective Effects. Oxid Med Cell Longev. 2021;3320325.
4. Eslam M, Sanyal AJ, George J, Panel IC. MAFLD: A Consensus-Driven Proposed Nomenclature for Metabolic Associated Fatty Liver Disease. Gastroenterology. 2020;158(7):1999-2014.e1.
5. Ding WX, Yang L. Alcohol and drug-induced liver injury: Metabolism, mechanisms, pathogenesis and potential therapies. Liver Res. 2019;3(3-4):129-31.
6. Benić MS, Nežić L, Vujić-Aleksić V, Mititelu-Tartau L. Novel Therapies for the Treatment of Drug-Induced Liver Injury: A Systematic Review. Front Pharmacol. 2021;12:785790.
7. Hoofnagle JH, Björnsson ES. Drug-Induced Liver Injury - Types and Phenotypes. N Engl J Med. 2019;381(3):264-73.
8. easloffice@easloffice.eu EAftSotLEa, Chair: CPGP, members P, representative: EGB. EASL Clinical Practice Guidelines: Drug-induced liver injury. J Hepatol. 2019;70(6):1222-61.
9. Kuna L, Bozic I, Kizivat T, Bojanic K, Mrso M, Kralj E, et al. Models of Drug Induced Liver Injury (DILI) - Current Issues and Future Perspectives. Curr Drug Metab. 2018;19(10):830-8.
10. Weiler S, Merz M, Kullak-Ublick GA. Drug-induced liver injury: the dawn of biomarkers? F1000Prime Rep. 2015;7:34.
11. Sundaram V, Björnsson ES. Drug-induced cholestasis. Hepatol Commun. 2017;1(8):726-35.
12. Kolarić TO, Ninčević V, Smolić R, Smolić M, Wu GY. Mechanisms of Hepatic Cholestatic Drug Injury. J Clin Transl Hepatol. 2019;7(1):86-92.
13. Ghabril M, Chalasani N, Björnsson E. Drug-induced liver injury: a clinical update. Curr Opin Gastroenterol. 2010;26(3):222-6.
14. Fu S, Wu D, Jiang W, Li J, Long J, Jia C, et al. Molecular Biomarkers in Drug-Induced Liver Injury: Challenges and Future Perspectives. Front Pharmacol. 2019;10:1667.

15. Devarbhavi H. An Update on Drug-induced Liver Injury. J Clin Exp Hepatol. 2012;2(3):247-59.

16. Shen T, Liu Y, Shang J, Xie Q, Li J, Yan M, et al. Incidence and Etiology of Drug-Induced Liver Injury in Mainland China. Gastroenterology. 2019;156(8):2230-41.e11.

17. Padda MS, Sanchez M, Akhtar AJ, Boyer JL. Drug-induced cholestasis. Hepatology. 2011;53(4):1377-87.

18. Grieco A, Forgione A, Miele L, Vero V, Greco AV, Gasbarrini A, et al. Fatty liver and drugs. Eur Rev Med Pharmacol Sci. 2005;9(5):261-3.

19. Rabinowich L, Shibolet O. Drug Induced Steatohepatitis: An Uncommon Culprit of a Common Disease. Biomed Res Int. 2015;2015:168905.

20. Eslam M, Newsome PN, Sarin SK, Anstee QM, Targher G, Romero-Gomez M, et al. A new definition for metabolic dysfunction-associated fatty liver disease: An international expert consensus statement. J Hepatol. 2020;73(1):202-9.

21. Farrell GC. Drugs and steatohepatitis. Semin Liver Dis. 2002;22(2):185-94.

22. Satapathy SK, Kuwajima V, Nadelson J, Atiq O, Sanyal AJ. Drug-induced fatty liver disease: An overview of pathogenesis and management. Ann Hepatol. 2015;14(6):789-806.

23. Kotiloglu G, Aki ZS, Ozyilkan O, Kutlay L. Tamoxifen-induced cirrhotic process. Breast J. 2001;7(6):442-3.

24. Buggey J, Kappus M, Lagoo AS, Brady CW. Amiodarone-Induced Liver Injury and Cirrhosis. ACG Case Rep J. 2015;2(2):116-8.

25. Kolaric TO, Nincevic V, Kuna L, Duspara K, Bojanic K, Vukadin S, et al. Drug-induced Fatty Liver Disease: Pathogenesis and Treatment. J Clin Transl Hepatol. 2021;9(5):731-7.

26. Özkan A, Stolley D, Cressman ENK, McMillin M, DeMorrow S, Yankeelov TE, et al. The Influence of Chronic Liver Diseases on Hepatic Vasculature: A Liver-on-a-chip Review. Micromachines (Basel). 2020;11(5).

27. Tsuda T, Tada H, Tanaka Y, Nishida N, Yoshida T, Sawada T, et al. Amiodarone-induced reversible and irreversible hepatotoxicity: two case reports. J Med Case Rep. 2018;12(1):95.

28. Daneshvar F. AMIODARONE-INDUCED CIRRHOSIS: A WELL KNOWN UNDERRECOGNIZED COMPLICATION. Journal of the American College of Cardiology; March 30, 2020; 75 (11_Supplement_1) 2307

29. Lewis JH, Ranard RC, Caruso A, Jackson LK, Mullick F, Ishak KG, et al. Amiodarone hepatotoxicity: prevalence and clinicopathologic correlations among 104 patients. Hepatology. 1989;9(5):679-85.

30. Huang CH, Lai YY, Kuo YJ, Yang SC, Chang YJ, Chang KK, et al. Amiodarone and risk of liver cirrhosis: a nationwide, population-based study. Ther Clin Risk Manag. 2019;15:103-12.

31. Schumacher JD, Guo GL. Mechanistic review of drug-induced steatohepatitis. Toxicol Appl Pharmacol. 2015;289(1):40-7.

32. Bjornsson ES. Epidemiology, Predisposing Factors, and Outcomes of Drug-Induced Liver Injury. Clin Liver Dis. 2020;24(1):1-10.

33. Kleiner DE, Chalasani NP, Lee WM, Fontana RJ, Bonkovsky HL, Watkins PB, et al. Hepatic histological findings in suspected drug-induced liver injury: systematic evaluation and clinical associations. Hepatology. 2014;59(2):661-70.

34. Zimmerman HJ. Hepatotoxicity: The Adverse Effects of Drugs and Other Chemicals on the Liver. Second ed. Philadelphia: Lippincot, Williams & Wilkins; 1999.

35. Macsween , RMN, Burt , AD, Portmann , BC, et al. Pathology of the Liver. 4th edition London: ELSEVIER; 2002.

36. Ramachandran R, Kakar S. Histological patterns in drug-induced liver disease. J Clin Pathol. 2009;62(6):481-92.

37. Chalasani N, Bonkovsky HL, Fontana R, Lee W, Stolz A, Talwalkar J, et al. Features and Outcomes of 899 Patients With Drug-Induced Liver Injury: The DILIN Prospective Study. Gastroenterology. 2015;148(7):1340-52.e7.

38. Allard J, Le Guillou D, Begriche K, Fromenty B. Drug-induced liver injury in obesity and nonalcoholic fatty liver disease. Adv Pharmacol. 2019;85:75-107.

39. Lettéron P, Sutton A, Mansouri A, Fromenty B, Pessayre D. Inhibition of microsomal triglyceride transfer protein: another mechanism for drug-induced steatosis in mice. Hepatology. 2003;38(1):133-40.

40. Lauressergues E, Staels B, Valeille K, Majd Z, Hum DW, Duriez P, et al. Antipsychotic drug action on SREBPs-related lipogenesis and cholesterogenesis in primary rat hepatocytes. Naunyn Schmiedebergs Arch Pharmacol. 2010;381(5):427-39.

41. Chaggar PS, Shaw SM, Williams SG. Effect of antipsychotic medications on glucose and lipid levels. J Clin Pharmacol. 2011;51(5):631-8.

42. Miele L, Liguori A, Marrone G, Biolato M, Araneo C, Vaccaro FG, et al. Fatty liver and drugs: the two sides of the same coin. Eur Rev Med Pharmacol Sci. 2017;21(1 Suppl):86-94.

43. Fromenty B, Pessayre D. Inhibition of mitochondrial beta-oxidation as a mechanism of hepatotoxicity. Pharmacol Ther. 1995;67(1):101-54.

44. Dowman JK, Tomlinson JW, Newsome PN. Pathogenesis of non-alcoholic fatty liver disease. QJM. 2010;103(2):71-83.

45. Pessayre D, Berson A, Fromenty B, Mansouri A. Mitochondria in steatohepatitis. Semin Liver Dis. 2001;21(1):57-69.

46. Begriche K, Massart J, Robin MA, Borgne-Sanchez A, Fromenty B. Drug-induced toxicity on mitochondria and lipid metabolism: mechanistic diversity and deleterious consequences for the liver. J Hepatol. 2011;54(4):773-94.

47. Suzuki A, Brunt E, Kleiner D, al. e. The use of liver biopsy evaluation in discrimination of idiopathic autoimmune hepatitis versus drug-induced liver injury. Hepatology. 2011;54(3):931–9.

48. Crawford JM. Histologic findings in alcoholic liver disease. Clin Liver Dis. 2012;16(4):699-716.

49. Fromenty B, Berson A, Pessayre D. Microvesicular steatosis and steatohepatitis: role of mitochondrial dysfunction and lipid peroxidation. J Hepatol. 1997;26 Suppl 1:13-22.

50. Pavlik L, Regev A, Ardayfio PA, Chalasani NP. Drug-Induced Steatosis and Steatohepatitis: The Search for Novel Serum Biomarkers Among Potential Biomarkers for Non-Alcoholic Fatty Liver Disease and Non-Alcoholic Steatohepatitis. Drug Saf. 2019;42(6):701-11.

51. Massart J, Begriche K, Moreau C, Fromenty B. Role of nonalcoholic fatty liver disease as risk factor for drug-induced hepatotoxicity. J Clin Transl Res. 2017;3(Suppl 1):212-32.

52. Lee J, Homma T, Kurahashi T, Kang ES, Fujii J. Oxidative stress triggers lipid droplet accumulation in primary cultured hepatocytes by activating fatty acid synthesis. Biochem Biophys Res Commun. 2015;464(1):229-35.

53. Miele L, Valenza V, La Torre G, Montalto M, Cammarota G, Ricci R, et al. Increased intestinal permeability and tight junction alterations in nonalcoholic fatty liver disease. Hepatology. 2009;49(6):1877-87.

54. Cani PD, Amar J, Iglesias MA, Poggi M, Knauf C, Bastelica D, et al. Metabolic endotoxemia initiates obesity and insulin resistance. Diabetes. 2007;56(7):1761-72.

55. Tilg H, Moschen AR. Evolution of inflammation in nonalcoholic fatty liver disease: the multiple parallel hits hypothesis. Hepatology. 2010;52(5):1836-46.

56. Dongiovanni P, Valenti L. Genetics of nonalcoholic fatty liver disease. Metabolism. 2016;65(8):1026-37

57. Morse BL, Kim RB. Is personalized medicine a dream or a reality? Crit Rev Clin Lab Sci. 2015;52(1):1-11.

58. Marino JS, Stechschulte LA, Stec DE, Nestor-Kalinoski A, Coleman S, Hinds TD. Glucocorticoid Receptor β Induces Hepatic Steatosis by Augmenting Inflammation and Inhibition of the Peroxisome Proliferator-activated Receptor (PPAR) α. J Biol Chem. 2016;291(50):25776-88.

59. Grieco A, Vecchio FM, Natale L, Gasbarrini G. Acute fatty liver after malaria prophylaxis with mefloquine. Lancet. 1999;353(9149):295-6.

60. Bruno S, Maisonneuve P, Castellana P, Rotmensz N, Rossi S, Maggioni M, et al. Incidence and risk factors for non-alcoholic steatohepatitis: prospective study of 5408 women enrolled in Italian tamoxifen chemoprevention trial. BMJ. 2005;330(7497):932.

61. Ninčević V, Omanović Kolarić T, Roguljić H, Kizivat T, Smolić M, Bilić Ćurčić I. Renal Benefits of SGLT 2 Inhibitors and GLP-1 Receptor Agonists: Evidence Supporting a Paradigm Shift in the Medical Management of Type 2 Diabetes. Int J Mol Sci. 2019;20(23).

62. Amacher DE, Chalasani N. Drug-induced hepatic steatosis. Semin Liver Dis. 2014;34(2):205-14.

63. Akbay E, Erdem B, Ünlü A, Durukan AB, Onur MA. Effects of N-acetyl cysteine, vitamin E and vitamin C on liver glutathione levels following amiodarone treatment in rats. Kardiochir Torakochirurgia Pol. 2019;16(2):88-92.

64. Kim G, Choi HK, Lee H, Moon KS, Oh JH, Lee J, et al. Increased hepatic acylcarnitines after oral administration of amiodarone in rats. J Appl Toxicol. 2020.

65. Massart J, Begriche K, Buron N, Porceddu M, Borgne-Sanchez A, Fromenty B. Drug-Induced Inhibition of Mitochondrial Fatty Acid Oxidation and Steatosis. Current Pathobiology Reports. 2013;1(3):147-57.

66. Fromenty B, Fisch C, Labbe G, Degott C, Deschamps D, Berson A, et al. Amiodarone inhibits the mitochondrial beta-oxidation of fatty acids and produces microvesicular steatosis of the liver in mice. J Pharmacol Exp Ther. 1990;255(3):1371-6.

67. Anthérieu S, Rogue A, Fromenty B, Guillouzo A, Robin MA. Induction of vesicular steatosis by amiodarone and tetracycline is associated with up-regulation of lipogenic genes in HepaRG cells. Hepatology. 2011;53(6):1895-905.

68. Cole LK, Jacobs RL, Vance DE. Tamoxifen induces triacylglycerol accumulation in the mouse liver by activation of fatty acid synthesis. Hepatology. 2010;52(4):1258-65.

69. Zhao F, Xie P, Jiang J, Zhang L, An W, Zhan Y. The effect and mechanism of tamoxifen-induced hepatocyte steatosis in vitro. Int J Mol Sci. 2014;15(3):4019-30.

70. Suddek GM. Protective role of thymoquinone against liver damage induced by tamoxifen in female rats. Can J Physiol Pharmacol. 2014;92(8):640-4.

71. Li T, Li X, Meng H, Chen L, Meng F. ACSL1 affects Triglyceride Levels through the PPARγ Pathway. Int J Med Sci. 2020;17(6):720-7.

72. Li LO, Ellis JM, Paich HA, Wang S, Gong N, Altshuller G, et al. Liver-specific loss of long chain acyl-CoA synthetase-1 decreases triacylglycerol synthesis and beta-oxidation and alters phospholipid fatty acid composition. J Biol Chem. 2009;284(41):27816-26.

73. Kawano Y, Cohen DE. Mechanisms of hepatic triglyceride accumulation in non-alcoholic fatty liver disease. J Gastroenterol. 2013;48(4):434-41.

74. Guzmán C, Benet M, Pisonero-Vaquero S, Moya M, García-Mediavilla MV, Martínez-Chantar ML, et al. The human liver fatty acid binding protein (FABP1) gene is activated by FOXA1 and PPARα; and repressed by C/EBPα: Implications in FABP1 down-regulation in nonalcoholic fatty liver disease. Biochim Biophys Acta. 2013;1831(4):803-18.

75. Tao LL, Ding D, Yin WH, Peng JY, Hou CJ, Liu XP, et al. TSA increases C/EBP-α expression by increasing its lysine acetylation in hepatic stellate cells. Mol Med Rep. 2017;16(5):6088-93.

76. Wandrer F, Frangež Ž, Liebig S, John K, Vondran F, Wedemeyer H, et al. Autophagy alleviates amiodarone-induced hepatotoxicity. Arch Toxicol. 2020;94(10):3527-39.

77. Singh AB, Kan CF, Dong B, Liu J. SREBP2 Activation Induces Hepatic Long-chain Acyl-CoA Synthetase 1 (ACSL1) Expression in Vivo and in Vitro through a Sterol Regulatory Element (SRE) Motif of the ACSL1 C-promoter. J Biol Chem. 2016;291(10):5373-84.

78. Wang Y, Nakajima T, Gonzalez FJ, Tanaka N. PPARs as Metabolic Regulators in the Liver: Lessons from Liver-Specific PPAR-Null Mice. Int J Mol Sci. 2020;21(6).

79. Ni XX, Li XY, Wang Q, Hua J. Regulation of peroxisome proliferator-activated receptor-gamma activity affects the hepatic stellate cell activation and the progression of NASH via TGF-β1/Smad signaling pathway. J Physiol Biochem. 2021;77(1):35-45.

80. Kremer JM, Galivan J, Streckfuss A, Kamen B. Methotrexate metabolism analysis in blood and liver of rheumatoid arthritis patients. Association with hepatic folate deficiency and formation of polyglutamates. Arthritis Rheum. 1986;29(7):832-5.

81. Tabassum H, Parvez S, Pasha ST, Banerjee BD, Raisuddin S. Protective effect of lipoic acid against methotrexate-induced oxidative stress in liver mitochondria. Food Chem Toxicol. 2010;48(7):1973-9.

82. Bath RK, Brar NK, Forouhar FA, Wu GY. A review of methotrexate-associated hepatotoxicity. J Dig Dis. 2014;15(10):517-24.

83. Meunier L, Larrey D. Chemotherapy-associated steatohepatitis. Ann Hepatol. 2020 Nov-Dec;19(6):597-601.

84. Labbe G, Pessayre D, Fromenty B. Drug-induced liver injury through mitochondrial dysfunction: mechanisms and detection during preclinical safety studies. Fundam Clin Pharmacol. 2008;22(4):335-53.

85. Patel V, Sanyal AJ. Drug-induced steatohepatitis. Clin Liver Dis. 2013;17(4):533-46, vii.

86. Luef G, Rauchenzauner M, Waldmann M, Sturm W, Sandhofer A, Seppi K, et al. Non-alcoholic fatty liver disease (NAFLD), insulin resistance and lipid profile in antiepileptic drug treatment. Epilepsy Res. 2009;86(1):42-7.

87. Szalowska E, van der Burg B, Man HY, Hendriksen PJ, Peijnenburg AA. Model steatogenic compounds (amiodarone, valproic acid, and tetracycline) alter lipid metabolism by different mechanisms in mouse liver slices. PLoS One. 2014;9(1):e86795.

88. Brüning A, Brem GJ, Vogel M, Mylonas I. Tetracyclines cause cell stress-dependent ATF4 activation and mTOR inhibition. Exp Cell Res. 2014;320(2):281-9.

89. Banerjee A, Abdelmegeed MA, Jang S, Song BJ. Zidovudine (AZT) and hepatic lipid accumulation: implication of inflammation, oxidative and endoplasmic reticulum stress mediators. PLoS One. 2013;8(10):e76850.

90. Gardner K, Hall PA, Chinnery PF, Payne BA. HIV treatment and associated mitochondrial pathology: review of 25 years of in vitro, animal, and human studies. Toxicol Pathol. 2014;42(5):811-22.

91. Yu YC, Mao YM, Chen CW, Chen JJ, Chen J, Cong WM, et al. CSH guidelines for the diagnosis and treatment of drug-induced liver injury. Hepatol Int. 2017;11(3):221-41.

92. Ford R, Schwartz L, Dancey J, Dodd LE, Eisenhauer EA, Gwyther S, et al. Lessons learned from independent central review. Eur J Cancer. 2009;45(2):268-74.

93. Wree A, Dechêne A, Herzer K, Hilgard P, Syn WK, Gerken G, et al. Steroid and ursodesoxycholic Acid combination therapy in severe drug-induced liver injury. Digestion. 2011;84(1):54-9.

94. Cicognani C, Malavolti M, Morselli-Labate AM, Sama C, Barbara L. Flutamide-induced toxic hepatitis. Potential utility of ursodeoxycholic acid administration in toxic hepatitis. Dig Dis Sci. 1996;41(11):2219-21.

95. Piotrowicz A, Polkey M, Wilkinson M. Ursodeoxycholic acid for the treatment of flucloxacillin-associated cholestasis. J Hepatol. 1995;22(1):119-20.

96. Kallinowski B, Theilmann L, Zimmermann R, Gams E, Kommerell B, Stiehl A. Effective treatment of cyclosporine-induced cholestasis in heart-transplanted patients treated with ursodeoxycholic acid. Transplantation. 1991;51(5):1128-9.

97. Velayudham LS, Farrell GC. Drug-induced cholestasis. Expert Opin Drug Saf. 2003;2(3):287-304.

98. Poupon RE, Poupon R, Balkau B. Ursodiol for the long-term treatment of primary biliary cirrhosis. The UDCA-PBC Study Group. N Engl J Med. 1994;330(19):1342-7.

99. Poupon RE, Lindor KD, Cauch-Dudek K, Dickson ER, Poupon R, Heathcote EJ. Combined analysis of randomized controlled trials of ursodeoxycholic acid in primary biliary cirrhosis. Gastroenterology. 1997;113(3):884-90.

100. Bataller R, Bragulat E, Nogué S, Görbig MN, Bruguera M, Rodés J. Prolonged cholestasis after acute paraquat poisoning through skin absorption. Am J Gastroenterol. 2000;95(5):1340-3.

101. Katsinelos P, Vasiliadis T, Xiarchos P, Patakiouta F, Christodoulou K, Pilpilidis I, et al. Ursodeoxycholic acid (UDCA) for the treatment of amoxycillin-clavulanate potassium (Augmentin)-induced intra-hepatic cholestasis: report of two cases. Eur J Gastroenterol Hepatol. 2000;12(3):365-8.

102. Wengrower D. Possible ticlopidine-induced cholestatic jaundice. Am Fam Physician. 2000;62(6):1258, 62.

103. Hunt CM, Washington K. Tetracycline-induced bile duct paucity and prolonged cholestasis. Gastroenterology. 1994;107(6):1844-7.

104. Uraz S, Tahan V, Aygun C, Eren F, Unluguzel G, Yuksel M, et al. Role of ursodeoxycholic acid in prevention of methotrexate-induced liver toxicity. Dig Dis Sci. 2008;53(4):1071-7.

105. Younossi ZM. Long-Term Outcomes of Nonalcoholic Fatty Liver Disease: From Nonalcoholic Steatohepatitis to Nonalcoholic Steatofibrosis. Clin Gastroenterol Hepatol. 2017;15(8):1144-7.

106. Ghazanfar H, Kandhi SD, Nawaz I, Javed N, Abraham MC, Farag M, et al. Role of Glucagon-Like Peptide-1 Receptor Agonists in the Management of Non-Alcoholic Steatohepatitis: A Clinical Review Article. Cureus. 2021;13(5):e15141.

107. Povsic M, Wong OY, Perry R, Bottomley J. A Structured Literature Review of the Epidemiology and Disease Burden of Non-Alcoholic Steatohepatitis (NASH). Adv Ther. 2019;36(7):1574-94.

108. Sheka AC, Adeyi O, Thompson J, Hameed B, Crawford PA, Ikramuddin S. Nonalcoholic Steatohepatitis: A Review. JAMA. 2020;323(12):1175-83.

109. Perumpail BJ, Khan MA, Yoo ER, Cholankeril G, Kim D, Ahmed A. Clinical epidemiology and disease burden of nonalcoholic fatty liver disease. World J Gastroenterol. 2017;23(47):8263-76.
110. Brunt EM, Wong VW, Nobili V, Day CP, Sookoian S, Maher JJ, et al. Nonalcoholic fatty liver disease. Nat Rev Dis Primers. 2015;1:15080.
111. Abou Assi R, Abdulbaqi IM, Siok Yee C. The Evaluation of Drug Delivery Nanocarrier Development and Pharmacological Briefing for Metabolic-Associated Fatty Liver Disease (MAFLD): An Update. Pharmaceuticals (Basel). 2021;14(3).
112. Oseini AM, Sanyal AJ. Therapies in non-alcoholic steatohepatitis (NASH). Liver Int. 2017;37 Suppl 1:97-103.
113. Zheng KI, Fan JG, Shi JP, Wong VW, Eslam M, George J, et al. From NAFLD to MAFLD: a "redefining" moment for fatty liver disease. Chin Med J (Engl). 2020;133(19):2271-3.
114. Ferron PJ, Gicquel T, Mégarbane B, Clément B, Fromenty B. Treatments in Covid-19 patients with pre-existing metabolic dysfunction-associated fatty liver disease: A potential threat for drug-induced liver injury? Biochimie. 2020;179:266-74.
115. Kanuri G, Bergheim I. In vitro and in vivo models of non-alcoholic fatty liver disease (NAFLD). Int J Mol Sci. 2013;14(6):11963-80.
116. Ricchi M, Odoardi MR, Carulli L, Anzivino C, Ballestri S, Pinetti A, et al. Differential effect of oleic and palmitic acid on lipid accumulation and apoptosis in cultured hepatocytes. J Gastroenterol Hepatol. 2009;24(5):830-40.
117. Gupta NA, Mells J, Dunham RM, Grakoui A, Handy J, Saxena NK, et al. Glucagon-like peptide-1 receptor is present on human hepatocytes and has a direct role in decreasing hepatic steatosis in vitro by modulating elements of the insulin signaling pathway. Hepatology. 2010;51(5):1584-92.
118. Kudaravalli P, John S. Sucralfate. 2022 Feb 25. In: StatPearls [Internet]. Treasure Island (FL): StatPearls Publishing; 2022 Jan.
119. Armstrong MJ, 2016 BatDSSA. Glucagon-like peptide-1 analogues in nonalcoholic steatohepatitis: From bench to bedside. Clin Liver Dis (Hoboken). 2017;10(2):32-5.
120. Armstrong MJ, Gaunt P, Aithal GP, Barton D, Hull D, Parker R, et al. Liraglutide safety and efficacy in patients with non-alcoholic steatohepatitis (LEAN): a multicentre, double-blind, randomised, placebo-controlled phase 2 study. Lancet. 2016;387(10019):679-90.
121. Kalogirou M, Sinakos E. Treating nonalcoholic steatohepatitis with antidiabetic drugs: Will GLP-1 agonists end the struggle? World J Hepatol. 2018;10(11):790-4.

122. Ohki T, Isogawa A, Iwamoto M, Ohsugi M, Yoshida H, Toda N, et al. The effectiveness of liraglutide in nonalcoholic fatty liver disease patients with type 2 diabetes mellitus compared to sitagliptin and pioglitazone. ScientificWorld Journal. 2012;2012:496453.
123. Feng W, Gao C, Bi Y, Wu M, Li P, Shen S, et al. Randomized trial comparing the effects of gliclazide, liraglutide, and metformin on diabetes with non-alcoholic fatty liver disease. J Diabetes. 2017;9(8):800-9.
124. Shao N, Kuang HY, Hao M, Gao XY, Lin WJ, Zou W. Benefits of exenatide on obesity and non-alcoholic fatty liver disease with elevated liver enzymes in patients with type 2 diabetes. Diabetes Metab Res Rev. 2014;30(6):521-9.
125. Fan H, Pan Q, Xu Y, Yang X. Exenatide improves type 2 diabetes concomitant with non-alcoholic fatty liver disease. Arq Bras Endocrinol Metabol. 2013;57(9):702-8.
126. Dong Y, Lv Q, Li S, Wu Y, Li L, Li J, et al. Efficacy and safety of glucagon-like peptide-1 receptor agonists in non-alcoholic fatty liver disease: A systematic review and meta-analysis. Clin Res Hepatol Gastroenterol. 2017;41(3):284-95.
127. Liava C, Sinakos E. Semaglutide for nonalcoholic steatohepatitis: closer to a solution? Hepatobiliary Surg Nutr. 2021;10(4):541-4.
128. Capehorn MS, Catarig AM, Furberg JK, Janez A, Price HC, Tadayon S, et al. Efficacy and safety of once-weekly semaglutide 1.0mg vs once-daily liraglutide 1.2mg as add-on to 1-3 oral antidiabetic drugs in subjects with type 2 diabetes (SUSTAIN 10). Diabetes Metab. 2020;46(2):100-9.
129. O'Neil PM, Birkenfeld AL, McGowan B, Mosenzon O, Pedersen SD, Wharton S, et al. Efficacy and safety of semaglutide compared with liraglutide and placebo for weight loss in patients with obesity: a randomised, double-blind, placebo and active controlled, dose-ranging, phase 2 trial. Lancet. 2018;392(10148):637-49.
130. Newsome P, Francque S, Harrison S, Ratziu V, Van Gaal L, Calanna S, et al. Effect of semaglutide on liver enzymes and markers of inflammation in subjects with type 2 diabetes and/or obesity. Aliment Pharmacol Ther. 2019;50(2):193-203.
131. Marso SP, Bain SC, Consoli A, Eliaschewitz FG, Jódar E, Leiter LA, et al. Semaglutide and Cardiovascular Outcomes in Patients with Type 2 Diabetes. N Engl J Med. 2016;375(19):1834-44.
132. Li S, Wang X, Zhang J, Li J, Liu X, Ma Y, et al. Exenatide ameliorates hepatic steatosis and attenuates fat mass and FTO gene expression through PI3K signaling pathway in nonalcoholic fatty liver disease. Braz J Med Biol Res. 2018;51(8):e7299.

133. Møllerhøj MB, Veidal SS, Thrane KT, Oró D, Overgaard A, Salinas CG, et al. Hepatoprotective effects of semaglutide, lanifibranor and dietary intervention in the GAN diet-induced obese and biopsy-confirmed mouse model of NASH. Clin Transl Sci. 2022;15(5):1167-86.
134. He Y, Ao N, Yang J, Wang X, Jin S, Du J. The preventive effect of liraglutide on the lipotoxic liver injury via increasing autophagy. Ann Hepatol. 2020;19(1):44-52.
135. Yu P, Xu X, Zhang J, Xia X, Xu F, Weng J, et al. Liraglutide Attenuates Nonalcoholic Fatty Liver Disease through Adjusting Lipid Metabolism via SHP1/AMPK Signaling Pathway. Int J Endocrinol. 2019;2019:1567095.
136. Wang YG, Yang TL. Liraglutide reduces fatty degeneration in hepatic cells via the AMPK/SREBP1 pathway. Exp Ther Med. 2015;10(5):1777-83.
137. Zhu CG, Luo Y, Wang H, Li JY, Yang J, Liu YX, et al. Liraglutide Ameliorates Lipotoxicity-Induced Oxidative Stress by Activating the NRF2 Pathway in HepG2 Cells. Horm Metab Res. 2020;52(7):532-9.
138. Decara J, Arrabal S, Beiroa D, Rivera P, Vargas A, Serrano A, et al. Antiobesity efficacy of GLP-1 receptor agonist liraglutide is associated with peripheral tissue-specific modulation of lipid metabolic regulators. Biofactors. 2016;42(6):600-11.
139. Kim KS, Lee BW. Beneficial effect of anti-diabetic drugs for nonalcoholic fatty liver disease. Clin Mol Hepatol. 2020;26(4):430-43.
140. Collection ATC. MTT Cell Proliferation Assay 2011. Available from: https://www.atcc.org/~/media/DA5285A1F52C414E864C966FD78C9A79.ashx. Date of access: 14.05.2022.
141. Strober W. Trypan blue exclusion test of cell viability. Curr Protoc Immunol. 2001;Appendix 3:Appendix 3B.
142. Zjalić M, Mustapić M, Glumac Z, Prološčić I, Blažetić S, Vuković A, et al. Construction of AC/DC magnetic syringe device for stimulated drug release, injection and ejection of nanocarriers and testing cytotoxicity. MethodsX. 2021;8:101312.
143. Akerboom TP, Sies H. Assay of glutathione, glutathione disulfide, and glutathione mixed disulfides in biological samples. Methods Enzymol. 1981;77:373-82.
144. Nair S, Singh SV, Krishan A. Flow cytometric monitoring of glutathione content and anthracycline retention in tumor cells. Cytometry. 1991;12(4):336-42.
145. Kizivat T, Smolić M, Marić I, Tolušić Levak M, Smolić R, Bilić Čurčić I, et al. Antioxidant Pre-Treatment Reduces the Toxic Effects of Oxalate on Renal Epithelial Cells in a Cell Culture Model of Urolithiasis. Int J Environ Res Public Health. 2017;14(1).

146. Felser A, Lindinger PW, Schnell D, Kratschmar DV, Odermatt A, Mies S, et al. Hepatocellular toxicity of benzbromarone: effects on mitochondrial function and structure. Toxicology. 2014;324:136-46.
147. Allard J, Bucher S, Massart J, Ferron PJ, Le Guillou D, Loyant R, et al. Drug-induced hepatic steatosis in absence of severe mitochondrial dysfunction in HepaRG cells: proof of multiple mechanism-based toxicity. Cell Biol Toxicol. 2021;37(2):151-75.
148. Zhou Y, Hua J, Barritt G, Liu Y, Tang BZ, Tang Y. Live Imaging and Quantitation of Lipid Droplets and Mitochondrial Membrane Potential Changes with Aggregation-Induced Emission Luminogens in an in Vitro Model of Liver Steatosis. Chembiochem. 2019;20(10):1256-9.
149. Vitins AP, Kienhuis AS, Speksnijder EN, Roodbergen M, Luijten M, van der Ven LT. Mechanisms of amiodarone and valproic acid induced liver steatosis in mouse in vivo act as a template for other hepatotoxicity models. Arch Toxicol. 2014;88(8):1573-88.
150. Sanoh S, Yamachika Y, Tamura Y, Kotake Y, Yoshizane Y, Ishida Y, et al. Assessment of amiodarone-induced phospholipidosis in chimeric mice with a humanized liver. J Toxicol Sci. 2017;42(5):589-96.
151. Leal S, Rocha L, Silva A, Faria J, Dinis-Oliveira RJ, Sá SI. Evaluation of progressive hepatic histopathology in long-term tamoxifen therapy. Pathol Res Pract. 2018;214(12):2115-20.
152. Resende AD, Leal S, Batista-Pinto C, Garcez F, Sá SI. Hepatic effects of long-term tamoxifen administration to cycling female rats. J Biochem Mol Toxicol. 2019;33(5):e22293.
153. Takahashi Y, Fukusato T. Histopathology of nonalcoholic fatty liver disease/nonalcoholic steatohepatitis. World J Gastroenterol. 2014;20(42):15539-48.
154. Tandra S, Yeh MM, Brunt EM, Vuppalanchi R, Cummings OW, Ünalp-Arida A, et al. Presence and significance of microvesicular steatosis in nonalcoholic fatty liver disease. J Hepatol. 2011;55(3):654-9.
155. Delli Bovi AP, Marciano F, Mandato C, Siano MA, Savoia M, Vajro P. Oxidative Stress in Non-alcoholic Fatty Liver Disease. An Updated Mini Review. Front Med (Lausanne). 2021;8:595371.
156. Zeng S, Wu F, Chen M, Li Y, You M, Zhang Y, et al. Inhibition of Fatty Acid Translocase (FAT/CD36) Palmitoylation Enhances Hepatic Fatty Acid β-Oxidation by Increasing Its Localization to Mitochondria and Interaction with Long-Chain Acyl-CoA Synthetase 1. Antioxid Redox Signal. 2022 Jun;36(16-18):1081-1100.

157. Yang Z, Yu GL, Zhu X, Peng TH, Lv YC. Critical roles of FTO-mediated mRNA m6A demethylation in regulating adipogenesis and lipid metabolism: Implications in lipid metabolic disorders. Genes Dis. 2022;9(1):51-61.
158. Ao N, Ma Z, Yang J, Jin S, Zhang K, Luo E, et al. Liraglutide ameliorates lipotoxicity-induced inflammation through the mTORC1 signalling pathway. Peptides. 2020;133:170375.
159. Petit JM, Cercueil JP, Loffroy R, Denimal D, Bouillet B, Fourmont C, et al. Effect of Liraglutide Therapy on Liver Fat Content in Patients With Inadequately Controlled Type 2 Diabetes: The Lira-NAFLD Study. J Clin Endocrinol Metab. 2017;102(2):407-15.
160. Yang M, Ma X, Xuan X, Deng H, Chen Q, Yuan L. Liraglutide Attenuates Non-Alcoholic Fatty Liver Disease in Mice by Regulating the Local Renin-Angiotensin System. Front Pharmacol. 2020;11:432.
161. Song JX, An JR, Chen Q, Yang XY, Jia CL, Xu S, et al. Liraglutide attenuates hepatic iron levels and ferroptosis in db/db mice. Bioengineered. 2022;13(4):8334-48.
162. Guo J, Li C, Yang C, Li B, Wei J, Lin Y, et al. Liraglutide reduces hepatic glucolipotoxicity-induced liver cell apoptosis through NRF2 signaling in Zucker diabetic fatty rats. Mol Med Rep. 2018;17(6):8316-24.
163. Flock G, Baggio LL, Longuet C, Drucker DJ. Incretin receptors for glucagon-like peptide 1 and glucose-dependent insulinotropic polypeptide are essential for the sustained metabolic actions of vildagliptin in mice. Diabetes. 2007;56(12):3006-13.
164. Liu X, Xu J, Rosenthal S, Zhang LJ, McCubbin R, Meshgin N, et al. Identification of Lineage-Specific Transcription Factors That Prevent Activation of Hepatic Stellate Cells and Promote Fibrosis Resolution. Gastroenterology. 2020;158(6):1728-44.e14.
165. Li J, Guo C, Wu J. The Agonists of Peroxisome Proliferator-Activated Receptor-γ for Liver Fibrosis. Drug Des Devel Ther. 2021;15:2619-28.
166. Quintero P, Arrese M. Nuclear control of inflammation and fibrosis in nonalcoholic steatohepatitis: therapeutic potential of dual peroxisome proliferator-activated receptor alpha/delta agonism. Hepatology. 2013;58(6):1881-4.
167. Bril F, Kalavalapalli S, Clark VC, Lomonaco R, Soldevila-Pico C, Liu IC, et al. Response to Pioglitazone in Patients With Nonalcoholic Steatohepatitis With vs Without Type 2 Diabetes. Clin Gastroenterol Hepatol. 2018;16(4):558-66.e2.
168. Sanyal AJ, Chalasani N, Kowdley KV, McCullough A, Diehl AM, Bass NM, et al. Pioglitazone, vitamin E, or placebo for nonalcoholic steatohepatitis. N Engl J Med. 2010;362(18):1675-85.

169. Cusi K, Orsak B, Bril F, Lomonaco R, Hecht J, Ortiz-Lopez C, et al. Long-Term Pioglitazone Treatment for Patients With Nonalcoholic Steatohepatitis and Prediabetes or Type 2 Diabetes Mellitus: A Randomized Trial. Ann Intern Med. 2016;165(5):305-15.
170. Mei S, Wang X, Zhang J, Qian J, Ji J. In vivo transfection of C/EBP-alpha gene could ameliorate CCL(4)-induced hepatic fibrosis in mice. Hepatol Res. 2007;37(7):531-9.
171. Tao LL, Cheng YY, Ding D, Mei S, Xu JW, Yu J, et al. C/EBP-α ameliorates CCl(4)-induced liver fibrosis in mice through promoting apoptosis of hepatic stellate cells with little apoptotic effect on hepatocytes in vitro and in vivo. Apoptosis. 2012;17(5):492-502.
172. Wang X, Huang G, Mei S, Qian J, Ji J, Zhang J. Over-expression of C/EBP-alpha induces apoptosis in cultured rat hepatic stellate cells depending on p53 and peroxisome proliferator-activated receptor-gamma. Biochem Biophys Res Commun. 2009;380(2):286-91.
173. Liu H, Zhan YL, Luo GJ, Zou LL, Li Y, Lu HY. Liraglutide and Insulin Have Contrary Effects on Adipogenesis of Human Adipose-Derived Stem Cells via Wnt Pathway. Diabetes Metab Syndr Obes. 2020;13:3075-87.
174. Sanz C, Vázquez P, Blázquez C, Barrio PA, Alvarez MeM, Blázquez E. Signaling and biological effects of glucagon-like peptide 1 on the differentiation of mesenchymal stem cells from human bone marrow. Am J Physiol Endocrinol Metab. 2010;298(3):E634-43.

11. CURRICULUM VITAE

First and Last Name: Tea Omanović Kolarić

Address: Šandora Petefija 17, 31000, Osijek, Croatia

Email address: tomanovic@mefos.hr

Phone number: (+385) 958839151

WORK EXPERIENCE

[13/05/2018 – Current] **Resident in Family medicine**

Faculty of Medicine Osijek/Faculty of Dental Medicine and Health

[30/09/2015 – Current] **University Research/Teaching Assistant**

Faculty of Dental Medicine and Health/Faculty of Medicine Osijek

[31/10/2016 – 30/03/2017] **Internship**

Health Center Osijek

EDUCATION AND TRAINING

[13/05/2018 – Current] **Resident in Family Medicine**

Faculty of Medicine/Faculty of Dental Medicine and Health Osijek

Address: J. Huttlera, 4/Crkvena, 21, 31000, Osijek, Croatia

[2015 – Current] **PhD student**

Postgraduate doctoral study of Biomedicine and health

Address: J. Huttlera, 4, 31000, Osijek, Croatia

[2008 – 2015] **Medical doctor**

Faculty of Medicine Osijek, University of J.J. Strossmayer in Osijek

Address: J. Huttlera, 4, 31000, Osijek, Croatia

[2004 – 2009] **High school graduate**

Catholic School Center Gymnasium

Address: 72000, Zenica, Bosnia and Herzegovina

[2004 – 2009] **Pianist**

Music High School

Address: 72000, Zenica, Bosnia and Herzegovina

HONOURS AND AWARDS

[2017]

Dean's Award for the annual seminar paper "The molecular mechanisms involved in the development of Drug-Induced Fatty Liver Disease (DIFLD) models and the use of Glucagon-like peptide-1 (GLP-1) analogues in the therapy of DIFLD in vitro"

Awarding institution: Faculty of Medicine Osijek

[2009] **Student of the generation;**

Awarding institution: Music High School

PUBLICATIONS

Omanovic Kolaric T, Kizivat T, Mihaljevic V, Zjalic M, Bilic-Curcic I, Kuna L, Smolic R, Vcev A, Wu G, Smolic M. Liraglutide exerts protective effects by downregulation of PPARγ, ACSL1 and SREBP-1c in Huh7 cell culture models of non-alcoholic steatosis and drug-induced steatosis. Curr Issues Mol Biol. 2022;44;3465–3480.

Ninčević V, Zjalić M, **Kolarić TO**, Smolić M, Kizivat T, Kuna L, et al. Renoprotective Effect of Liraglutide Is Mediated via the Inhibition of TGF-Beta 1 in an LLC-PK1 Cell Model of Diabetic Nephropathy. Curr Issues Mol Biol. 2022;44(3):1087-114.

Kuna L, Zjalic M, Kizivat T, Roguljic H, Nincevic V, **Omanovic Kolaric** T, et al. Pretreatment of Garlic Oil Extracts Hampers Epithelial Damage in Cell Culture Model of Peptic Ulcer Disease. Medicina (Kaunas). 2022;58(1)

Kolaric TO, Nincevic V, Kuna L, Duspara K, Bojanic K, Vukadin S, et al. Drug-induced Fatty Liver Disease: Pathogenesis and Treatment. J Clin Transl Hepatol. 2021;9(5):731-7.

Duspara K, Bojanic K, Pejic JI, Kuna L, **Kolaric TO**, Nincevic V, et al. Targeting the Wnt Signaling Pathway in Liver Fibrosis for Drug Options: An Update. J Clin Transl Hepatol. 2021;9(6):960-71.

Kishta S, Tabll A, **Omanovic Kolaric T**, Smolic R, Smolic M. Risk Factors Contributing to the Occurrence and Recurrence of Hepatocellular Carcinoma in Hepatitis C Virus Patients Treated with Direct-Acting Antivirals. Biomedicines. 2020;8(6).

Ninčević V; Kizivat T; **Omanović Kolarić T**; Kuna L; Cindrić A; Banovac A, et al. Influence of caffei**ne on crystallization and amelioration ofoxidative stress on in vitro model of urolithiasis.** Collegium antropologicum, 44 (2020), 3; 121-125 doi:10.5671/ca.44.3.2

Ninčević V, **Omanović Kolarić T**, Roguljić H, Kizivat T, Smolić M, Bilić Ćurčić I. Renal Benefits of SGLT 2 Inhibitors and GLP-1 Receptor Agonists: Evidence Supporting a Paradigm Shift in the Medical Management of Type 2 Diabetes. Int J Mol Sci. 2019;20(23).

Kolarić TO, Ninčević V, Smolić R, Smolić M, Wu GY. Mechanisms of Hepatic Cholestatic Drug Injury. J Clin Transl Hepatol. 2019;7(1):86-92.

Raguz Lucic N, Jakab J, Smolic M, Milas AM, **Omanovic Kolaric** T, Nincevic V, et al. Primary Care Provider Counseling Practices about Adverse Drug Reactions and Interactions in Croatia. J Clin Med. 2018;7(9).

Smolić M; **Omanović T**; Božić I; Bilić-Čurčić I; Smolić R; Včev A. Pharmacogenomic Testing in the Era of Patient- Tailored HCV Treatment. Update on Hepatitis C / Smolić, Martina; Včev, Aleksandar ; Y. Wu, George (ur.). Rijeka: InTech, 2017. str. 173-189

Božić I; Omanović T; Kuna L; Kizivat T; Smolić R; Včev A; Smolić Martina. **Pharmacogenomics: sex gender differences and application in pediatrics.** Southeastern European medical journal, 1 (2017), 1; 108-120

PROJECTS

MEFOS-IP-2021, Osobitosti izražaja biljega i gena endotelne disfunkcije u

bolesnika sa šećerenom bolesti tipa 2 liječenih SGLT2 inhibitorima, suradnik

MEFOS-IP 2019, Procjena staničnih modela za poboljšanu predikciju

lijekovima uzrokovane masne promjene jetre (IP2019-10), suradnik

FDMZ-VIF 2018, Osobitosti tamoksifenom izazvane steatoze i

steatohepatitisa u modelu metabolički funkcionalnih ljudskih jetrenih stanica", voditelj

ZUP 2018, Razlike u pojavnosti hipoglikemije nakon treninga jakosti I aerobnog tipa vježbanja u bolesnika sa šećernom bolesti tipa 1 (ZUP2018-90), suradnik

MEFOS-VIF 2018, Osobitosti amiodaronom izazvane steatoze i steatohepatitisa u modelu metabolički funkcionalnih ljudskih jetrenih stanica (VIF2018-MEFOS-10), suradnik

MEFOS-VIF 2017, Osteoblastični biljezi u procjeni nuspojava inhibitorima aromataze (VIF2017- MEFOS-5) suradnik

MEFOS- VIF 2016, Molekularni mehanizmi djelovanja liraglutida u staničnim modelima gastrointestinalnih i kardiovaskularnih bolesti, suradnik

CONFERENCES AND SEMINARS

[26/09/2018 – 29/09/2018] Kognitivni poremećaji u praksi liječnika obiteljske medicine. Zlatibor, Srbija; IX Kongres opšte medicine Srbije sa međunarodnim učešćem, **invited lecture**

Omanovic Kolaric, Tea; Nincevic, Vjera; Kizivat, Tomislav; Zjalic, Milorad; Kuna, Lucija; Bili- Curcic, Ines; Smolic, Robert; Vcev, Aleksandar; Wu, George; Smolic, Martina; Liraglutide reduces hepatosteatosis in NAFLD and drug-induced fatty liver cell culture models through PPARγ signaling pathway. // 3rd European Fatty Liver Conference; Maastricht, Nizozemska, 2022. str. 1-1

Omanovic Kolaric, Tea; Nincevic, V; Kizivat, Tomislav; Zjalic, Milorad; Kuna, Lucija; Bilic-Curcic, Ines; Smolic, Martina; Assessment of therapeutic effect of liraglutide in newly established cell culture model of non-alcoholic and drug-induced fatty liver disease. // Journal of Hepatology / Angeli, Paolo (ur.); London, UK: ELSEVIER, 2022. str. 718-719 doi:10.1016/S0168-8278(22)01755-X

Omanović Kolarić, Tea; Ninčević, Vjera; Kizivat, Tomislav; Kuna, Lucija; Zjalić, Milorad; Bilić- Ćurčć, Ines; Vukadin, Sonja; Roguljić, Hrvoje; Včev, Aleksandar; Smolić, Martina;

Amiodarone and tamoxifen induced fatty liver injury and possible in vitro protective effect of GLP-1RA cotreatment. // 8th European Congress of Pharmacology; Prag, Češka, 2021. str. 1-1

Kuna, Lucija; Zjalic, Milorad; Kizivat, Tomislav; Roguljic, Hrvoje; Nincevic, Vjera; **Omanovic Kolaric, Tea**; Vcev, Aleksandar; Smolic, Martina; Smolic, Robert; Garlic extracts act synergistically with lansoprazole against sodium taurocholate-induced ulcer disease in AGS cell culture model// 8th European Virtual Congress of Pharmacology (EPHAR 2021), December 6-8, 2021; Prag, Češka, 2021. str. 1-1

Roguljić, Hrvoje; Smolić, Martina; Kuna, Lucija; Smolić, Robert; Arambašić, Jerko; Kizivat, Tomislav; Ninčević, Vjera; Vukadin, Sonja; **Omanovic Kolaric, Tea**; Bilić Ćurčić, Ines; Včev, Aleksandar; LJUTA PAPRIKA „STARA PRIJATELJICA“ S NOVOM ULOGOM. // 13. međunarodni znanstveno-stručni skup HRANOM DO ZDRAVLJA; Osijek, 2021. str. 1-1)

Kuna, Lucija; Smolic, Robert; Smolic, Martina; Kizivat, Tomislav; Zjalic, Milorad; Nincevic, Vjera; Roguljic, Hrvoje; Vukadin, Sonja; **Omanovic Kolaric, Tea**; Vcev, Aleksandar; PREDTRETMAN ČEŠNJAKOVIM ULJEM SMANJUJE OŠTEĆENJE NASTALO DJELOVANJEM NaT-a U AGS MODELU ULKUSNE BOLESTI. // 13. međunarodni znanstveno-stručni skup HRANOM DO ZDRAVLJA; Osijek, 2021. str. 1-1

Omanović Kolarić, Tea; Ninčević, Vjera; Kuna, Lucija; Kizivat, Tomislav; Smolić, Robert; Smolić, Martina. ASSESSMENT OF HEPATOSTEATOGENIC EFFECTS IN CELL CULTURE MODEL OF DRUG INDUCED FATTY LIVER DISEASE // 9. Hrvatski kongres farmakologije s međunarodnim sudjelovanjem, Zagreb, 2019. str. 135-135

Kuna, Lucija; Kizivat, Tomislav; Smolić, Robert; **Omanović Kolarić, Tea**; Ninčević, Vjera; Včev, Aleksandar; Smolić, Martina; THE ACTIVITY OF GARLIC EXTRACTS (ALLIUM SATIVUM) TO THE EPITHELIAL DAMAGE CAUSED BY SODIUM TAUROCHOLATE IN A CELL CULTURE MODEL OF ULCER DISEASE. // 9. Hrvatski kongres farmakologije s međunarodnim sudjelovanjem; Zagreb, 2019. str. 136-136

Kizivat, Tomislav; Ninčević, Vjera; Cindrić, Anita; **Omanović Kolarić, Tea**; Kuna, Lucija; Smolić, Robert; Bilić-Ćurčić, Ines; Smolić, Martina; EFFECTS OF CAFFEINE ON DEVELOPMENT OF OXIDATIVE STRESS AND CRYSTALLIZATION ON IN VITRO MODEL OF OXALATE UROLITHIASIS. // 9. Hrvatski kongres farmakologije s međunarodnim sudjelovanjem; Zagreb, 2019. str. 132-132

Omanović Kolarić, Tea; Raguž-Lučić, Nikola; Ninčević, Vjera; Smolić, Martina; Stavovi liječnika obiteljske medicine o stalnoj provedbi kontrole farmakoterapije. // Knjiga sažetaka X. Kongresa Društva nastavnika obiteljske medicine "SMJERNICE U PRAKSI OBITELJSKOG LIJEČNIKA"; Zagreb, Hrvatska, 2019. str. 180-181

Omanović Kolarić, Tea; Ninčević, Vjera; Raguž- Lučić, Nikola; Jakab, Jelena; Kuna, Lucija; Smolić, Robert; Bilić-Ćurčić, Ines; Včev, Aleksandar; Smolić, Martina; Seniority of primary care physicians is associated with positive attitudes toward regular pharmacotherapy control habits. // PROGRAM AND ABSTRACTS- 11th ISABS Conference on Forensic and Anthropologic Genetics and Mayo Clinic Lectures in Individualized Medicine / Primorac, Dragan; Schanfield, Moses; Vuk-Pavlović, Stanimir; Kayser, Manfred; Ordog, Tamas (ur.). Zagreb, 2019. str. 165-165

Omanović Kolarić, Tea; Ninčević, Vjera; Kuna, Lucija; Kizivat, Tomislav; Včev, Aleksandar; Smolić, Martina; KLINIČKI ZNAČAJNE INTERAKCIJE HRANE I LIJEKOVA. // Knjiga sažetaka s 12. međunarodnog znanstveno- stručnog skupa HRANOM DO ZDRAVLJA; Osijek, Hrvatska, 2019. str. 75-75

Ninčević, Vjera; Kizivat, Tomislav; Cindrić, Anita; **Omanović Kolarić, Tea**; Kuna, Lucija; Smolić, Robert; Bilić Ćurčić, Ines; Smolić, Martina; POTENTIAL OF CAFFEINE TREATMENT ON OXIDATIVE STRESS AND CRYSTALLIZATION INHIBITION IN CELL CULTURE MODEL OF OXALATE UROLITHIASIS. // Knjiga sažetaka s 12. međunarodnog znanstveno- stručnog skupa HRANOM DO ZDRAVLJA; Osijek, Hrvatska, 2019. str. 73-73

Kuna, Lucija; Kizivat, Tomislav; Smolic, Robert; **Omanovic Kolaric, Tea**; Nincevic, Vjera; Vcev, Aleksandar; Smolic, Martina; GASTROPROTECTIVE EFFECT OF GARLIC EXTRACTS (ALLIUM SATIVUM) ON AMELIORATING DAMAGE CAUSED BY SODIUM TAUROCHOLATE IN A CELL MODEL OF ULCER DISEASE. // Knjiga sažetaka s 12. međunarodnog znanstveno- stručnog skupa HRANOM DO ZDRAVLJA; Osijek, Hrvatska, 2019. str. 66-66

[23/05/2018 – 25/05/2018] Assessment of the relevance of the specific scientific skills at Postgraduate doctoral study of Biomedicine and Health in Osijek; Rejkjavik, Island; **Omanovic Kolaric T**, Nincevic V, Smolic M. Assessment of the relevance of the specific scientific skills ORPHEUS CONFERENCE

[27/02/2018 – 01/03/2018] IDENTIFICATION OF POTENTIAL DRUG-TARGETS FOR DRUG INDUCED FATTY LIVER DISEASE. Vaals The Netherlands; **Omanovic T**, Kizivat T, Nincevic V, Raguz-Lucic N, Jakab J, Kuna L; Smolic R; Bilic-Curcic, I; Vcev A and Smolic M; 2nd European Fatty Liver Conference (EFLC2018)

[10/12/2018 – 12/12/2018] Knowledge, attitudes and counseling about drug-drug interactions among primary care physicians (PCPs) in Croatia; London, UK; Raguz Lucic N, Milas AM, Jakab J, Kralik K, **Omanovic T**, Nincevic V, Smolic M; Pharmacology 2018

[31/05/2017 – 02/06/2017] EVALUATION OF MOLECULAR MECHANISM DIFFERENCES IN IN VITRO MODELS OF DRUG INDUCED AND FATTY-ACIDS INDUCED NAFLD; Seville, Spain; **Omanovic T**, Kizivat T, Raguz-Lucic N, Nincevic V, Jakab J, Kuna L, Smolic R, Bilic-Curcic I, Vcev A, Smolic M.; The 1st International Conference on Fatty Liver

[03/05/2017 – 05/05/2017] Evaluation of Mentoring Workshop organized within the Faculty of Medicine Osijek; Klaipeda, Lithuania; **Omanovic T**, Raguz-Lucic N, Volaric N, Smolic M, Vcev A; ORPHEUS conference 2017 “PhD Training in Health Sciences and Biomedicine from the Interdisciplinary Perspective"

[2017] In vitro assessment of molecular mechanisms of free fatty acids-induced and drugs-induced fatty liver disease; Opatija; **Omanović Kolarić, Tea**; Ninčević, Vjera; Jakab, Jelena; Kuna, Lucija; Kizivat, Tomislav; Raguž- Lučič, Nikola; Abičić, Ivan; Smolić, Robert; Včev, Aleksandar; Bilić- Ćurčić, Ines; Smolić, Martina; Abstract book: 7th Croatian Congress of Obesity str. 11-12

[2017] Establishing the model of adipogenesis in vitro; Opatija; Jakab, Jelena; **Omanović Kolarić, Tea**; Kuna, Lucija; Ninčević, Vjera; Kizivat, Tomislav; Volarić, Nikola; Žulj, Marinko; Smolić, Robert; Včev, Aleksandar; Bilić-Čurčić, Ines; Smolić, Martina; Abstract book: 7th Croatian Congress of Obesity str. 29-30

[2016] Pharmaceutical residues in the aquatic environment Osijek; Kuna, Lucija; Jakab, Jelena; **Omanović, Tea**; Raguž-Lučić, Nikola; Smolić, Martina; Včev, Aleksandar; 7th International Scientific and Professional Conference Water for all - Book of Abstracts/ Habuda-Stanić, Mirna (ur.); Osijek: Prehrambeno-tehnološki fakultet Osijek, 2017. str. 79-79

[2016] Urolithiasis and Osteoporosis: Clinical Relevance and Therapeutic Implications; Osijek; Bilić-Čurčić, Ines; Milas-Ahić, Jasminka; Smolić, Martina; Smolić, Robert; Mihaljević, Ivan;

Tucak Zorić, Sandra; **Omanović, Tea**; Kuna, Lucija; Jakab, Jelena: Knjiga sažetaka: 12. osječki urološki dani, 5. osječki nefrološki dani, 4. sekcija medicinskih sestara i tehničara urologije i nefrologije Osijek 2017. str. 30-30

[2015] UTJECAJ USPJEŠNE ANTIVIRUSNE TERAPIJE NA KVALITETU ŽIVOTA BOLESNIKA OBOLJELIH OD KRONIČNOG VIRUSNOG HEPATITISA C. Osijek; Smolić Martina, **Omanović Tea**, Ragužˇ-Lučić Nikola, Kuna Lucija, Jakab Jelena, Smolić Robert, Včev Aleksandar.; Primarna i sekundarna prevencija bolesti suvremenog čovjeka

[2015] CASE REPORT: BETTER GLYCEMIC CONTROL AFTER LIRAGLUTIDE THERAPY IN DIABETES MELLITUS TYPE II.; Zagreb; Matus Helena, Miler Valentina, Šimić Iivana, **Omanović Tea**, Bilić-Ćurčić Ines; Croatian Student Summit 12 (CROSS 12) 2016.

[2015] Bone Mineral Density in Relation to Componenets of Metabolic Syndrome in Postmenopausal Women with Diabetes Type 2; Dubrovnik; Bilić-Čurčić, Ines; Smolić, Martina; Smolić, Robert; Ninčević, Vjera; **Omanović, Tea**; Včev, Aleksandar; IUAES - World anthropologies and privatization of knowledge: engaing anthropology in public

ORGANISATIONAL SKILLS

Organisation of various conferences

2016. 3rd International Monothematic Conference on Viral Hepatitis C (IMC-HCV-2016), 29.9.- 1.10.2016., Orahovica. Organizer

2017. Tenth ISABS Conference on Forensic and Anthropologic Genetics and Mayo Clinic Lectures in Individualized Medicine Member of Organizing Committee

2017. 4th International Monothematic Conference on Viral Hepatitis C (IMC-HCV-2017). Organizer

2018. 5th International Monothematic Conference on Viral Hepatitis C (IMC-HCV-2018). Or ganizer

2019. 6th International Monothematic Conference on Viral Hepatitis C (IMC-HCV-2019). Or ganizer

PARTICIPATION IN CONFERENCES

Participation in conferences

2015. 2nd International Monothematic Conference on Viral Hepatitis C (IMC-HCV-2015)

2015. Budućnost zdravstvene industrije, 20. listopada 2015. Mala dvorana Vatroslav Lisinski

2016. 4th Central Eastern European Symposium on Free Nucleic Acids in Non-Invasive Prenatal Diagnosis, Split, 25-26 May 2016

COURSES AND CERTIFICATES

2017. LETNJA ŠKOLA KLINIČKE FARMAKOLOGIJE, 25. avgust - 4. septembar 2017. godine, Ohrid, Makedonija

2016. Erasmus+ programu 2016 za mobilnost osoblja- laboratory work in Pecs

2016. Festival znanosti 18.-23.4.2016. in Osijek

2016. Temeljne vještine edukatora u biomedicini i zdravstvu, te interdisciplinarnim područjima znanosti (međunarodni tečaj 1. kategorije), 7-10 December, 2016, Osijek, Croatia

2016. Workshop for mentors, December 7, 2016, Osijek, Croatia

2016. qPCR basics and best practices for effective planning, realization and data analysis. Mannheim, Germany, 27th October 2016

2016. Tečaj za osposobljavanje osoba koje rade s pokusnim životinjama (B kategorija), 17-26 November; Zavod za animalnu fiziologiju, Prirodoslovno-matematički fakultet Zagreb, Hrvatska

2015. PhD course in Pecs 14.-18.12.2015., Laboratory immunetechinques in molecular biology research

2014. European Medical Students Orchestra and Choir (EMSOC), Bilbao 2014.

MEMBERSHIPS

Hrvatski liječnički zbor, member

Hrvatska liječnička komora, member

Hrvatsko društvo za humanu genetiku, member

Hrvatsko društvo farmakologa, member

Hrvatsko društvo za preciznu personaliziranu medicinu, member

International Society for Applied Biological Sciences (ISABS), member

LANGUAGE SKILLS

Mother tongue(s): Croatian

Other language(s):

English: LISTENING C1 **READING** C1 **WRITING** B2 **SPOKEN PRODUCTION** B2 **SPOKEN INTERACTION** B2

German: LISTENING B1 **READING** B1 **WRITING** B1 **SPOKEN PRODUCTION** B1 **SPOKEN INTERACTION** B1